University of Nottingham

UK | CHINA | MALAYSIA

MRI and Molecular Imaging studies of post-prandial gastrointestinal motility and peptide response in health and Crohn's disease

Dissertation submitted to the University of Nottingham for the degree of Doctor of Philosophy

Asseel Khalaf

Nottingham Digestive Diseases Centre, School of Medicine,

University of Nottingham, UK

List of abbreviations

^{99m}Tc	Technetium-99m
a.u.	Arbitrary units
ANOVA	Analysis of variance
ARC	Arcuate nucleus
AUC	Area under the curve
BRC	Biomedical Research Centre
bTFE	Balanced turbo field echo sequence
CCK	Cholecystokinin
CD	Crohn's disease
CDAS	Crohn's disease activity score
CDEIS	Crohn's disease endoscopic index of severity
CgA	Chromogranin A
CRP	C-reactive protein
CT	Computed tomography
DICOM	Digital Imaging and Communications in Medicine
DRAM	Dual Registration of Abdominal Motion
EEC	Enteroendocrine cells
ELISA	Enzyme-linked immunosorbent assay
fC	Faecal calprotectin
GEMRIGS	Gastric emptying by MRI and gamma scintigraphy
GI	Gastrointestinal
GIP	Glucose-dependant insulinotropic polypeptide
GLP-1	Glucagon-like peptide 1
GMP	Good Manufacturing Practice

GS	Gamma scintigraphy
HV	Healthy volunteer
IBD	Inflammatory bowel disease
ICC	Intra-class correlation coefficient
MaRIA	Magnetic resonance index of activity
mDIXON	Multiple echo time Dixon method
MEGS	Magnetic Resonance Enterography Global Score
MIC	Motility in Crohn's disease
MIP	Maximum intensity projection
MMC	Migratory motor complex
MRCP	Magnetic resonance cholangiopancreatography
MRE	Magnetic resonance enterography
MRI	Magnetic resonance imaging
NDDC	Nottingham Digestive Disease Centre
PP	Pancreatic polypeptide
PYY	Peptide YY
QMC	Queen's Medical Centre
RF	Radiofrequency
RIA	Radioimmunoassay
ROI	Region of interest
SBCE	Small bowel capsule endoscopy
SBWC	Small bowel water content
SD_{JAC}	Standard deviation of the Jacobian
SEM	Standard error of the mean
SENSE	SENSitivity Encoding

Sn	Sensitivity
Sp	Specificity
SPAIR	SPectral Attenuated Inversion Recovery
SPECT	Single photon emission computed tomography
SPIR	Spectral presaturation with inversion recovery
SPMIC	Sir Peter Mansfield Imaging Centre
TE	Echo time
TFE	Turbo field echo
TMF	Trial Master File
TR	Repetition time
UCL	University College London
US	Ultrasonography
VAS	Visual analogue scale
WAPS	Weighted average position score
WGT	Whole gut transit

Table of contents

List of figures

List of tables

Acknowledgments

The past few years have been a life-changing experience for me and this work would not have been possible without the help and support of many people. First and foremost, I would like to thank God Almighty for giving me the power and strength to pursue my dreams.

I would like to express my special thanks and appreciations to my great supervisor Dr Luca Marciani, thank you for your guidance, support and for the invaluable advices. Thanks for giving me the skills that improved me and for encouraging me to grow as a researcher. Without your kind words and motivations, I would not have had the confidence to excel academically.

I would like to express my sincere thanks for the support throughout this project, the constructive suggestions, and the critical advices of my co-supervisor Dr Gordon Moran. I also would like to acknowledge the constant guidance and valuable input of Prof Penny Gowland. A very special thanks to Dr Caroline Hoad, thank you for teaching me various methods and techniques and for answering all my questions no matter how busy you were.

I would like to express my sincere gratitude to all those at the Biomedical Research Centre (BRC), Sir Peter's Mansfield Imaging Centre (SPMIC), and the Medical physics department who helped me throughout my studies. I gratefully acknowledge the funding received towards my PhD from Kuwait University. I also greatly appreciate the financial support received for the study in Chapter 5 from Kuwait

Foundation for the Advancement of Sciences (KFAS) under project code CB17-63NR-01.

To my family, I express my gratitude for the support through good and bad times. A heartfelt thank you to my Mum, without your prayer for me I would not have come this far. To my beloved son and daughter, thank you for always listening and cheering me up! I’m thankful to my sister, for unconditionally loving me and for always being there for me. My acknowledgement would be incomplete without thanking my best friends. Thank you, my friends, for the unconditional friendship, for the motivations, for believing in me, and for being by my side throughout this PhD.

Abstract

Introduction: Crohn's disease (CD) patients suffer postprandial symptoms such as chronic diarrhoea, abdominal pain, bloating, weight loss and nutritional abnormalities. The changes in the regulation of gut hormones and gut dysmotility are believed to play a role but these are rarely studied together in the postprandial state in an unprepared bowel. This project aimed to: (a) develop an MRI methodology to assess fasting and postprandial intestinal motility and gut peptides using a soup test meal intervention in healthy volunteers and (b) to use this methodology to investigate the pathophysiological fasting and postprandial responses in CD.

Methods: Sixteen CD patients with active disease (age 36±3 years, BMI 26±1 kg/m^2) and 20 healthy volunteers (age 31±3 years, BMI 24±1 kg/m^2) participated. They underwent baseline and postprandial MRI scans, symptom questionnaires, and blood sampling at intervals for 270 minutes following a 400 g soup meal (204 kcal). Gastric volume, gall bladder volume, small bowel water content, small bowel motility, whole gut transit, GLP-1, PYY, and CCK were measured. A new processing technique was developed and used to quantify small bowel motility from cine MRI data. A standard magnetic resonance enterography (MRE) test was also performed at the end of the feeding study to measure disease activity. An assessment of gastric emptying of the soup meal by MRI and gamma scintigraphy (GS) was also carried out.

Key results: (mean±SEM) The healthy volunteers had significantly higher fasting motility index (106±13 a.u.) compared to CD subjects (70±8 a.u., $p<0.05$). The average time to empty half of the stomach contents ($T_{1/2}$) in healthy volunteers and CD subjects was 43±4 min, 63±7.5 min respectively. A significant difference was seen in the area under the curve of small bowel water content in CD subjects (19778±2119 mL/min) compared to healthy volunteers (14197±1249 mL/min, $p<0.05$). A significant increase was noted in fasting plasma measures of total GLP-1 in CD subjects compared to healthy volunteers (CD 50±8 µg/mL versus HV 13±3 µg/mL, $p<0.0001$) with a significantly higher postprandial GLP-1 (AUC CD: 12725 versus HV: 2400, $p<0.0001$). Fasting PYY levels increased significantly in CD subjects compared to the healthy volunteers (CD 236±16 pg/mL versus HV 118±12 pg/mL, $p<0.0001$) with a significant postprandial increase in levels in CD subjects compared to healthy volunteers (AUC CD 62782±4313 pg/mL versus HV: 34744±3169 pg/mL, $p<0.0001$). Fasting and postprandial CCK levels were not significantly different between CD subjects and healthy volunteers. CD subjects showed a significantly higher fasting fullness scores compared to healthy volunteers (CD 21±6 mm versus HV 5±3 mm, $p<0.01$). The meal challenge induced a significant postprandial increase in all symptoms scores in CD subjects compared to healthy volunteers ($p<0.05$). Gastric emptying carried out by MRI and GS correlated well ($r=0.95$, $p<0.0001$)

Conclusions: Multiple gastrointestinal motility, peptide and symptom responses were successfully measured in a single study session. The optimised MRI motility technique was sensitive to changes in motility induced by feeding. Small bowel motility and different physiological outcomes were successfully quantified in unprepared small bowel during fasting and after a nutrient soup meal in patients with CD and healthy volunteers. Gastric emptying of the soup meal can also be translated to gamma scintigraphy. These techniques will be useful for studying physiopathological pathways in different groups. The improved understanding of gastrointestinal pathophysiology will allow a better of understanding of the aetiology of symptoms in these patient groups with consequent identification of better therapeutic targets.

1. Introduction

1.1 The digestive system

The digestive system is responsible for the breakdown of various foods and liquids and for the absorption of nutrients into the body by mechanical and chemical processes. The gastrointestinal (GI) tract (Figure 1) of the digestive system is approximately 9 m long from the mouth to the anus. It is regulated intrinsically and extrinsically by neural and hormonal regulatory mechanisms.

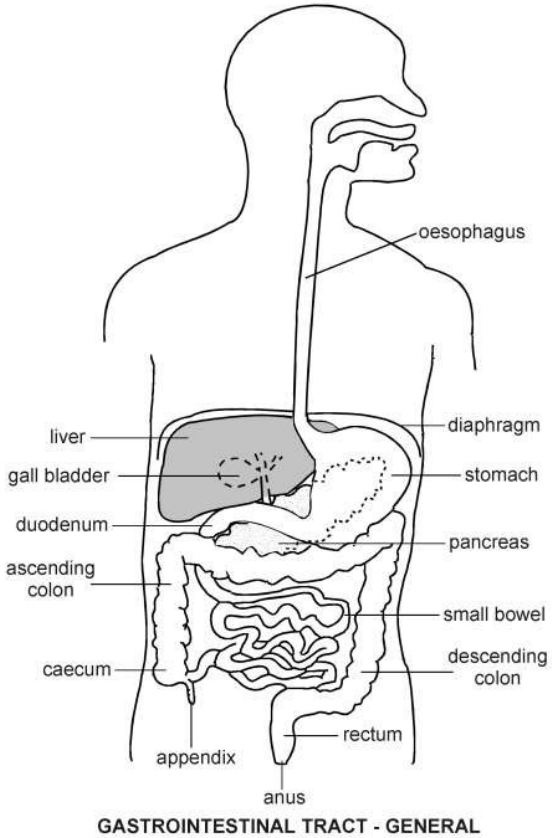

Figure 1: Diagram illustrating the gastrointestinal tract. Diagram authored by Dr Beverley Kenny, 30 Jul 2010. Date accessed 05 March 2018.

1.1.1 Stomach

The stomach is the most distensible part of the GI tract. It is a reservoir for ingested food and drink and the site for breakdown of food into chyme, which is controlled mainly by mechanical, chemical and enzymatic processes[1, 2]. Upon swallowing, food chime from the mouth reaches the stomach where it undergoes dilution, digestion and mixing by peristalsis and gastric and salivary juices. Following that, the chyme is delivered to the duodenum at a controlled rate and it is further degraded into molecular components by digestive enzymes[3].

Gastric emptying

After food intake, the proximal part of the stomach relaxes and acts as a reservoir for the food. Following that, a tonic contraction will redistribute the food towards the distal part of the stomach and a repeatable contraction of the antrum will facilitate in the breakdown and mixing the contents with gastric juices[3]. Subsequently, the process of mechanical digestion will start by pushing the food against a closed pylorus through gastric muscles. Food contents will exit the antrum of the stomach through the pylorus into the duodenum. This process is known as gastric emptying and is controlled by neurohormonal factors[3, 4].

1.1.2 Small intestine

The primary digestive organ of the body is the small intestine. It is the longest part of the GI tract and it is divided into duodenum, jejunum and ileum. The primary function of the small bowel is the digestion and absorption of food nutrients through complex secretory, absorptive and mechanical processes. The movement of the small bowel helps mixing the chyme with bile and pancreatic enzymes and propels the chyme to the colon[5]. Mechanical segmentation contractions of the intestinal muscles allow the chyme to be mixed with digestive juices and allow the nutrients to be absorbed. Transport along the bowel is achieved by the peristaltic contractions of the small bowel which are caused by the enteric nervous system. Small bowel digestion can be divided into mechanical and chemical digestion. Absorption in the small intestine is facilitated by the combined intestinal and pancreatobiliary juices.

Small bowel motility regulation

Small bowel motility is characterized by different types of contractions and waves that control mixing and propel the chyme through the gut. It has two forms of motility patterns; fasting (starvation) pattern and the fed pattern[2, 6]. Throughout fasting, small bowel motility is determined by a type of waves called the migrating motor complexes (MMCs), which consist of three different phases, repeated approximately every 2 hours and coordinated by neural and hormonal factors[7]. The MMC force the chyme to travel down the intestine during the fasting state. Upon feeding,

the MMC is replaced by the postprandial (fed) pattern. The postprandial intestinal motility is triggered by the luminal distention and is modulated by the luminal nutrients[8]. Another type of contractile pattern is the stationary segmenting contractions which help in mixing and pushing the chyme.

One of the important factors that regulate the amount of nutrients absorbed by the intestine, is the intestinal transit time[2]. Typically, the transit time of the small bowel is approximately 1-4 hours in healthy humans[9].

1.1.3 Colon

The large intestine, or colon, is the last part of the digestive system and it consists of six parts: cecum, ascending colon, transverse colon, descending colon, sigmoid colon and rectum. The waste materials (faeces) are processed in the colon and are ultimately excreted through the anus.

1.2 Gastrointestinal peptides and their physiological roles

The largest endocrine organ in the human body is the enteroendocrine system and it is made up of enteroendocrine cells (EEC). The EEC represent ~1% of the entire intestinal epithelium[10] and they produce more than 20 hormones[11]. Gastrin, somatostatin, PYY, secretin, CCK, GLP-1, 5-HT and GIP are some examples of EEC hormones[11]. The EEC act like

sensors of the luminal contents (mainly nutrients) and function to secrete different amine and peptide hormones in response to food intake[10]. A variety of gastrointestinal peptides are secreted from different EEC. Each peptide/amine has a specific function and is secreted by cells in definite anatomical locations in the GI tract[11].

These hormones regulate different homeostatic functions in the GI tract such as postprandial secretion and motility and they have a role in regulating satiation during food intake. They act indirectly by activating the vagal nerve[12] or directly by entering the blood stream and sending signals to the arcuate nucleus (ARC) in the hypothalamus[13]. Some of the peptides more relevant to this work are briefly described below.

1.2.1 Cholecystokinin (CCK)

Cholecystokinin (CCK) is an endogenous gut hormone released from the I cells of the proximal duodenum and jejunum[12]. CCK was the first hormone shown to have an effect on appetite regulation[14]. CCK has a short half-life of only 1-2 minutes[12]. It acts mainly through two receptors, the CCK1 and CCK2 receptors[1]. It is secreted in response to ingestion of fat or protein in the small intestine[12]. It has been discovered that only long-chain fatty acids (>C10) can stimulate I cells to release CCK[15] through G-protein coupled receptor 40 (CPR 40)[16].

The level of CCK increases over 10-30 minutes after food intake[12]. The main functions of CCK are the stimulation of gall bladder contraction, stimulation of pancreatic secretions and delay of gastric emptying[12]

which eventually contributes to increased feelings of satiety and fullness and termination of food intake[13]. Exogenous administration of CCK resulted in decreasing meal size, thus showing the role of CCK in modulating appetite in humans[17].

1.2.2 Peptide YY (PYY)

Peptide YY (PYY) is secreted from L cells of the small and large intestine with the highest concentrations within the terminal ileum[12]. PYY is a member of the pancreatic polypeptide (PP) peptide family and it acts by binding to G-protein receptors, Y1 and Y2 receptors[1].

PYY is mainly stimulated by protein; however, fats and carbohydrates also stimulate its release[18]. Plasma levels of PYY are relatively low in the fasted state with levels rising within 30 minutes after a meal stimulus[19]. PYY affects the GI system by slowing the meal transit[12] through a delay in gastric emptying and increasing the GI transit time (known as ileal brake)[20]. Exposure of the ileum to fatty acids decreases jejunal[21] and duodenal motility[22] through PYY-mediated mechanisms, while parenteral administration of PYY 3-36 delays gastric emptying[23]. In animal models, CCK and PYY were shown to interact in the postprandial state to control gut secretory and motor function[12]. In humans, postprandial release of PYY from the distal ileum after a fat load in the proximal gut has been shown to be CCK-mediated[24].

1.2.3 Glucagon-like peptide 1 (GLP-1)

Glucagon-like peptide 1 (GLP-1) has a key role in increasing satiety and it enhances insulin release[25]. Similar to PYY, GLP-1 is released from L cells of the distal small intestine and large intestine[26]. After an oral glucose load, GLP-1 has an incretin effect through stimulating insulin secretion by acting on pancreatic beta receptors[27]. Consequently, the released insulin stimulates the uptake of blood glucose by liver, muscle and adipose tissue thus contributing to glucose homeostasis[28].

GLP-1 is mainly stimulated by carbohydrates and it has a half-life of 2 minutes. The release of GLP-1 starts 10-15 minutes after a meal and again it peaks after 30-60 minutes[27]. It delays gastric emptying[25] and decreases small bowel motility separately; its effects have been shown both in murine models[29] and, more recently, in humans[30, 31].

Peptide	Secreted from	Main function
CCK	I cells of the proximal duodenum and jejunum.	- To stimulate gall bladder contraction. - To stimulate pancreatic secretions. - To delay gastric emptying.
PYY	L cells of the small and large intestine.	- To delay gastric emptying. - To increase GI transit time (ileal brake)
GLP-1	L cells of the distal small intestine and large intestine.	- It has an incretin effect. - Acts as an ileal brake

Table 1: Summary of gut peptides and their main function

1.3 Evaluation of the GI tract

Different techniques are used to evaluate and visualise the anatomy and the pathology of the gastrointestinal (GI) tract to obtain the correct diagnosis and also to study transit time and motility in the gut. Some of these modalities will be explained briefly:

1.3.1 Manometry

Manometric recording of motility is one method performed by inserting a solid-state or water perfused catheter into a selected portion of the gut[32]. This technique is invasive and requires skilled specialist operators[32]. In

addition, hydrogen breath test is another method to measure the intestine transit time[2].

1.3.2 Endoscopy

Endoscopy is a useful modality to directly visualize the gut mucosa in combination with histology from biopsies. It is an essential initial tool to diagnose and distinguish different types of inflammatory bowel disease (IBD)[33]. It is also an important modality in evaluating treatment responses and therapeutic outcomes. However, endoscopy is not useful at measuring transmural inflammation. Therefore, cross sectional imaging is required like computed tomography (CT) and Magnetic resonance imaging (MRI).

Small bowel capsule endoscopy (SBCE)

Recently, a wireless capsule has been used to measure regional intestinal transit time and gastric emptying[34]. Capsule data from healthy volunteers and patients with gastroparesis showed a significant increase in transit times in patients compared to healthy control[34]. SBCE has an important role in assessing intestinal mucosa, disease extent and severity and in evaluating mucosal healing[35]. Although capsule endoscopy is sensitive in detecting inflammatory lesions, the use is limited in patients with small bowel obstruction[36].

1.3.3 Conventional radiological examinations

Abdominal non-contrast radiography can be used to differentiate normal and abnormal gas accumulations, air fluid levels and calcifications. Positive and negative oral luminal contrast agents can be used to image peristalsis, emptying and pathological changes like stenosis, inflammation or neoplastic changes[37].

1.3.4 Ultrasonography

Ultrasonography (US) is an imaging technique that provides good soft tissue capabilities. It is a safe technique without any radiation exposure. US is used to detect wall thickening, disturbed wall morphology, oedema and lymphadenopathy in inflammatory bowel diseases[38]. Moreover, Doppler imaging techniques can be used to examine the perfusion of the intestinal wall and the surrounding tissues[37]. In addition, transabdominal US and colour Doppler US have been used to acquire qualitative and quantitative information regarding intestinal motility and gastric emptying[39]. Although US is a non-invasive technique and does not disturb the normal motility of the GI tract, it is an operator-dependant technique and the views are limited by intestinal gas.

1.3.5 Computed tomography

Multi detectors CT scanners are used to assess the abdominal viscera[40]. Non-contrast enhanced CT allows the detection of free intra-abdominal air and intestinal obstruction[37]. Additionally, contrast materials in CT are

used to enhance imaging of the bowel wall which is very useful in inflammatory bowel diseases[41]. Non-contrast and contrast enhanced CT scanning has been used to provide cross sectional images of the intestinal loops. The main advantage of modern CT scanners is that they permit fast acquisition of thin slices which reduces the motion artefacts; the images can then undergo multi-planar reconstruction in any direction[37]. The use of ionizing radiation in CT is the major disadvantage[42].

1.3.6 Gamma scintigraphy

Gamma scintigraphy (GS) is useful in imaging the upper GI, particularly in emptying and motility disorders[43]. It is the gold standard examination for assessing gastric emptying with the use of radiolabelled test meals. It is a simple, easy test that produce quantitative data on gastric emptying and GI transit with the use of small amount of ionising radiation[37]. Both scintigraphy and single photon emission computes tomography (SPECT) are used for transit and gastric emptying studies of the GI tract[43]. Radiolabelled white cell scanning using 111-indium or 99mTc has been used in evaluating inflammation and assessing disease extension in IBD[44-46].

1.3.7 Magnetic resonance imaging

MRI is a medical imaging modality that provides excellent soft tissue contrast and spatial resolution compared to other modalities. Newly

developed fast sequences and modified techniques have overcome the long acquisition time in GI MRI[47]. High resolution and better image quality using modified protocols and new sequences can enhance patient diagnosis[48]. This makes it the technique of choice in repeated scanning, also because of the lack of radiation exposure.

Basic principles

MRI uses the inherent magnetic resonance properties of the hydrogen protons. Hydrogen protons are electrically charged and spin around their own axis and as such they exhibit a magnetic moment. In a quantum mechanic description the radiofrequency (RF) pulse applied excites the protons[49]. When they then decay to a lower energy state the energy released can be detected using receiver coils to build the MR image. In a semi-classical framework, when placed inside a strong magnetic field, the protons are subject to a torque and precess about the field with a specific frequency called the Larmor frequency. Application of radiofrequency waves at this specific frequency tilts the magnetization away from the direction of the main field and after excitation a signal can be detected using receiver aerials (coils). When the RF pulse is switched off, the magnetisation returns to its original state, a process called relaxation[49]. The original magnetization starts to recover and the received energy is transferred to the surrounding, termed T1 relaxation. Different molecules have different T1, for example, fat has shorter T1 than water. At the same time, protons begin to dephase (spin out of

phase) when the RF pulse if turned off. The time needed for the tissue to dephase is termed T2 relaxation.

MRI and small bowel motility

The use of MRI is increasing in the field of gastrointestinal diseases because of the lack of radiation exposure, which is a major concern in repeated scanning[50]. It has been used to measure small bowel transit time and motility and to study small bowel diseases[51, 52]. To clearly visualize the small bowel, the bowel segment should be distended to offer a good contrast against the adjacent walls[47]. MR Enterography (MRE) has been used previously to image small bowel motility[47]. The methodology involves ingesting large amounts (~ 1L) of fluid to distend the bowel artificially. The fluid usually contains a combination of osmotic agents and fiber hydrogel agents which assist in avoiding fast reabsorption of the liquid[53]. One study evaluated the viability of cine MRI in 10 volunteers to evaluate small bowel peristaltic motion by drug-induced motility changes[54]. The results showed that MRI is a reliable method in evaluating motility and in monitoring the effect of different pharmacological factors[54].

The evaluation of small bowel motility is usually achieved using subjective qualitative assessment by a radiologist, thus researchers investigated different methods to quantify objectively motility using MRI methods. The ability of MRI to quantify the variability in small bowel motility using motility analysis software after pharmacological

intervention has been presented in another study with healthy volunteers[55]. The volunteers received either neostigmine (a prokinetic agent) or saline and the second group received either Butlyscoplamine (an inhibitor of bowel motility) or saline[55]. The software quantified motility showing good repeatability and captured the changes induced by the administration of pharmacological drugs[55]. Another objective method to visualise and quantify global bowel motility with MRI is by using motility mapping, displayed using a colour-coded scaling similar to that used in conventional manometry (Figure 2)[56]. This work was done on four healthy subjects and eight patients with IBD. The segments with abnormal bowel movement were identified and correlated with motility maps in the eight patients using colour-coded motility mapping[56].

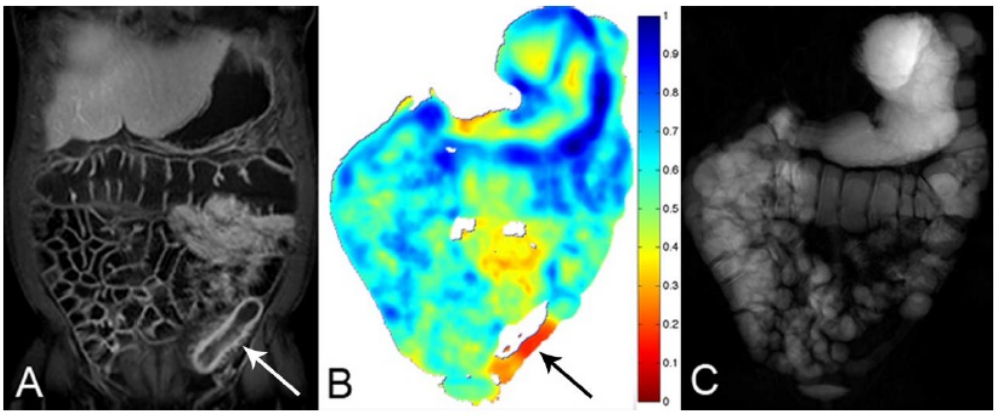

Figure 2: Example of MRI mapping. MRI (A, C) and motility coloured map finding (B) of a 45-year old patient with CD[56]. Arrow in (A) is showing segmental wall thickening, increased contrast enhancement, and low-grade irregular stenosis of the descending colon. Arrow in (B) is showing the segment affected in red, which indicates low motility.

Odille et al investigated a quantitative method to assess motility using MR images[57]. Quantifying motility using MRI is challenging with the presence of complex motion patterns. Therefore, the authors used image registration technique to derive a parametric map which can be used to quantify motility. They presented a novel non-rigid image-based technique for automated small bowel motility analysis from dynamic MRI images[57]. Small bowel motility was assessed in a total of 10 patients with CD (confirmed histologically). This quantitative assessment was validated against small bowel motility measured manually by two experienced radiologists[57]. Recently, a different automatic analytical software called Motasso has been validated in 25 patients with clinical indication for small bowel MRI by comparing it directly with manual measurements of small bowel motility by two experienced radiologist[58]. The parameters measured by hand and by the software in this study correlated significantly between the methods. These results showed that the software-assisted evaluation of motility can reliably and accurately measure small bowel motility[58]. Furthermore, the decrease in motility following an administration of glucagon in 10 healthy volunteers was assessed with the use of tagged MR imaging (which is a motion sensitive technique that looks at the changes in the tag pattern)[59]. The techniques was able to detect the drug-induced changes in motility[59].

The literature summarised above leads to the conclusion that small bowel motility can be quantified using MRI and that the MRI method is sensitive to changes induced by pharmacological interventions.

1.4 Crohn's disease

Crohn's disease (CD) is an IBD. It is a chronic condition characterised by patchy, transmural inflammation of the GI tract[60]. IBD affects around 0.2% of the human population with a UK-wide prevalence of ~250,000 patients, with specifically CD affecting 80,000 patients in the UK alone[61]. The estimated costs of IBD to NHS is around £720 million with an average of £3,000 per patient per year[62].

CD may have a pan-enteric distribution but most commonly it affects the distal ileum and the colon (Figure 3)[61]. Inflammation affects the terminal ileum in about 60% of small intestinal inflammation cases[63].

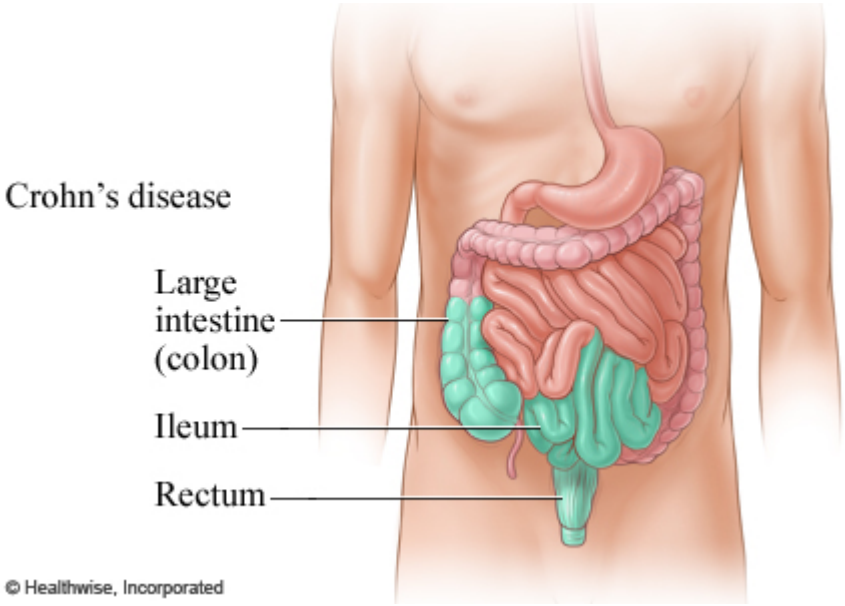

Figure 3: Diagram of the most common sites of Crohn's disease © Healthwise, Inc. date accessed 15 Nov 2015

1.4.1 Aetiology

The aetiology and the pathology of CD are not well understood[60] but these are widely believed to be multifactorial. A combination of immune, genetic and environmental factors is thought to induce the intestinal inflammation in response to an intraluminal bacterial antigen stimulus[64]. Intestinal inflammation in CD is considered to be generated by the adaptive immune system[65]. Immune dysregulation in a genetically susceptible host has been long believed to play a major role in the aetiopathogenesis of the disease[66]. Familial aggregation is confirmed in CD and a large number of genes that might contribute to the disease have been identified[65].

Additionally, impaired ecology of the intestinal gut microbiota has been suggested to participate in the pathogenesis of the disease as it contributes to the regulation of inflammation[67]. Data from different studies suggested a possible role of the gut microbiota in the development of IBD[68, 69]. Furthermore, an alteration in the expression of tight junction proteins has been shown, leading to an increase in intestinal permeability and thus migration of bacterial antigens in the lamina propria with consequent triggering of the adaptive immune response[70].

Finally all these variables at the patient-level are modified by environmental factors. A history of smoking, obesity and a western life style are all implicated in the development of CD[60].

1.4.2 Disease classification

The Montreal classification of CD[71] classifies CD according to the age of onset (A) disease location (L) and disease behaviour (B) as described in Table 2.

<table>
<tr><th colspan="3">Montreal classification of Crohn's disease</th></tr>
<tr><td>Age at diagnosis (A)</td><td>Disease location (L)*</td><td>Disease Behaviour (B)</td></tr>
<tr><td>A1 16 years or younger</td><td>L1 Terminal ileum</td><td>B1 nonstricturing nonpenetrating</td></tr>
<tr><td>A2 17-39 years</td><td>L2 Colon</td><td>B2 stricturing</td></tr>
<tr><td rowspan="2">A3 over40 years</td><td>L3 Ilecolon</td><td rowspan="2">B3 penetrating</td></tr>
<tr><td>L4 Upper GI</td></tr>
</table>

Table 2: Summary of Montreal CD classification[71] according to the (A) age at diagnosis, (L) disease location, (B) disease behaviour. *A perianal disease modifier may be added in the presence of perianal fistulas. This will not be discussed any further in this thesis.

1.4.3 Symptoms

CD can present with a variety of symptoms but nutritional abnormalities are a very common problem in this disease. Up to 85% of IBD patients suffer from nutritional deficiencies with protein-calorie malnutrition common when in an active phase of the disease[72] Micronutrient deficiencies are also a recognisable issue in remission[73]. In CD, up to 75% of hospitalized patients are malnourished[74]. Increased intestinal losses, anorexia and inflammation appear to contribute to malnutrition in

CD[74]. Most patients' symptoms in CD occur postprandially after feeding rather than after a prolonged fast.

CD patients suffer from acute or chronic diarrhoea, abdominal pain, bloating, and weight loss[60]. Specific symptoms of CD may vary in between patients but this tends to depend broadly on the predominant disease location. Patients with a predominant colonic distribution of the disease tend to present mainly with chronic diarrhoea and rectal bleeding, while patients with small bowel disease can present with a change in bowel habit, abdominal pain and predominant obstructive symptoms.

These symptoms have a significant influence on patients' lives. In a survey study of 5636 patients 75.6% of the patients reported that symptoms affected their ability to enjoy leisure activities like travel, dining and sports and in 68.9% the symptoms affected their ability to perform at workplace[75].

1.4.4 Diagnosis

A number of investigations may be needed to diagnose CD as a significant number of related symptoms can be non-specific and shared with other common conditions like irritable bowel syndrome, coeliac disease, intra-abdominal malignancy and ulcerative colitis. There is no single gold standard test to diagnose CD. The diagnosis is confirmed by clinical evaluation and a combination of haematological, biochemical, endoscopic, histological and imaging-based investigations[61]. Initial

mandatory laboratory tests include full blood count, urea and electrolytes, liver function tests, and C-reactive protein (CRP)[60]. The most common findings in the laboratory tests in patients with CD are anaemia, a high white cell count, thrombocytosis, and raised inflammatory markers[60].

Faecal calprotectin (fC), a granulocyte protein shed into faeces by the inflamed bowel, has been used in recent years as a marker of disease activity. Meta-analyses estimate it has 80-87% sensitivity (Sn) and 68-82% specificity (Sp) for clinical[76] and endoscopic[77] CD activity, and 78% Sn and 73% Sp to predict relapse[78].

Recent data have indicated that fC might be less sensitive as a marker of small bowel disease[79]. To this effect, the correlation co-efficient of faecal calprotectin with endoscopic and histological parameters of disease activity is reduced in small bowel disease when compared to large bowel disease[80].

Different imaging modalities are available to diagnose and evaluate the extent and the severity of the disease and to investigate the suspected complications. A plain abdominal x-ray is sometimes necessary for the initial assessment of patients with CD in order to exclude obstructive complications[61]. Endoscopic examination through a colonoscopy is the gold standard investigation as it provides the opportunity of a close inspection of the intestinal mucosa and the ability to obtain histological samples for microscopic assessment of the disease. Intuitively, colonoscopy is highly useful for colonic disease but has a limited role in the diagnosis and follow-up of small bowel disease

especially if this has a proximal or mid small bowel location as it cannot be reached[60]. A simple endoscopic score system for CD (SES-CD) is used in clinics based on endoscopic variables[81]. Small bowel capsule endoscopy (SBCE) has a high sensitivity for detecting small bowel disease but the effectiveness of this modality is limited by inter-observer variability and limited availability within medical institutions. Moreover, it is impossible for SBCE to assess the extra luminal disease extent[82].

Ultrasound has also been used in the diagnosis of CD. It has the ability to visualise the changes in the bowel wall without the use of ionising radiation. The contribution of newly developed techniques in intestinal ultrasound has been shown in CD. Contrast-enhanced ultrasonography (CEUS) demonstrated a high sensitivity and specificity in predicting disease activity in CD[83] and in evaluating postoperative recurrence in CD[84]. Another interesting method is the ultrasound elastrography. This method evaluates the changes in tissue elasticity and stiffness in pathological conditions[85]. Recent studies based on this technique suggested that it can be used in evaluating CD[86, 87]. In addition, a multi-centre clinical trial has been launched recently aimed to compare and evaluate the diagnostic accuracy of MRI and ultrasound in CD[88].

Recently, MRI and CT have been widely used because of their accuracy in detecting small bowel inflammatory lesions[60]. Additionally, both MRI and CT are capable of indicating the disease extension and activity based on the wall thickness and increased intravenous contrast

enhancement[60]. CT is widely available and is less time-consuming than MRI[61], however the use of MRI in CD assessment has recently increased for specific reasons. One major disadvantage of CT is the high radiation exposure specially with repeated examinations[82]. MRI has better soft tissue contrast and multi-planar capability. Moreover, MRI is superior in detecting CD complications and the lack of radiation exposure, together with improved infrastructure, availability and technology makes it the technique of choice for CD patients[61]. For these reasons MRI has become a recommended technique especially with the modern hardware and software[61].

MRI has the ability to detect luminal and extra luminal features of CD[89]. The degree of wall thickness, bowel wall enhancements and wall oedema are important signs of disease activity which can be assessed using MRI[90] (Figure 4). Another important sign of CD is the abnormal alteration in bowel motility which can be examined using MRI[91]. In addition, MRI has the ability to detect fat wrapping (creeping fat) in CD[92] which is one of the disease's features defined by the unusual changes in the appearance of mesenteric adipose tissue in CD patients[93].

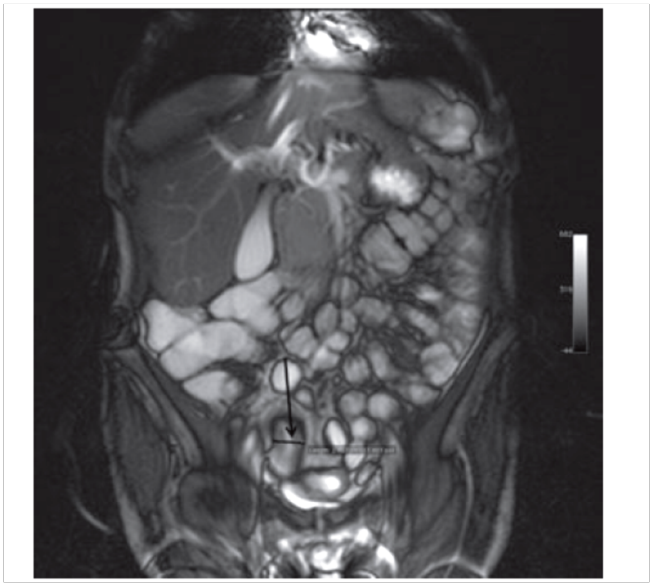

Figure 4: Example of MRI findings seen in CD[94]. MRI image of the entire abdomen illustrating the terminal ileum (arrow) showing wall thickening, comb sign, and edema in the surrounding mesenterial tissue[94].

Advantages of MRI in assessing CD patients

One of the most important benefits of MRI is the lack of radiation exposure. This is more critical in CD patients because the disease affects mostly young patients. Also, CD patients often need repeated scanning to assess the disease activity and progress, and also to monitor treatment outcomes, making repeated radiation exposure by CT an unsuitable option in the long term. In addition, patients with CD have background risk of neoplasia[95]. MRI has instead potential advantages for the assessment of disease activity and patient management[89]. The role of MRI has expanded and researchers are investigating its use in monitoring and evaluating treatment therapies[96, 97].

New and emerging MRI techniques have important advantages in measuring disease activity in CD. A significant decrease in contrast enhancement from active to remission in CD was reported with the use of contrast-enhanced T1-weighted MRI [98]. The study also demonstrated a significant decrease in wall thickness from active to remission phase suggesting the importance of MRI in detecting pathological changes[98]. Additionally, the ability of MRI in detecting fibrosis in CD lesions has been shown from analysing 44 segments of 41 patients [99] . An adequate distention of the bowel can be achieved artificially through nasoduodenal intubation in MRI enterolysis[100] and in MRI enterography. MRI enterolysis showed a similar accuracy to conventional enteroclysis (under fluoroscopic guidance) as a diagnostic method in evaluating CD in patients[101]. In addition, Frokjaer et al[102] showed that MRI is superior to conventional enteroclysis in visualising the entire small bowel pathology with less patient discomfort. Another sign of CD is the high mural signal intensity on T2-weighted fat-saturated images which might indicate the presence of mural oedema and contribute to disease activity[90].

1.4.5 Management

There is no actual cure for CD. The choice of management of Crohn's disease depends on the severity, the site and the behaviour of the disease[103]. Therapeutic options in the management of the disease include nutritional supplementation, smoking cessation, drug therapy, and surgery in severely active or complicated stricturing and penetrating

disease[61]. Smoking cessation resulted in a 65% reduction in the risk of relapse compared to continued smokers[104]. The aim of the drug therapy is to reduce the inflammatory burden, attenuate or halt disease progression, control the symptoms and optimise quality of life. A variety of drug therapies have been used such as antibiotics, corticosteroids, aminosalicylates, thiopurines, methotrexate, vedolizumab, ustekinumab and anti-TNF therapy[61]. Even with appropriate medications and nutrition, patients may ultimately need surgery to reduce the disease's symptoms and complications. It has been reported that surgery may be required in up to 75% of CD patients after 10 years of the disease[105]. Recent data highlight a rate of 35% in the first decade with the risk of a second operative procedure of 25% in the next 5 years[106]. A very recent data showed an overall decrease in the surgical resection rates in CD[107].

1.4.6 Peptide dysregulation in CD

In patients with intestinal inflammation, nutritional deficiency is a very common and important clinical problem[108]. The causes of malnutrition are multifactorial and biological processes other than structural disease have a key role[109]. In addition, poor appetite, satiety and reduced food intake contribute to the nutritional imbalance in CD[109]. Satiety signals produced by gut peptides play a critical role in CD. Changes in the regulation of GI peptides in inflammatory bowel disease are believed to play a fundamental role in the control of food intake. Intestinal inflammation in CD has been associated with increased GI peptides and

these peptides have an effect on GI function. This might suggest a link between the alteration in intestinal physiology and malnutrition in CD. The link between peptides regulations in CD and the aversive symptoms is inadequately understood.

Animal models

The effect of inflammation on food intake has been studied in a mice model of upper gut infection (Trichinella spiralis). Elevated CCK plasma levels were demonstrated with reduced food intake in the affected mice[110]. Food intake was increased after treating the mice with CCK1 receptor antagonist loxiglumide[110]. Worthington et al [111]also investigated the alteration in feeding in a mice model of enteritis (induced by Trichinella spiralis). They obsereved a a reduction in feeding from 6-10 days post infection with a significant increase in CCK positive I cells in wild-type mice. This was attenuated in the genetically modified mice lacking CCK[111]. These observations indicate that the intestinal inflammation and the increase in CCK may be linked to the reduced food intake.

Human studies

Historical data in eight patients with severe malabsorption showed increase in various gut hormones compared to 12 controls[112]. In another study, patients with digestive disorders showed elevated plasma levels of PYY[113]. In a study done on patients suffering from giardiasis, a

significant increase in their postprandial CCK levels was reported compared to healthy controls. Following treatment with metronidazole, plasma CCK levels were normalised and patient symptoms like nausea bloating and anorexia were abolished[114]. This suggests a link between intestinal inflammation and the increase in GI peptides and its potential reversibility.

CD data

Few studies have considered the EEC peptides in CD and their role is poorly understood. In an early study, ileum specimens were taken from 10 patients with CD. They demonstrated a significant increase in the EEC population in the ileum measured using immunostaining[115]. Furthermore, at the tissue level, a significant increase in EEC peptide expression was seen in the terminal ileum of CD patients[116]. GLP-1 and chromogranin A (CgA) cells in the terminal ileum were increased by 2.5 fold in CD patients while PYY cells were unchanged[116]. In the same study, mRNA expression of the gut peptides was examined and the results showed a significant increase in the gene expression of CgA and GLP-1 peptides but not PYY[116].

In a study using breath test, gastric emptying and gut peptides were investigated in 13 CD patients and 13 healthy controls[117]. A 50% delayed gastric emptying (measured by $T_{1/2}$) was noted with elevated postprandial levels of gut hormones like CCK, PYY and GLP-1[117]. In another CD patients study, the link between EEC peptides and appetite

related symptoms was investigated in a cohort of 17 patients and 13 healthy controls. An increase in fasting and postprandial plasma PYY levels was seen and it was associated with symptoms like nausea and bloating[109]. After treatment, plasma PYY levels were normalised thus suggesting a link between EEC peptides and disease activity[109]. Recently, Keller et al evaluated gastric emptying in 20 healthy controls and 13 CD patients during active disease and following treatment. Delayed gastric emptying and elevated levels of GLP-1 were noted in CD patients compared to controls[118]. After 3-4 months of treatment, gastric emptying was accelerated and the peptides levels were significantly decreased[118].

Although there is little research aimed at investigating the link between patient symptoms and altered EEC secretions in small bowel CD, symptoms are believed to result from changes in peptide regulation[119].

1.5 Assessment of disease activity in Crohn's disease

The gold-standard assessment of mucosal healing in CD relies on endoscopy. However, this invasive procedure needs to be repeated to monitor the disease activity[120]. The disadvantages of endoscopy include risk of bowel perforation, difficulty to reach the distal small bowel, patient discomfort, the use of sedation and poor patient acceptance[121]. Furthermore, colonoscopy is not easily accessible for all patients and it can only assess the mucosal side of the lumen[122]. In parallel, the growing

interest in cross sectional imaging of IBD attracted the attention towards using CT in evaluating the disease activity. The use of intravenous contrast medium in CT improves the evaluation of bowel wall changes in patients with CD[123]. However, the major disadvantage of CT is the use of ionizing radiation[42] as discussed before. The use of US has been suggested to measure disease activity, however, gas interposition limited its use[124]. This technique is well tolerated by patients, but high inter-operator variability has been noticed when using US.

MRI has the potential to overcome these limitations with the lack of ionising radiation, high soft tissue contrast[120], and high diagnostic precision in the evaluation of luminal and extra-luminal lesions[125]. Moreover, MRI is now a well-established non-invasive diagnostic technique in IBD with high sensitivity and specificity in detecting the disease[126, 127]. It is ideally appropriate in the management of CD because it is safe, accurate and well-tolerated[123]. In addition, MRI has the ability to assess the ileocolonic region in all CD patients compared to 72% of the patients using colonoscopy[121].

1.5.1 Scoring systems

Magnetic Resonance Index of Activity (MaRIA)

MRI analysis of disease activity in CD relies on structural changes such as bowel wall thickness, mucosal ulceration, wall oedema (estimated using a “fluid sensitive” MRI scan) (Figure 5) and increased blood supply (estimated by giving an intravenous contrast agent)[121]. These variables

are combined in a scoring index called a Magnetic Resonance Index of Activity (MaRIA)[121]. This scoring system has been used to evaluate the ability of MRI to assess inflammation in CD and to monitor responses to therapeutic interventions[121]. It was validated against Crohn's Disease Endoscopic Index of Severity (CDEIS)[128] (an index for determining the severity of CD using endoscopy). In this study, fifty patients with active (n=35) and inactive (n=15) CD were examined using ileocolonoscopy and MRI. As in colonoscopy, the bowel in the MRI image is divided into six segments to quantify disease activity (distal ileum, ascending, transverse, descending, sigmoid colon and rectum)[121]. Based on the MRI findings in each of the segments, the MaRIA score is calculated using this formula: MaRIA (segment) = 1.5 x wall thickness (mm) + 0.02 x Relative Contrast Enhancement + 5 oedema + 10 x ulceration[121]. A global MaRIA score can be measured by adding the values of all the segments[121]. In this study, the CD findings using both modalities were compared using the two scoring systems. They concluded that MRI can be used as an alternative to endoscopy in measuring disease activity in CD[121].

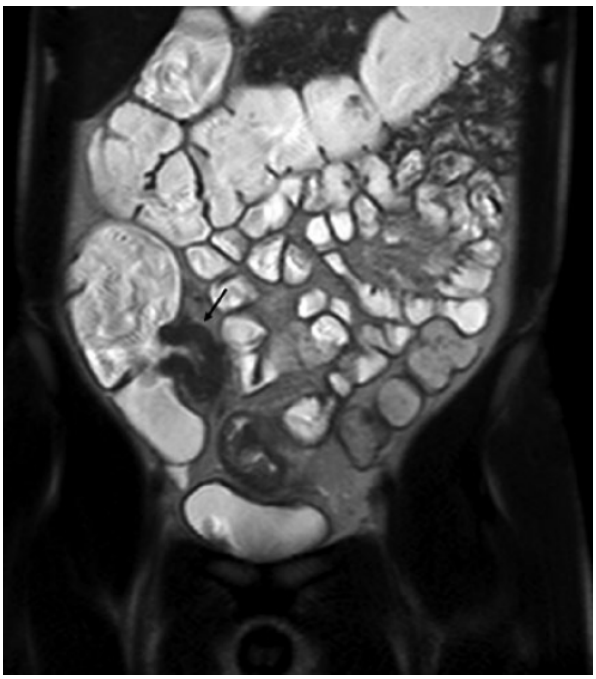

Figure 5: Example of MRE image showing wall thickening of the terminal ileum (black arrow)[129].

Magnetic Resonance Enterography Global Score (MEGS)

MEGS is another MRE-based scoring index for CD. It was developed from a previous index called Crohn's disease activity score (CDAS) which was proposed by Steward et al[130]. MEGS was developed to better define the disease extent and findings and was validated against CRP and stool calprotectin[131]. This score looked at different variables like segmental mural thickness, mural oedema, mural contrast enhancement, segmental disease length, enlarged mesenteric lymph nodes, and abscesses and fistulae[132, 133].

1.5.2 MRI and motility in CD

Patient symptoms in CD maybe related to the alteration of small bowel motility but studies are lacking in this area. Recent data have highlighted that MRI may be a reliable method in evaluating motility in CD patients. Froehlich et al[91] showed an increase in CD lesion detection rate in forty patients using cine MRE sequences compared to standard MRE imaging. They demonstrated an association of motility changes with small bowel wall changes in the affected small bowel locations in CD patients[91]. Knuesel et al[50] investigated the difference in contrast enhancement of the small bowel segments with and without active CD in thirteen patients. A significant increase in contrast uptake has been shown compared to normal segments with the use of dynamic MRE[50].

In a retrospective study on 91 patients with stricturing CD, our collaborators from University College London investigated hypomotility within strictured and prestricture bowel using the automated software described by Odille et al[57] using MRE[134]. They indicated a significant reduction in small bowel motility within the stricture compared to normal and pre-stricture bowel after measuring bowel calibre and small bowel motility in each region of interest (ROI)[134].

In CD, Menys et al[135] examined and compared the motility in the terminal ileal with histopathological severity of inflammation in 28 patients with CD. Their data suggested a negative correlation between terminal ileal motility and histopathological measure of disease activity and anatomical MRI biomarkers in CD[135]. In addition, they showed that

motility assessed using cine MRI was related to the severity of inflammation in CD[135]. Following these findings, the relationship between small bowel motility and luminal inflammation has been further investigated by another group of researchers. Elevated levels of fC and CRP in 13 patients were significantly linked to changes in small bowel motility assessed by MRI with the use of a dedicated small bowel motility software (Motasso)[136].

In a recent study investigating CD patients' response to anti-TNF α as a medical therapy, 46 patients underwent MRE before and after the treatment, MaRIA score and CRP were measured[137]. The decrease in motility was correlated to the severity of mural inflammation and was improved rapidly with successful treatment[137]. The results concluded a significant improvement in small bowel motility with the medical therapy, thus proposing that motility can be a valuable indicator of treatment response[137].

1.6 Aims and hypothesis

The literature briefly reviewed here established the dysregulation of enteroendocrine postprandial responses in CD. It also established the presence of gut dysmotility and postprandial patient's symptoms in CD. These parameters have not however been studied comprehensively in a non-invasive fashion in an un-prepared bowel. This highlights the need to investigate further the pathophysiological postprandial responses in CD.

Based on the literature we hypothesised that a test meal challenge in patients with CD will cause postprandial symptoms with upregulation of GI peptides such as CCK, GLP-1 and PYY and altered GI motility, and this project therefore aimed to:

a) Develop an MRI methodology to assess post-prandial intestinal motility (gastric emptying, small bowel motility and whole gut transit) in a single study session.

b) Use this methodology to measure intestinal motility, EEC peptide response and symptoms in the fasted and fed state in active small bowel CD and compare these to healthy volunteers (HV).

A further aim of this work was to broaden the translatability of the meal challenge to another imaging modality such as gamma scintigraphy.

1.7 Thesis outline

The work started with a literature review on MRI methods to assess gastrointestinal function[138] and a study in healthy volunteers using a soup test meal intervention[139]. This is described in Chapter 2. The study aimed to develop and optimise the MRI protocols to collect MRI parameters of motility throughout the gut. Small bowel motility was the primary outcome and other outcomes included small bowel water content, gall bladder volume, gastric volumes and whole gut transit in the fasted and postprandial state. Plasma EEC peptides and symptoms visual analogue scale (VAS) also were collected and analysed. This part of the project was used not only to set up the protocols and analysis but also to collect reference data for the following study in patients. The development and evaluation of the new analysis methods [140] is described in Chapter 3.

From the initial study and methods the work developed into the CD study described in Chapter 4. The same protocol was applied in a cohort of CD patients with active disease. The difference in small bowel motility between patients and healthy volunteers was evaluated.

A final study aimed to extend and compare the use of the meal challenge with another common imaging modality, gamma scintigraphy, to enable wider uptake of some of the methodology. This is described in the last experiemental chapter, Chapter 5.

The rationale underpinning this work is that increased knowledge of the relationship between measures of hypomotility and aversive

symptoms in CD will allow future targeting using pharmacological modulation to improve motility and patient symptoms.

2. Motility in Crohn's disease 1 (MIC1)

This work was accepted as an oral presentation at the Midlands Academy of Medical Sciences in April 2016 under the abstract entitled 'MRI study of postprandial Gastrointestinal Motility and gut peptides' and has been published in the journal Neurogastroenterology and Motility[139]. It was also accepted as an oral presentation at the European Society for Magnetic Resonance in Medicine and Biology (ESMRMB) in October 2016 and the abstract has been published on springerlink.com under the abstract entitled 'MRI study of postprandial Gastrointestinal Motility and gut peptides'. This work was presented also as a poster in the American Association of Pharmaceutical Scientists (AAPS) Annual Meeting in November 2017.

2.1 Introduction

MRI has recently come to the fore offering repeatable means to measure global and segmental motility of the small bowel[137] without the use of ionising radiation. However most MRI protocols for small bowel motility are undertaken in the fasting state with a bowel artificially distended with large amounts of contrast agent and not in the physiological state. Patient symptoms in gastrointestinal diseases commonly precipitate in the postprandial state rather than after a prolonged fast. It thus comes as a rather major limitation that most MRI motility investigations are carried out in the fasted state and in prepared bowel.

Advances in the availability of MRI scanners, increases in the speed of acquisition and growing acceptance of this method for the investigation gastrointestinal disease have driven the role of MRI in the assessment of GI pathophysiology. A number of techniques to assess motility in the fasted and prepared bowel during an MRE are now available[136] enabling rapid, reproducible and sensitive assessment of intestinal motility to complement morphological changes seen through structural imaging[55, 57].

In this study we aimed to develop a methodology to assess gastric emptying, gallbladder contraction, small bowel water content, small bowel intestinal motility, gut peptides and symptom scores in a single session using MRI in a fed and physiological state, and to collect initial reference data for the study in active CD patient.

2.2 Methodology

This study was approved by the local Ethics Committee of the University of Nottingham (H19062014) and was registered on clinicaltrials.gov with identifier NCT02717117. All participants gave informed written consent.

2.2.1 Subjects

Fifteen healthy volunteers (age 29±10 years, BMI 24±5 kg/m^2) were recruited from the local campus population. Eligibility criteria are shown below and any potential participants scoring highly on the depression scale questionnaire were excluded. Standard MRI safety exclusion

criteria were also applied. A total of 28 subjects were consented and 13 (who met exclusion criteria) were excluded.

2.2.2 Eligibility

Inclusion criteria:

- Healthy volunteer, male or female.
- Age range – 18-75 years.
- BMI – 18-30 kg/m^2.
- Able to understand English language.

Exclusion criteria:

- Any history of gastrointestinal disease (inflammatory bowel disease, smokers who are unable to refrain from midnight until after test finishes, a history of bowel resections or any gastric surgery, history of pancreatic insufficiency, thyroid disease, and/or diabetes).
- Subjects currently (or in the last three months) participating in another research project.
- Pregnancy or breastfeeding.
- MRI contraindication (e.g. pacemaker).
- Use of medication that could affect gastrointestinal function (history of usage of proton-pump inhibitor or any medication that affects gastric emptying or small bowel transit).

2.2.3 Test meal challenge

The test meal consisted of: tinned cream of chicken soup (400g) or mushroom for vegetarians (Heinz, Wigan, UK) (Figure 6). The nutrient content of this meal/100g was: energy (kcal) 51, protein 1.5 g (1.5%), carbohydrate 4.7 g (4.5%) and fat 2.9 g (2.9%). This meal challenge had been previously shown to induce reliably a GI peptide response[109,114]. All subjects finished their soup without any adverse events.

Figure 6: Image of the cream of chicken soup and cream of mushroom soup meal used in the study (400g, Heinz, Wigan, UK).

2.2.4 Study design

This study had an open label design. Participants were given 5 MRI transit marker capsules (20 mm x 7 mm) filled with 0.4 mL 15 μM Gadoteric acid, an MRI contrast agent, to take home. They were instructed to swallow these 24 h before attending the unit for their study day and undergoing the baseline MRI scans as previously described[141]. They were asked to fill in a questionnaire to ensure adherence to the study day restrictions.

The subjects were asked to fast from 2000 hrs the previous evening and to avoid alcohol, caffeine, strenuous exercise and any medication that could affect gut function for 18 h before the experiment.

On the day of the scan, the participants attended at the 1.5T Philips Achieva MRI scanner (Philips Healthcare, Best, the Netherlands) at the Sir Peter Mansfield Imaging Centre (SPMIC) unit at the University Park Campus, University of Nottingham (Figure 7). Participants were cannulated intravenously by a research nurse on arrival and underwent a baseline fasting scan (defined at t = -20 min time point), together with a fasting baseline blood sample. A 60 min interval between cannulation and acquisition of baseline measurements was introduced to allow the subjects to normalise to a baseline calm physiological state. Following this, they were asked to consume all their test meal within a maximum time of 20 min then the subjects underwent a first immediate postprandial scan (defined as t = 0 min).

This was followed by data collection (MRI, questionnaire data and 10 mL blood samples) time points every 15 min for the first 60 min and then every 30 min up to 270 min. Blood samples were collected by a research nurse. The first 2 mL of each sample was discarded to avoid contamination with the saline used to maintain patency. Blood was collected into vacutainer tubes containing 0.325 mL of aprotinin, (Trasylol, Bayer) (Dorset, England).

At each time point, the MRI procedures took approximately 15 minutes, including subject positioning on the scanner bed, setup of the

MRI scans and data collection. For the first 60 minutes the subjects were kept inside the scanner. After this the subjects were kept sitting upright in a quiet lounge next to the scanner for the rest of the study day except for the subsequent MRI acquisitions. At each time point, they filled a 100 mm VAS symptoms questionnaire scoring their feeling of fullness, bloating, distension, abdominal pain/discomfort and nausea[109]. The VAS anchors were from 'not' to 'extremely' (appendix A). At the end of the 270 min the participants were discharged.

Figure 7: The 1.5T Philips Achieva MRI scanner at the Sir Peter Mansfield Imaging Centre (SPMIC) at the University Park Campus, University of Nottingham.

2.2.5 MRI protocol

MRI scanning was carried out supine. Participants were scanned using a range of sequences. At each time point scans were acquired to assess

gastric volume[142], gall bladder volume[143], small bowel water content[144] and small bowel motility[55]. In addition, at baseline the position of the MRI marker capsules was determined to measure whole gut transit time[141].

Gastric emptying was assessed using a balanced gradient echo sequence (bTFE) acquiring 50 contiguous axial slices with reconstructed in-plane resolution 2.0x1.77 mm^2, slice thickness 5 mm and 0 mm slice gap, echo time (TE)=1.5 ms, repetition time (TR)=3.0 ms, flip angle 80º, SENSitivity Encoding (SENSE) 2.0 within one breath hold of ~16 s. This imaging sequence yields good contrast between the stomach contents and other abdominal organs. Samples containing mobile water appear brighter than viscous samples with reduced water content and mobility.

The content of apparent freely mobile water in the small bowel was assessed as previously described[144] using a single-shot fast spin echo sequence acquiring 24 contiguous coronal slices with reconstructed in-plane resolution 0.78x0.78mm^2, slice thickness 7 mm and slice gap 0 mm, TE=320 ms, TR=8000 ms, spectral presaturation with inversion recovery (SPIR) fat saturation within one breath hold of 24 s. This sequence yields high-intensity signal from areas with freely mobile fluid and low signal from poorly mobile or bound water and all other body tissues.

Small bowel motility was assessed using a single slice cine MRI acquisition set at six contiguous parallel coronal planes through the small bowel (to capture all the bowel loops). Data were acquired using a bTFE sequence with reconstructed in-plane resolution 1.49x1.7 mm^2, TE=1.52

ms, TR=3.0 ms, flip angle 80º, SENSE 2.0 at a repetition time of 1 image per second for a duration of 1 minute for each plane with gentle free breathing throughout the acquisition.

Whole gut transit was assessed using two different Coronal 3D T1 weighted turbo field echo (TFE) sequences. Each of these was acquired at two stations with a 30 mm overlap. Firstly, a T1 weighted 3D TFE sequence with SPectral Attenuated Inversion Recovery (SPAIR) fat saturation was acquired. Sequence parameters for each station were as follows: TE=1.9 ms, TR=4.0 ms, flip angle= 10°, field of view= 250x398x160 mm^3. Acquired resolution 2.3x2.3x5 mm^3, reconstructed to 1.4x1.4x2.5 mm^3, with a 288x288 reconstructed matrix. 64 slices were acquired with a half-scan factor of 0.7 in the phase direction and 0.85 in the slice direction in a 23 s breath hold. The second sequence, another T1-weighted 3D TFE sequence with a 2-echo readout and mDIXON (multi-point Dixon method) reconstruction of the water only images[145] was acquired with increased resolution using SENSE. Thirty six maximum intensity projection (MIP) images were generated from this data to create a 3D view of the colon to aid in defining the position of the capsules. Imaging parameters at each station were as follows: TE1/TE2= 1.4/2.5 ms, TR= 3.8 ms, flip angle= 10°, field of view= 250x371x200 mm^3. Acquired resolution 1.8x1.8x3.6 mm^3, reconstructed to 1.0x1.0x1.8 mm^3, with a 384x384 reconstructed matrix. 111 slices were acquired with a SENSE factor of 2.0 in the phase direction in a 22 s breath hold.

The gall bladder volume was assessed at baseline at every acquisition time point up to 60 min postprandially[143]. This was carried out using the same images as for the gastric volumes as previously described[142].

2.2.6 Plasma collection and peptides assays analysis

On the morning of the test, 0.325 mL of aprotinin was added to vacutainer tubes (BD-361017, BD Diagnostics, Oxford) by a lab technician for collection for each time point aiming for a final volume of 6.5 mL. Fasting 10 mL blood sample was drawn in a syringe by a research nurse and the correct amount transferred to the tubes. After the test meal, data were acquired every 15 min for the first 60 min and every 30 min thereafter to 270 min. Twelve samples were taken totalling 120 mL. Samples were centrifuged at 3000 rpm for 10 min and stored temporarily on ice[109] before being stored at -80°C. Plasma peptides (total GLP-1, total PYY) were analysed through enzyme-linked immunosorbent assay (ELISA) techniques (Millipore, UK) as previously shown[109]. The concentrations of serum CCK were measured by radioimmunoassay (RIA) (Euro Diagnostic Products, Sweden) as previously shown[146]. The peptides were analysed by the laboratory technicians in the Biomedical Research Centre (BRC).

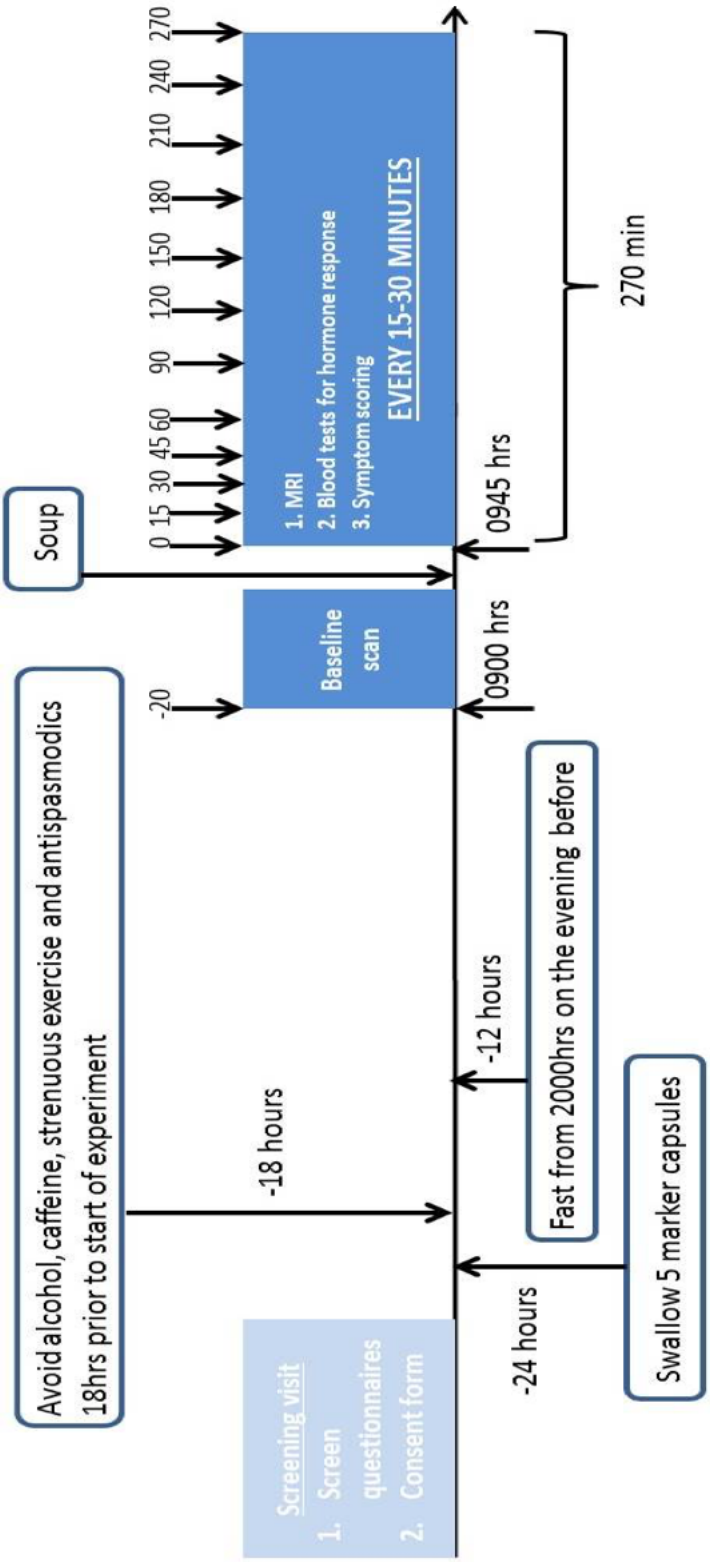

Figure 8: Diagram of the study protocol followed in MIC1 study.

2.2.7 Data analysis

Motility assessment

The small bowel motility assessment was carried out in collaboration with University College London (UCL) and Motilent Ltd. Motilent is a medical imaging technology company that offers imaging analysis services for the quantitative investigations of the GI tract. All anonymised dynamic data (Digital Imaging and Communications in Medicine (DICOM) file format) were sent to Motilent and processed with Dual Registration of Abdominal Motion (DRAM) (Motilent, Ford, UK). DRAM first removes respiratory motion[147] before applying the optic flow registration as previously described by Odille et al[57] to capture local deformation caused by bowel wall motion and model intensity changes caused by luminal flow. Registration results were further analysed using a customised graphical user interface written in MATLAB (MathWorks, Natick, MA, USA) by Dr. Caroline Hoad (Figure 9).

Published methods of assessing small bowel motility have been applied in MRE[55, 57]. MRE involves artificially inflating the bowel lumen which stimulates wall movement and allows the movement of the bowel wall to be tracked during the registration process. The aim of our project was to measure postprandial motility in a physiological rather than an artificially distended state. Since postprandial small bowel motility does not produce the same motion or appearance of the lumen as in MRE, a different approach to assessing the small bowel motility was required. The technique used in this study quantified the motility of the bowel using

the pixel signal changes through the time series, within a defined ROI placed over the small bowel loops. The metric was calculated as follows: For each pixel in the registered dataset, a power spectrum of the intensity changes across the time series was calculated and then summed across all frequencies. This metric was termed the total power, and reflected bowel motility, both in terms of segmental oscillations and bolus movement of contents, typically seen postprandially[148].

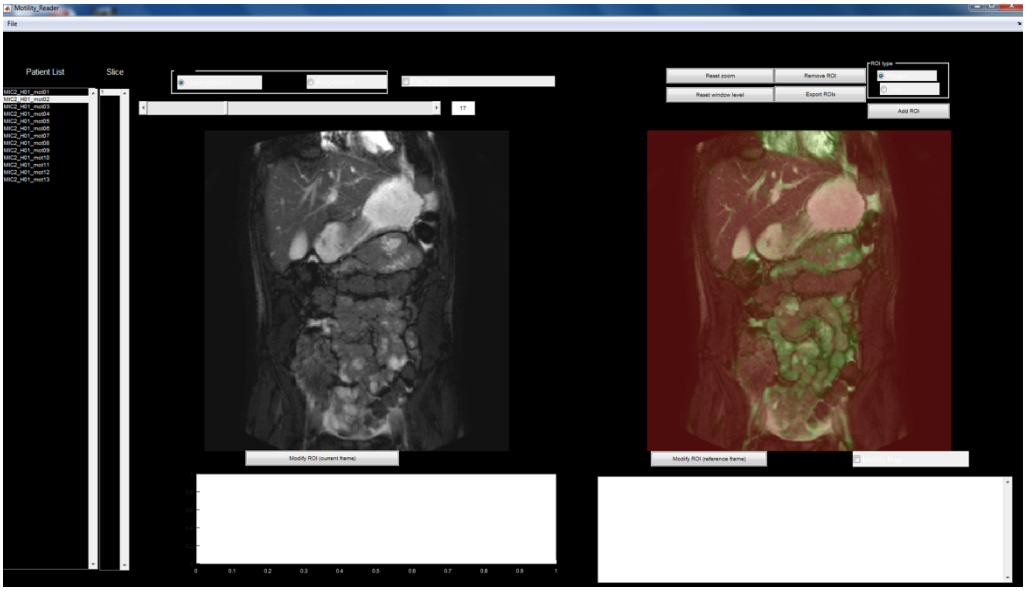

Figure 9: A screenshot of the motility assessment program written by Dr. Caroline Hoad in MATLAB (MathWorks, Natick, MA, USA) using a customised graphical user interface.

Two independent observers (AK, CH) drew ROIs manually over all the loops of the small bowel in all the slices for each imaging datasets (Figure 10). From these ROIs the mean total power across all small bowel pixels was calculated. A larger total power motility index represents higher small bowel motility.

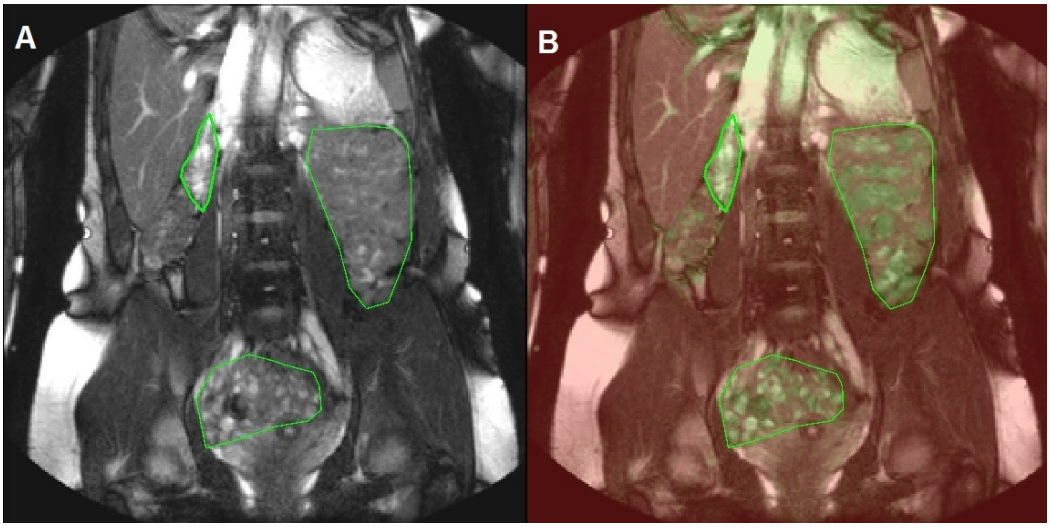

Figure 10: Example of a reference image (A) and a motility map (B) for a healthy volunteer. ROIs were placed on the reference image to include small bowel loops only.

Small bowel water content (SBWC)

The small bowel water content (SBWC) was measured as previously described[144], using in house software written by Dr. Caroline Hoad in IDL® (Research Systems Inc. Boulder, Colorado, USA. Briefly, this method assumed that any pixel with signal intensity above a calculated threshold in the heavily T2-weighted coronal images is filled with freely mobile water. ROIs were drawn manually around the small bowel loops and structures such as blood vessels, bladder, stomach and gall bladder were excluded (Figure 11).

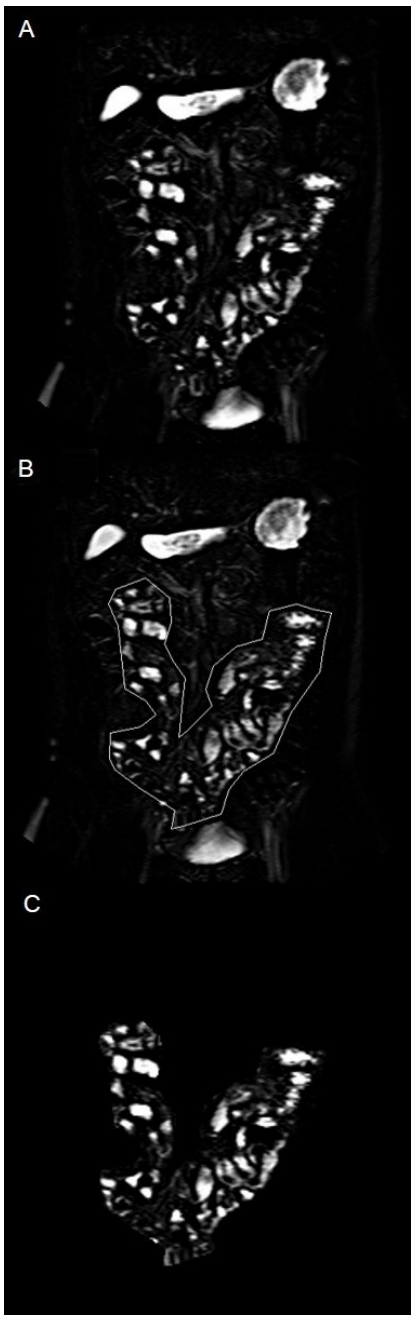

Figure 11: Examples of use of the SBWC analysis software. Images were acquired using magnetic resonance cholangiopancreatography (MRCP) sequence. (A) Small bowel loops filled with water before excluding the other structures. (B) ROIs drawn around the small bowel loops only. (C) Other structures were excluded leaving the small bowel loops only.

Gall bladder and gastric volumes

The gall bladder and gastric volumes were quantified using in house software written by Dr. Caroline Hoad in IDL® (Research Systems Inc. Boulder, Colorado, USA). This method uses a semi-automatic technique to define the content of the stomach and gas within the stomach on each image slice[142] (Figure 12). Total gastric volume was calculated as the sum of the stomach contents and any gas. Postprandial gastric content volumes were fitted to a 5 parameter equation[149] to model the emptying process and allow the calculation of the gastric half-emptying time ($T_{1/2}$).

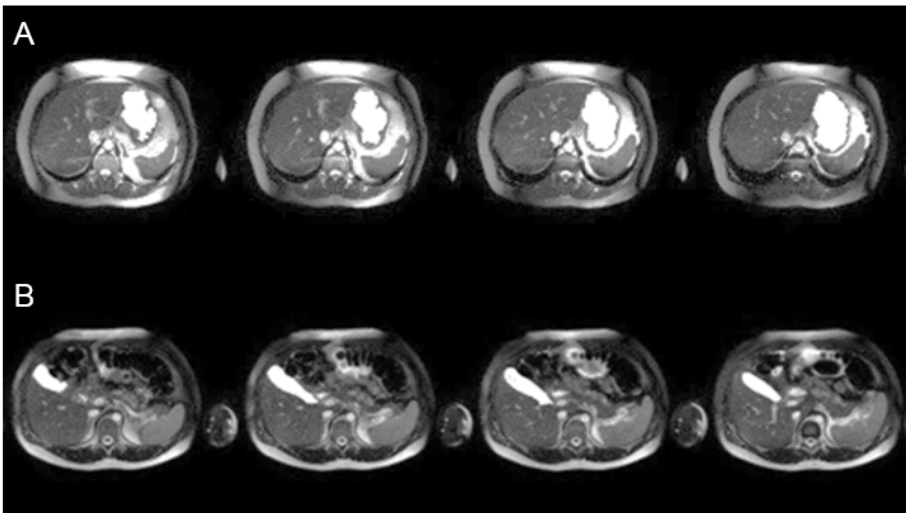

Figure 12: Illustrations of the processing analysis algorithm for the measurement of (A) gastric volumes and (B) gallbladder volumes.

Whole gut transit (WGT)

Whole gut transit was assessed as previously described[141]. From the two sets of MRI images a transit score was calculated by sub-dividing the bowel into eight sections and each capsule was scored according to its

position in the colon at 24 hr (Figure 13). A weighting factor was calculated for each capsule depending on the difference of the capsule score from the median capsule score as described previously[141].

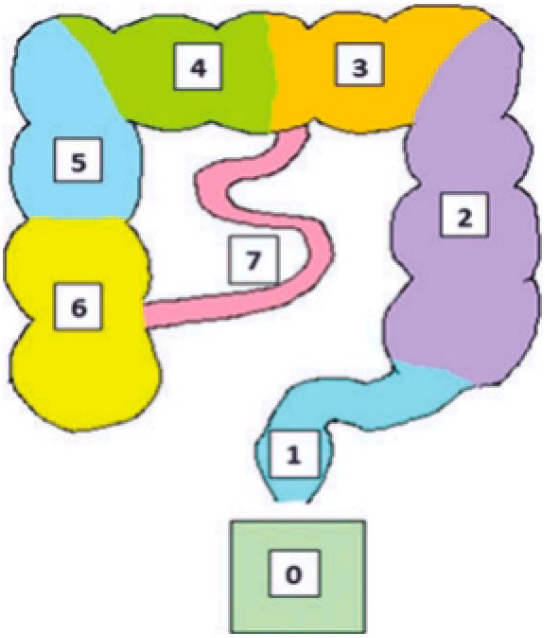

Figure 13: Diagram illustrating the segmented colon used to score the MRI capsules according to their location at 24 hr[141]. 0 = not found, 1 = sigmoid and rectum, 2 = descending colon, 3= left transverse colon, 4 = right transverse colon, 5 = upper ascending colon, 6 = lower ascending colon, 7 = small bowel.

Visual analogue scale (VAS)

Symptoms regarding appetite, satiety and abdominal pain were scored at each time point on previously used questionnaires[109] (appendix A).

2.2.8 Statistical analyses

Due to the pilot nature of this study, it was not possible to calculate a sample size, but similar studies done by our group have used similar-sized cohorts[109, 143, 150]. The data are expressed as mean±standard error of the mean (SEM). Normality of the data were assessed using Shapiro–Wilk's test. One-way analysis of variance (ANOVA) was used to assess the significance of differences. When the analysis of variance was significant, post hoc test assessments of the individual time points were performed using the Dunnett's (for parametric data) or Dunn's (for nonparametric data) test to account for multiple comparisons. All statistical analyses were performed using GraphPad Prism 7.01 (La Jolla, USA). A p-value less than 0.05 was considered statistically significant.

2.3 Results

All fifteen healthy volunteers (9 female, 6 male, age 29.3±2.7 years and BMI 24±1.3 Kg/m^2) completed the study and tolerated the experimental procedures well without any adverse event.

Small bowel motility

From Figure 14 it can be seen that small bowel motility index rose significantly ($p<0.0001$) throughout the study time with a significant increase ($p<0.05$) at t= 0 min and t=15 min when compared to fasting motility index. The total power value of small bowel motility increased

significantly from fasting 108.9±14.7 arbitrary units (a.u.) to a maximum of 209.7±19.9 a.u. immediately after feeding (t=0 min, p<0.0001) and then gradually decreased back to around baseline (121.3±15.9 a.u.) in 90 minutes. The motility index rose again at 120 min to 149.2±119.4 a.u. and decreased back again to 95.6±11.9 a.u. at 240 min. Figure 15 shows an example of a motility maps in fasted and fed state of one healthy subject generated by the used motility software.

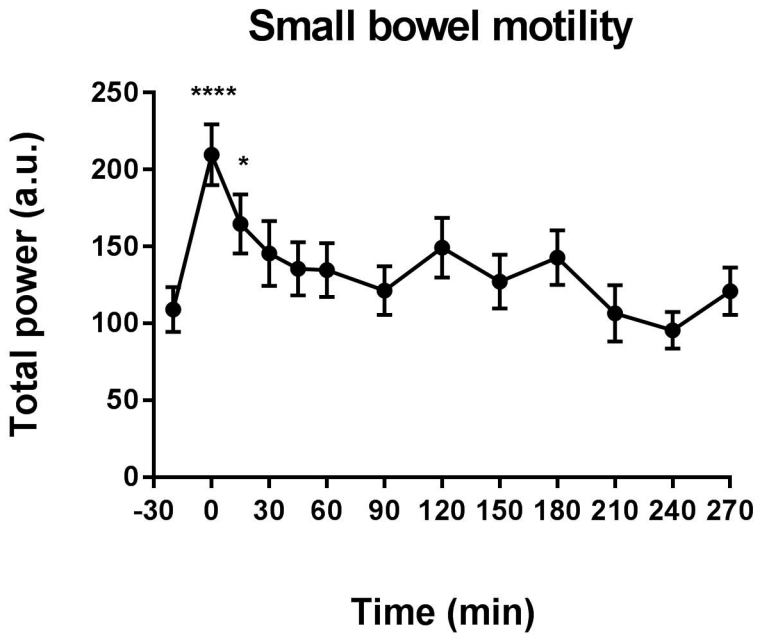

Figure 14: Time courses of the small bowel motility. Data are mean ± SEM from n=15 healthy volunteers. **** p<0.0001 and *p<0.05 versus fasting value.

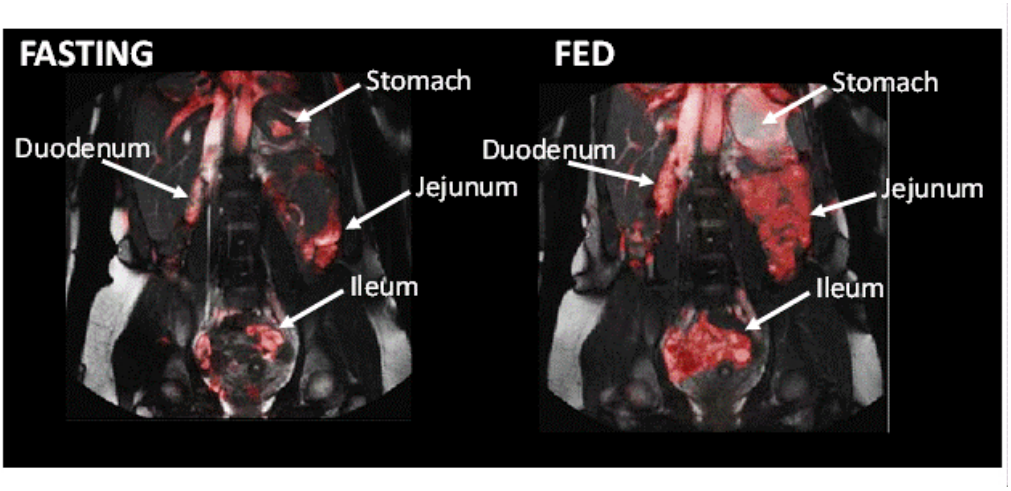

Figure 15: Examples of fasting and fed state small bowel motility maps respectively for one participant using the total power spectrum. Red colour represents the areas with higher motility.

Gallbladder volumes

The changes in gallbladder volumes with time are shown in Figure 16. The gallbladder volumes significantly decreased ($p<0.0001$) throughout the postprandial time points compared to the fasting volume. The meal induced a moderate and significant postprandial decrease in the gall bladder volume from 19±2 mL (mean±SEM) at baseline to 12±2 mL immediately after feeding t=0 min ($p<0.0001$).

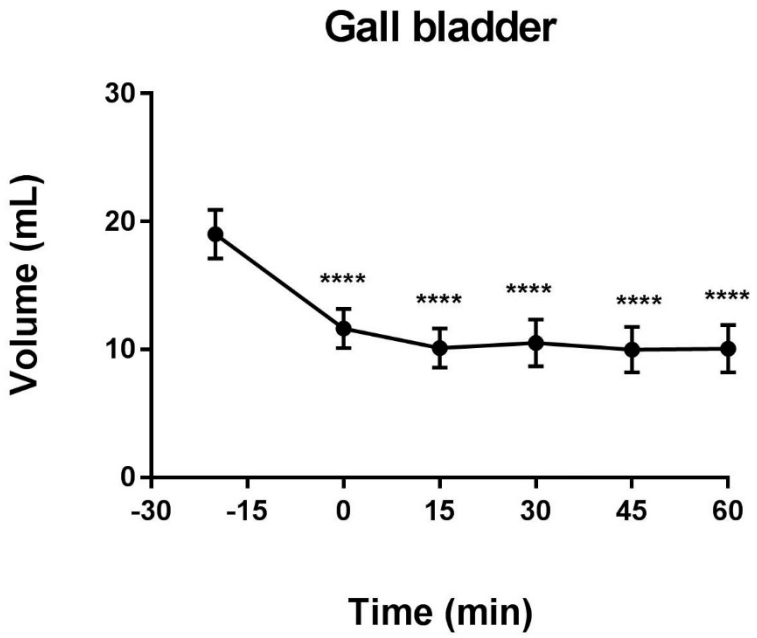

Figure 16: Time courses of the gallbladder volume. Data are mean ± SEM from n=15 healthy volunteers. **** p<0.0001 versus fasting value.

Gastric volumes

The baseline gastric volumes showed a small amount of resting gastric juice of 26±7 mL. Gastric content volumes rose significantly upon feeding to 418±17 mL at t=0 min ($p<0.0001$) after which the stomach volume declined and went back to baseline (37±7 mL) at 150 min (Figure 17). The postprandial volumes were significantly higher than baseline ($p<0.05$) at all time points except at t=150 min. The average time to empty half of the stomach contents ($T_{1/2}$) was 46±5 min.

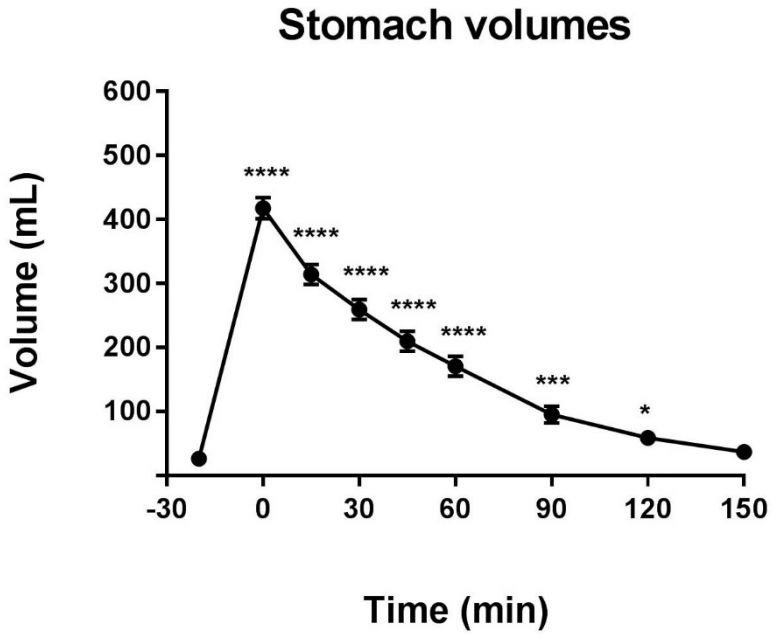

Figure 17: Time course of the stomach content volumes. Data are mean ± SEM from n=15 healthy volunteers. **** p<0.0001, ***p<0.001 and *p<0.05 versus fasting value.

Small bowel water content

The data in Figure 18 show a relatively small amount of fasting (t= -20 min) small bowel water content of 39±2 mL. The test meal induced a significant ($p<0.05$) change in small bowel water content across the different time points. Immediately after the soup meal was ingested, the small bowel water content increased to a maximum of 51±2 mL ($p<0.05$) at 15 min. The volume decreased towards baseline (38±2 mL) at 60 min after which a second, higher peak at 180 min is clearly seen with a volume of 65±3 mL.

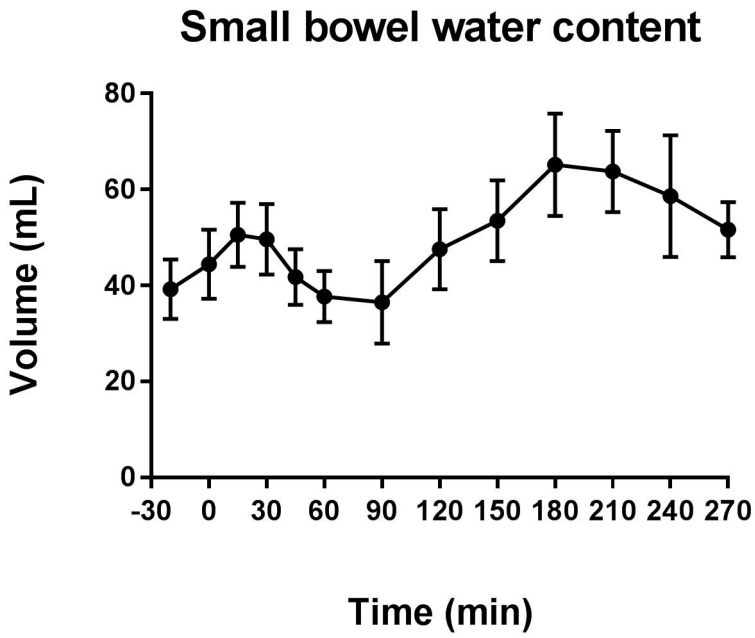

Figure 18: Time courses of the small bowel water contents. Data are mean ± SEM from n=15 healthy volunteers.

Whole gut transit (WGT)

The median average weighted position score (WAPS) of the MRI capsules was 1.0 (0-3.8). As described previously[141], the WAPS at 24 hr was converted to WGT in hours, giving a median whole gut transit time of 33 h.

Total GLP-1

Ingestion of the meal induced significant changes in plasma measures of total GLP-1 ($p<0.01$) (Figure 19). The mean GLP-1 data from healthy volunteers showed a postprandial peak from fasting volume of 15±3 µg/mL to 22±4 µg/mL (t=0 min). The GLP-1 levels dropped (12±3 µg/mL)

after 30 minutes and remained around baseline levels for the duration of the study time points.

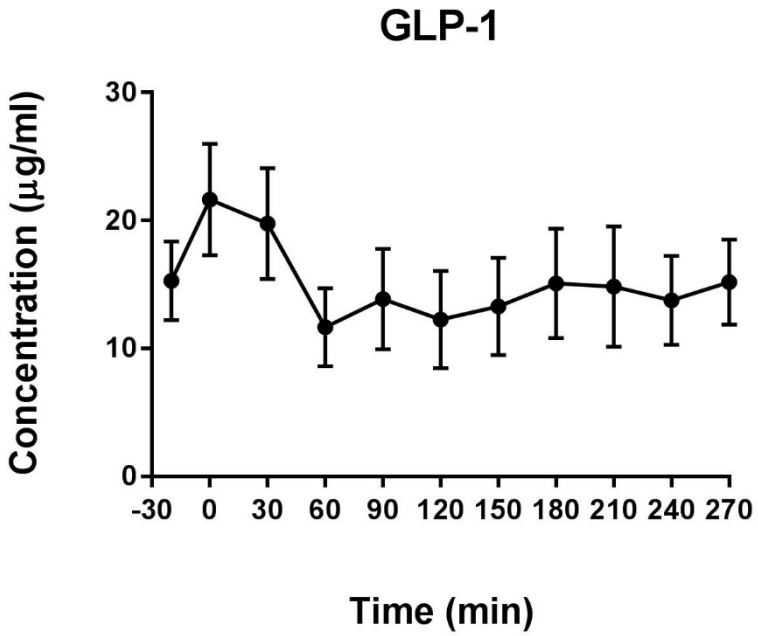

Figure 19 Time courses of the GLP-1 levels. Data are mean ± SEM from n=15 healthy volunteers.

PYY

PYY levels increased significantly ($p<0.001$) from fasting 98±10 pg/mL to 149±14 pg/mL at 30 min postprandially in healthy volunteers (Figure 20). PYY returned to baseline after 2 hours postprandially and later dropped even further to reach 71±13 pg/mL at 270 min. A significant increase ($p<0.05$) was noted from t=0 min to t=90 min compared to fasting levels.

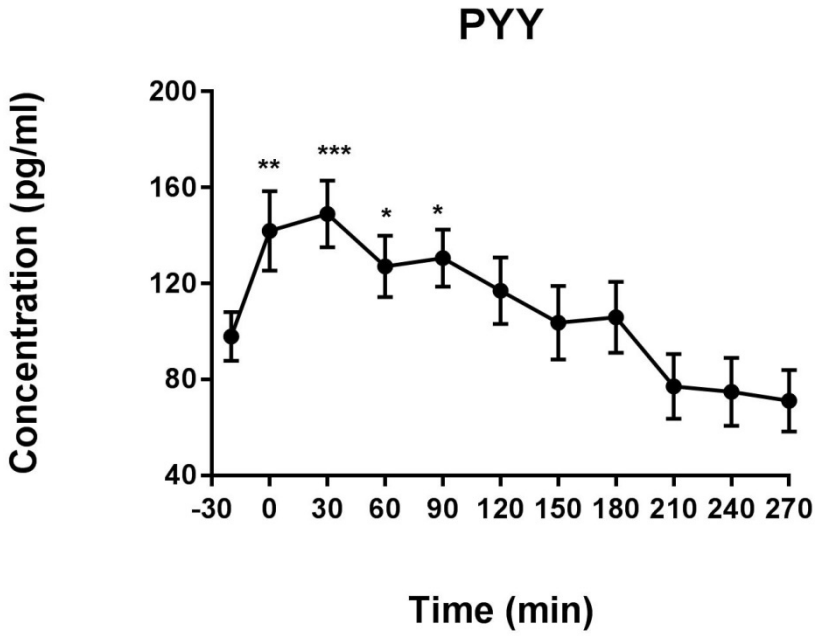

Figure 20: Time courses of the PYY levels. Data are mean ± SEM from n=15 healthy volunteers. *** p<0.001, ** p<0.01 and *p<0.05 versus fasting value.

CCK

The plasma CCK concentrations (Figure 21) showed a significant increase ($p<0.05$) immediately after feeding to 60 min in comparison to fasting concentrations. The CCK levels increased significantly ($p<0.01$) from fasting 0.40±0.06 pmol/mL to 0.94±0.1 pmol/mL at t=30 min and then steadily decreased after 60 min to reach baseline (0.4±0.01 pmol/mL) for the rest of the study day.

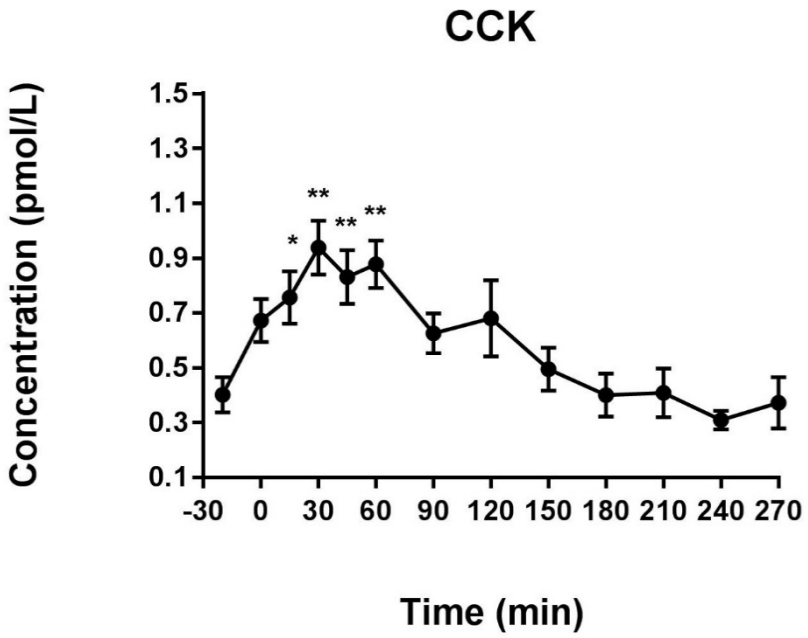

Figure 21: Time courses of the CCK plasma levels. Data are mean ± SEM from n=15 healthy volunteers. **p<0.01 and *p<0.05 versus fasting value.

Symptom VAS data

The VAS score for fullness increased from 9±5 mm to 44±5 mm at 0 min and 41±6 mm at 30 min postprandially ($p<0.001$). This increase returned to baseline thereafter. Bloating, distention, pain and nausea scores did not change significantly compared to fasting scores (Table 3).

Time point (min)	Fullness	Bloating	Distention	Pain/ discomfort	Nausea/ sickness
-20	9±5	7±3	4±2	1±1	6±4
0	44±5**	9±3	4±2	0±0	2±2
15	41±6*	10±3	5±3	0±0	2±2
30	41±6**	6±3	3±2	0±0	1±1
45	37±7	7±3	3±2	0±0	1±1
60	31±7	5±3	2±2	0±0	1±1
90	26±6	5±3	3±3	0±0	0±0
120	20±6	7±4	3±2	0±0	1±1
150	13±4	4±2	1±1	0±0	0±0
180	12±5	2±1	1±1	0±0	0±0
210	7±4	1±1	1±1	0±0	0±0
240	5±2	0±0	1±1	0±0	0±0
270	3±1	0±0	0±0	0±0	0±0

Table 3: Visual analogue scale (100 mm VAS scores) **p<0.001 and *p<0.05 versus fasting value.

2.4 Discussion

To our knowledge, this is the first study to measure and quantify fasting and postprandial small bowel motility in an unprepared small bowel, without artificially distending the bowel using large volumes of oral contrast media. The soup meal challenge was effective in inducing

multiple physiological end-points. The measured physiological parameters were within the normal range for a healthy cohort as shown previously[143, 150, 151]. The meal was a good stimulus for GLP-1, PYY and CCK because of its carbohydrate (4.5%) and fat (2.9%) content.

In this work, the motility of the unprepared small bowel was measured in response to a nutrient meal. Mean small bowel motility peaked immediately postprandially. This early increase may be due to the fact that meal bolus move rapidly through the duodenum and upper jejunum. Additionally, a rapid gastro-ileal reflex would facilitate emptying of the distal small bowel content into the ascending colon. At approximately 90 minutes and when the emptying of the stomach has almost completed, the small bowel motility decreased back to baseline. This decrease is matched with maximal plasma levels of GLP-1 and PYY[152], which have previously been associated with delayed small bowel transit[153]. Another peak in mean small bowel motility was seen at 120 min. There may be various possible explanations for this change. Between 90 and 120 min, mean plasma levels of PYY and GLP-1 dropped back to around baseline levels hence minimising their effect on small bowel motility. At a similar time period the small bowel water content rose likely due to an increase in intestinal and pancreatico-biliary secretions. This pronounced bowel distention could be a stimulus itself for smooth muscle contraction[154] and might cause the observed increase in the measured small bowel motility.

Gastric emptying was similar to our previous observations whereby following a solid meal with a drink, there was an initial rapid gastric emptying in the first 0 to 75 min, followed by slower phase of emptying. There was an immediate postprandial increase in mean reported fullness VAS fasting state with a decline to baseline within ~ 180 min. A bimodal peak in small bowel water content was observed in the postprandial state up to 270 min. The subjects' mean fasting baseline small bowel water content reached the first peak at 15 min with the volume then decreased towards baseline at 60 min in an early 'gastric phase' presenting the gastric emptying phase, after which a second peak at 180 min of the later 'intestinal phase'[143] was clearly seen. The early drop observed is possibly representative of the absorption of water and the available nutrients. This net absorption together with an activated postprandial gastro-ileal reflex resulting in emptying the contents of the distal ileum into the ascending colon, which leads to a decrease in small bowel water content. The increase in pancreatico-biliary and enterocyte secretion might be the reason behind the second peak or the intestinal phase[155].

In response to the carbohydrate content within the meal, the plasma levels of GLP-1 increased rapidly. The total carbohydrate load is one of the main factors governing gastric emptying[156] and the absorption of simple digestible carbohydrates through the proximal duodenum resulted in an increase in GLP-1 secretion and a delay in gastric emptying[25]. The level of CCK usually increases 10-30 minutes after food

intake[12] as was confirmed in our results. Gall bladder contracted within 20 min of meal ingestion which would explain the 50% decrease in gall bladder volume.

In this study, the whole gut transit time in a healthy population was a median of 33 hours. This is similar to our previous reports of 31 hours using the same methodology in a similar population[141].

There were limitations in this study. The meal used was small in both volume and energy, hence providing a submaximal stimulus to the GI tract. The reason behind the choice of this meal is due to its known effects on GI peptide response[109] and also because it could be tolerated in patient population. Moreover, it could be prepared and administered easily and in a timely fashion in a clinical setting.

In this study we have established an unprecedented platform for measuring postprandial small bowel motility in human subjects using MRI, and compared this to known physiological GI peptide responses and symptoms. This work shows that using such methodology is feasible. The length of our study is such that it may be difficult to implement in a busy clinical setting as is, though one could choose to scan only during the early postprandial time where the response is maximal. Presently intestinal motility had only been measured in the fasting state or on a bowel prepared with large volumes of luminal contrast, which may be less relevant to some of the post prandial symptoms experienced by patients. Mapping out such post-prandial physiological changes in

disease groups will help us to better understand the cross-link between symptoms and altered gastrointestinal physiology.

3. The new analysis technique

3.1 Introduction

In this work, a new image processing technique was used to generate motility data based on power spectrum analysis (total power) of voxel signal changes with time after image registration. This is because most investigations of bowel function are generally undertaken in the fasted state with the bowel prepared by large volumes of contrast media, but feeding often precipitates symptoms in GI diseases. Therefore studying them in the unprepared physiological state is interesting and valuable. This work has been published in the journal Neurogastroenterology and Motility[140].

On MRI the unprepared small bowel has a very different appearance compared to the prepared bowel required for MRE (Figure 22). In MRE, the bowel is filled with luminal contrast media to distend the walls which may itself disturb the underlying physiology. Moreover, in the prepared bowel there is a clear definition of the bowel walls and peristaltic motion is easily visible while in the unprepared bowel, the bowel wall is not always visible. Therefore a different approach for quantifying the motility of the unprepared small bowel was developed, based on the change in signal intensity between time points, within a defined ROI placed over the small bowel loops.

Reproducibility of the motility measurements was assessed using the 15 healthy volunteers' data from the MIC1 study. In addition, intra

and inter-observer variability were assessed. The technique's sensitivity to changing motility was tested in response to feeding using two motility analysis techniques, the total power and the standard deviation of the Jacobian (SD_{JAC}), a previous published metric for motility[55].

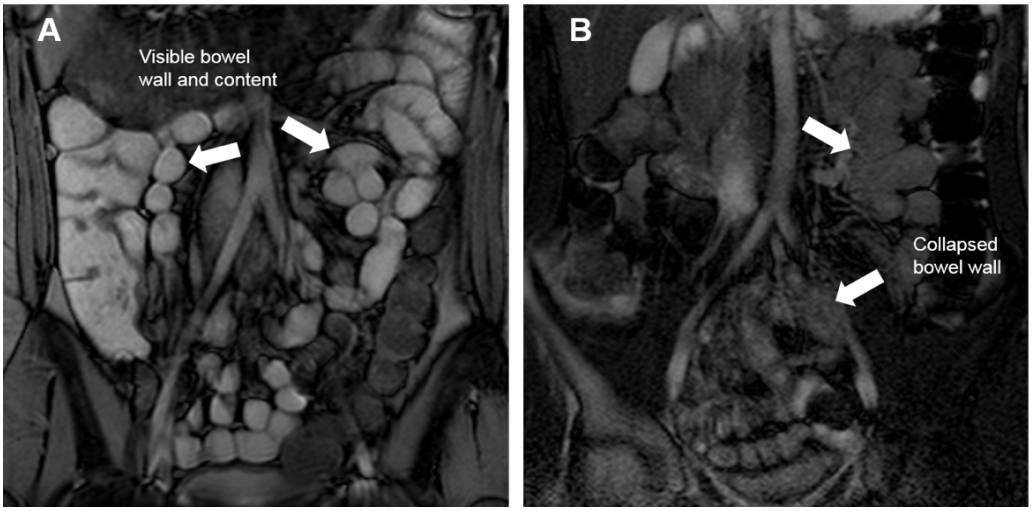

Figure 22: Illustration of the difference between (A) a prepared bowel which is distended and with clear definition of the bowel wall and bright luminal contents and (B) an unprepared bowel, more collapsed and with less visible bowel wall.

3.2 Methodology

3.2.1 Motility assessment

Inter-observer variability

Two observers, one experienced (Caroline Hoad, over 10 years) in viewing small bowel MRI data and one less experienced (Asseel Khalaf, less than 2 years) drew regions of interest around all the visible small

bowel segments across the 6 coronal slices acquired for all 15 subjects scanned at all time points pre and post-test meal.

Intra-observer variability

The same two observers drew regions around the visible small bowel segments from a subset of six subjects (chosen to have different body composition: 3 normal BMI (22.3, 22.9 22.9 kg/m^2) and 3 high BMI (30.6, 27.1, 29.1 kg/m^2) analysed twice. The changing body composition resulted in images with very different contrast of the edges of the small bowel loops and therefore represented a wide range of tissue contrast that would be seen across all subjects. Regions were defined by drawing the ROIs to include only the visible small bowel loops ignoring intra-abdominal visceral fat and other tissues; the regions were defined twice on the images with at least one month interval between observations.

Changing motility in response to feeding using two motility metrics

The strength of correlation between two motility analysis techniques was examined using the total power and the SD_{JAC}. SD_{JAC} looks at the geometric changes from image registration and is currently used for small bowel motility in the prepared bowel. In addition, the change in both metrics with feeding was determined by looking at the mean change in the metric between the fasted (t= -20min) and the immediately postprandial data (t= 0 min).

3.2.2 Statistical analysis

All statistical analysis was carried out using Graph Pad Prism 7.01 (La Jolla, USA). All data were tested for normality using Shapiro–Wilk's test. Inter-observer variability was investigated by using a Bland-Altman plot[157] to determine the 95% confidence limits of agreement. The correlation between observers and intra-observer variability were measured using the Intra-class correlation coefficient (ICC). The Pearson correlation coefficient was used to measure the strength of correlation between the measurement of motility using the total power and the SD_{JAC} for the fasting and immediately postprandial data sets.

3.3 Results

Visualisation of high motility regions

Example total power spectrum maps of fasting and postprandial data for one subject are shown in Figure 23. Example maps of SD_{JAC} are also shown for comparison. The total power spectrum maps show lower values in regions of known low motility (e.g. liver) compared to the SD_{JAC} maps.

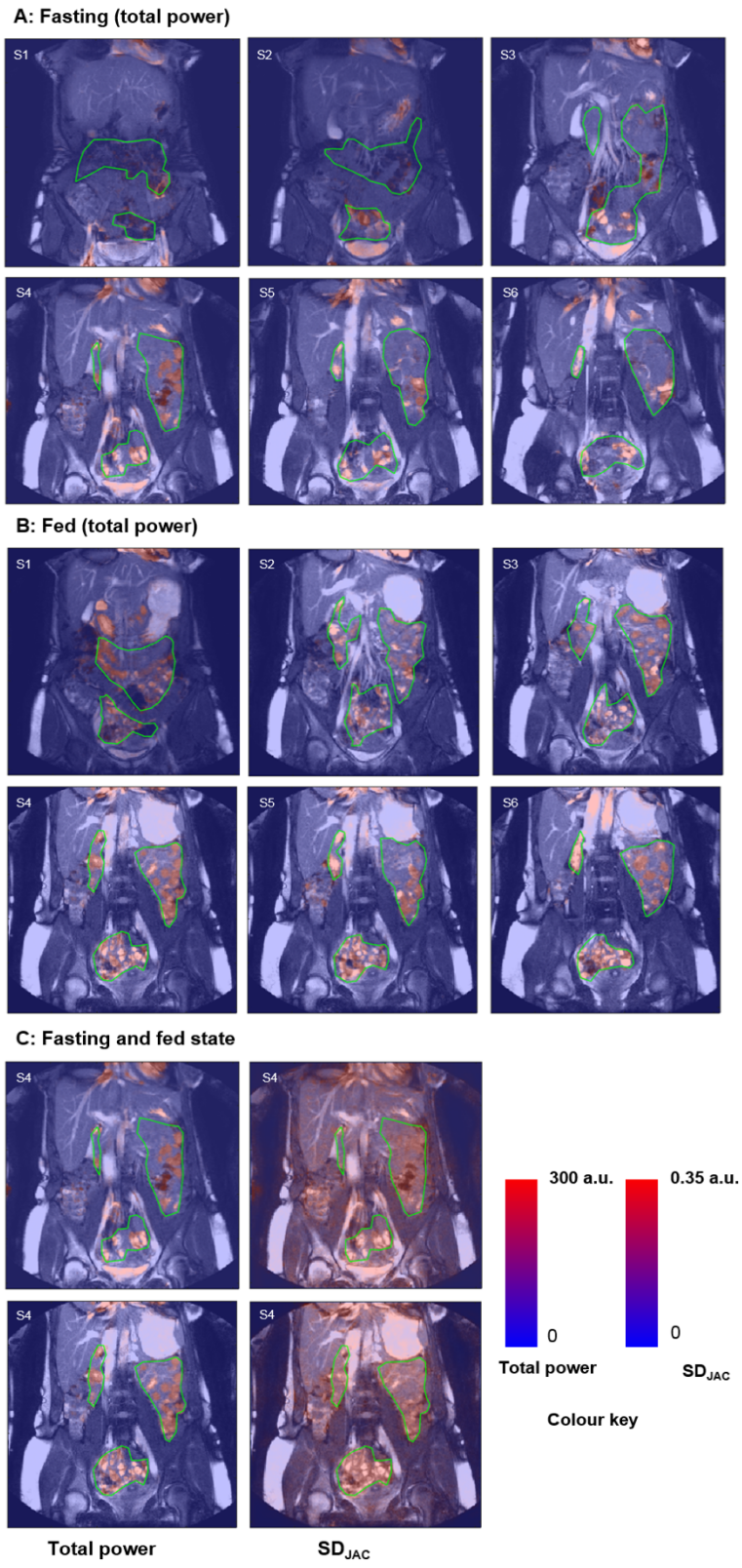

Figure 23: Example of motility maps generated by the software for a single volunteer across the 6 slices acquired, visualising the areas of high

motility. A and B illustrate the fasting and the fed state motility maps. C Represents the different motility maps generated by the total power spectrum and SD_{JAC} motility parameters. S: slice number. Regions of small bowel have been highlighted on the images.

Inter-observer variability of small bowel motility

The variation in both total power and SD_{JAC} across different time points averaged over all healthy volunteers, at each time point, and covering all regions of small bowel from the 6 slices, measured by each observer is shown in Figure 24A. This graph shows low measured motility at baseline in the fasting state followed by a significant increase postprandially which then persists for the majority of the imaging period. The degree of correlation between two observers was assessed using the ICC to be 0.979 and $p<0.0001$, $n=195$ (Figure 24B). Inter-observer variability was assessed using the Bland Altman plot (Figure 24C) which showed a mean difference of 8.5 a.u. between small bowel motility measurements, with a 95% confidence interval of -28.9 to 45.9 a.u. as indicated by the upper and lower dotted lines.

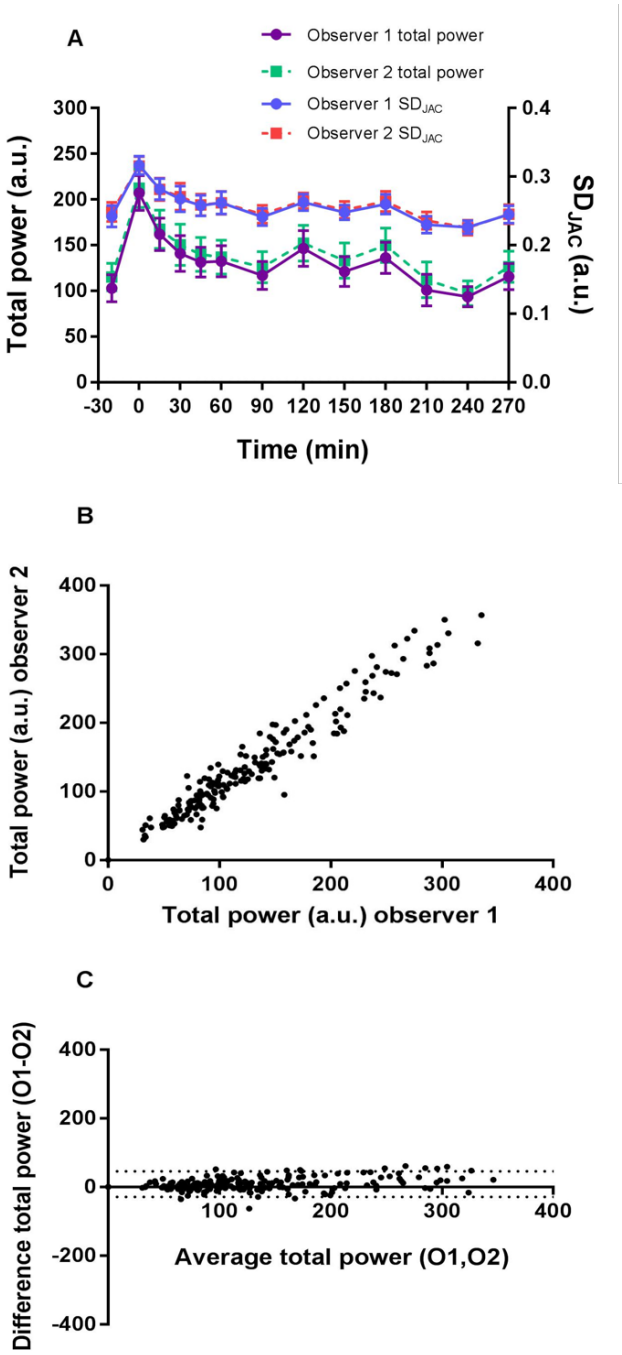

Figure 24: A. plot of the small bowel motility assessed with total power and SD_{JAC} across time points, measured by two observers. B. Correlation of inter-observer data for total power spectrum data. C. Bland–Altman plot showing the 95% limits of agreement in total power results. (Mean difference: thick solid line, mean ±2 standard deviations: dotted lines).

Intra-observer variability of small bowel motility

Correlation between the two analyses for the total power spectrum performed by each observer was also assessed using the ICC and Bland-Altman limits of agreement (Table 4), showing good agreement between the analyses (ICC > 0.9 for all data). Figure 25 displays the plots of the total power measurements against time for the six subjects with normal and high BMI, showing good agreement between analyses at most time points for both body compositions.

	ICC	Bland-Altman
Observer 1	0.992 P<0.0001 n=78	MD 6.1 a.u. 95% CI -7.2 to 19.4 a.u. Measurement Range (27.2 – 254.5 a.u.)
Observer 2	0.960 P<0.0001 n=78	MD 1.0 a.u. 95% CI -41.2 to 43.19 a.u. Measurement Range (28.4 – 281.0 a.u.)

Table 4: Table summarising the total power ICC and Bland-Altman from observer 1 (experienced, over 10 years) and observer 2 (less experienced, less than 2 year). MD – Mean Difference; CI – Confidence Interval.

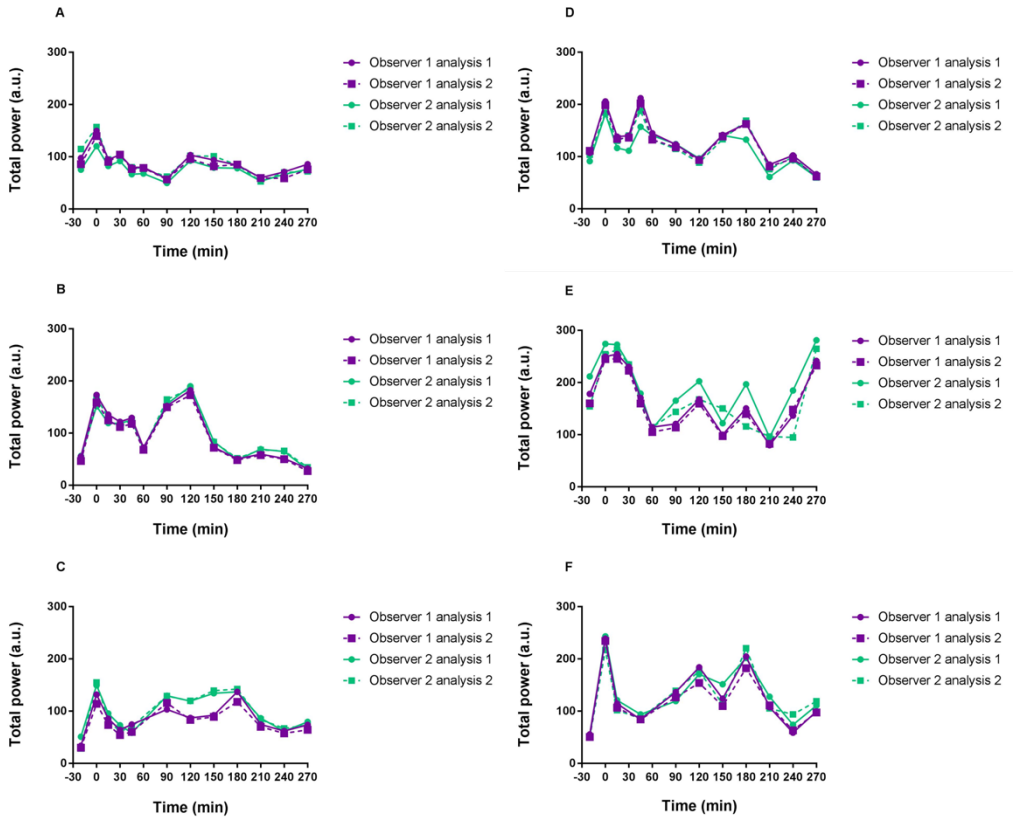

Figure 25: Graphs showing the repeated analysis of total power for the (A,B,C) normal and (D,E,F) high BMI subject measured by the two observers.

Small bowel motility changes in response to feeding

The subjects showed an increase between their fasting and initial postprandial motility measurement for both analysis methods (total power and SD_{JAC}), (Figure 26). The correlation between the techniques was significant ($r=0.9$, $p<0.0001$, $n=30$).

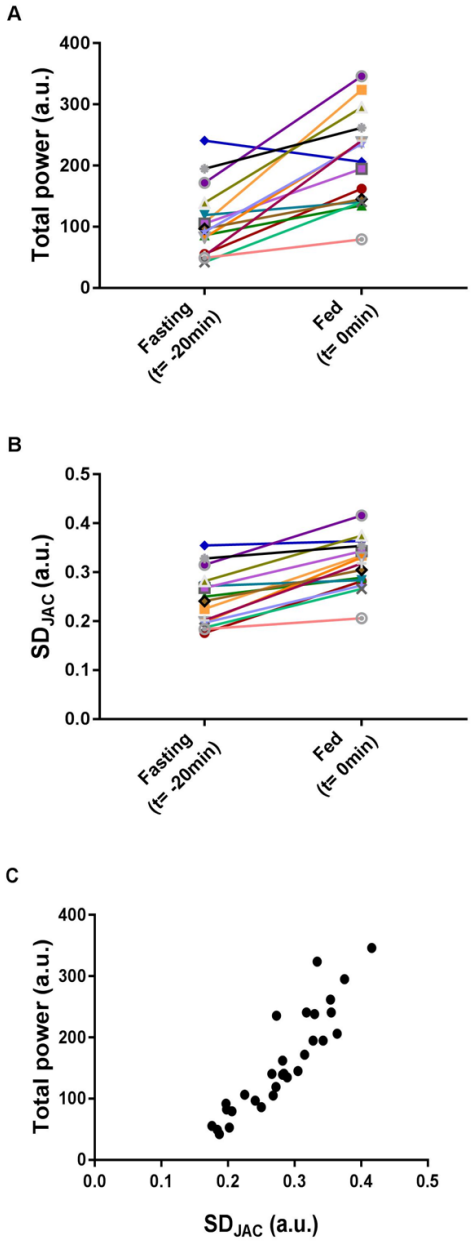

Figure 26: Graph illustrating the difference in small bowel motility during fasting and immediately after feeding using the two different motility parameters across all the 15 subjects. A. The fasting and fed small bowel motility measured by total power. B. The fasting and fed small bowel motility measured by SD_{JAC}. C. Correlation between the two parameters of the fasting and fed data (r=0.9, p<0.0001, n=30). Individual subjects have the same colour coding across A and B.

3.4 Discussion

In this work we evaluated the new technique for the analysis of small bowel motility from MRI images in unprepared bowel. The maps of total power spectrum indicated a better discrimination of the bowel tissue compared to the more widely published SD_{JAC}[55, 57, 137] with lower noise in the regions where non/low-motility is expected, and a bigger dynamic range of motility indices.

The appearance of the unprepared bowel, which may contain multiple collapsed loops (which are not always easily identified) means that the definition of the ROIs is more subjective than for the prepared bowel with distended lumen. However our inter-observer variability data suggested that ROI definition had a small effect on the results compared to the changes in motility seen following ingestion of the meal. Excellent correlation between observers was seen across the whole range of total power spectrum measurement acquired and the Bland-Altman limits of agreement were low compared to the range of values measured. The postprandial changes over time showed a rapid increase in motility following ingestion of the soup meal with levels returning towards baseline much later after the meal had been consumed[139].

Intra-observer variability was also low with a small range of Bland-Altman limits of agreements for both observers across two very different body shapes. The ICC was excellent with all data greater than 0.9.

This work presents a new analysis of MRI data to assess the motility in the physiological fasting and postprandial states using

registered MRI datasets. The MRI method proposed removes the need for intubating subjects, which can be a stressful procedure, often requiring fluoroscopy to place the catheter and rarely covering the entire length of the small bowel. Scintigraphy transit studies[158] involving ionising radiation do not normally provide information about the motor patterns seen in the small bowel. The proposed techniques (including further frequency analysis of the power spectra) will be useful to study the time scales of contractile activity and regional patterns along the gastrointestinal tract in health and disease.

There were limitations to this work. Due to the time consuming nature of drawing all the individual ROIs on the motility data the intra-observer repeated measurements were confined to just 6 subjects, not the full 15 available (used for the inter-observer data). Drawing of ROIs for a single time point took up to 10 minutes depending on the anatomy including the loading of each data set into the software. However, the intra-observer data were chosen from subjects who had very different small bowel anatomical appearances due to their differing BMIs, providing the observers with contrasting data for drawing the regions.

This method showed excellent agreement between measurements of intra and inter observers as well as showing the sensitivity of the technique to changes in motility induced by ingestion of a meal. Therefore, we planned to use this new image processing technique for the analysis of small bowel motility in unprepared bowel of CD patients

and to compare this to the healthy volunteers. This will be discussed in detail in the following chapter.

4. Motility in Crohn's disease 2 (MIC2)

The MRI protocol developed in MIC1 was acceptable to the healthy volunteer's cohort. The soup meal was able to produce physiological responses and we were able to collect reference data to start the CD patient's study. Our new small bowel motility technique showed an excellent agreement between the measurements of intra and inter-observers variability. In the following chapter the patient's study will be discussed in detail showing the results in comparison to the healthy volunteer's data.

This work was accepted as a poster presentation at the European Crohn's and Colitis Organization (ECCO) in February 2018 and at the British Society of Gastroenterology (BSG) in June 2018.

4.1 Introduction

Intestinal inflammation in CD is associated with an increase in PYY, GLP-1 and CCK[109] and recent literature has shown that small bowel motility in CD negatively correlates to intestinal inflammation[135]. Small bowel motility in CD is linked to patient symptoms like abdominal pain[159]. We hypothesize that some of these symptoms may be linked to the increased expression and postprandial responses in key GI peptides and to the alteration in intestinal motility.

Our aim was to use the methodology developed for MIC1 to assess gut peptide, small bowel motility and patient symptom response to the

soup meal challenge in CD patients and to evaluate the difference in small bowel motility between patients and healthy volunteers groups. This work will help us understand the aetiology of the altered intestinal physiology and its link to patient's symptoms in intestinal inflammation due to CD.

4.2 Methodology

4.2.1 Subjects

Sixteen CD patients with active small bowel disease (age 36±3 years, BMI mean 26±1 kg/m^2) were recruited from NHS outpatient clinics. Twenty Healthy volunteers (age 31±3 years, BMI mean 24±1 kg/m^2) were recruited from the local campus population (15 healthy volunteers from MIC study and 5 extra volunteers where recruited to complete the sample size (10 females and 10 males)).

This study was approved by the Research Ethics Committee (NRES approval 15/EM/0003) and R&D approval 14GGA043. It was registered on clinicaltrials.gov with identifier NCT03052465. All participants gave informed written consent. This part of the study investigated a cohort of CD patients with active disease and healthy volunteers. Patients' eligibility criteria are shown below. The healthy participants' eligibility criteria from MIC1 were used here too. Standard MRI exclusion criteria were applied.

4.2.2 Patients eligibility

Inclusion criteria:

A cohort of non-obese CD patients aged 18-75 years (BMI 18-30) with active disease defined as Harvey-Bradshaw index score (HBI) of 5-16[160] and at least one o f the following:

- Ulceration seen at ileocolonoscopy, aiming for SES-CD of 4-19[161] in the absence of complicated disease or,
- Intestinal inflammation or deep ulceration seen on CT or MRE, with the disease activity quantified via the MaRIA score[121] or,
- Faecal calprotectin of >250µg/g[161, 162], or
- C-Reactive protein >5mg/dl.

These measures of disease activity were to be taken ideally within 4 weeks of recruitment as part of their standard care. No change in management had happened between the screening visits and the scan visits.

Stable doses of immunosuppressive agents, corticosteroids or biological agents were permitted. No changes in medication were allowed at inclusion until data collection of the outcome measures has been completed. All participants had a good command of the English language and had the capacity to give informed written consent.

Exclusion criteria:

Potential participants with any of the following criteria were excluded:

- Malignant disease.
- Stricturing or penetrating disease.
- Smoking history.
- History of bowel resections or any gastric surgery.
- History of pancreatic insufficiency.
- BMI <18 or >30 Kg/m^2.
- Significant cardiovascular or respiratory disease.
- Diabetes mellitus.
- Thyroid disease.
- Current Infection.
- Neurological or cognitive impairment.
- Significant physical disability.
- Significant hepatic disease or renal failure.
- Abnormal blood results other than those explained by CD in CD participants.
- Subjects currently (or in the last three months) participating in another research project.
- Pregnancy or breastfeeding.
- Contraindications for MRI (e.g. pacemaker).
- Proton-pump inhibitor usage or any medication that affects gastric emptying or small bowel transit (hyoscine butylbromide or mebeverine).

4.2.3 Study design

In this study, the same protocol as developed for MIC1 was used with only the exception of the MRI whole gut transit test and the addition of a standard MRE test, performed at the end of the postprandial study, to measure disease activity.

4.2.4 MRI Protocol

Subjects were scanned using the 1.5T Philips Achieva MRI scanner (Philips Healthcare, Best, the Netherlands) at the Sir Peter Mansfield Imaging Centre, University of Nottingham. They underwent a baseline fasting scan and then they were asked to consume the soup meal within 20 min. This was followed by postprandial scans at regular intervals. Subjects were scanned using the same MRI sequences described in MIC1 study and the data (MRI, questionnaire data and 10 mL blood samples) were collected in the same way.

At the end of the 270 min CD subjects were given a volume (750 mL-1250 mL) of contrast agent to drink (within 60 minutes) (Figure 27) and a further MRI scan (within 30 minutes) was undertaken to quantify disease activity.

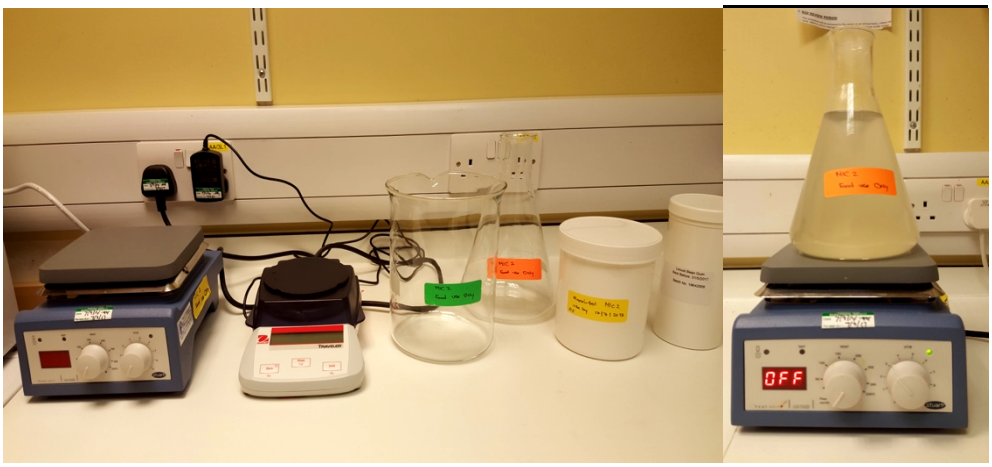

Figure 27: Image showing the oral contrast preparations.

4.2.5 Peptide assays

Plasma peptides (total GLP-1, total PYY) were analysed as described in MIC1 through ELISA techniques (Millipore, UK)[109] and the concentrations of serum CCK were measured by RIA (Euro Diagnostic Products, Sweden)[146]. The peptides were analysed by the laboratory technicians in the BRC.

4.2.6 MRI measures of disease activity

At the end of the series, subjects were given 60 minutes to drink 750-1250 mL of an oral contrast solution (5% mannitol). Oral contrast solution was prepared according to the standard operating procedures (SOP) shown in Appendix B.

The small bowel was scanned as previously described[121, 163] before and 10 minutes after 40 mg of hyoscine butyl bromide was injected intravenously by a physician to reduce small bowel motility.

Patients were scanned within 30 minutes of the oral contrast. Initially a true fast imaging with a steady sequence was acquired in the coronal plane. Axial T1 sequences were acquired before and 70 s after intravenous administration of 0.2 mL/kg body weight of gadolinium chelate (gadodiamide 0.5 mmol/l) at a rate of 2 mL/s.

MRE variables were evaluated by a Nottingham University Hospitals clinical GI MRI radiologist with > 10 years' experience (Dr. Khalid Latief) in each segment including: bowel wall thickening, enhancement of the bowel wall after administration of intravenous contrast with gadolinium (relative contrast enhancement), presence of ulcers, mural oedema, regional enlarged lymph nodes (>10 mm), peri-enteric vascularization (comb sign), peri-enteric fluid, fat stranding, and fibro-fatty proliferation (table 5). The MaRIA score in each segment was calculated according to a formula, as previously defined[121]. One subject with a low MaRIA score (3.39) was excluded from this study.

Variables contributing to MaRIA score	Bowel wall thickness
	Enlarged regional mesenteric lymph nodes
	Presence of mural oedema
	Presence of mucosal ulceration
	Presence of pseudopolyps in the lumen
	Quantitative measurement of wall signal intensity before and after the contrast
	Relative contrast enhancement of the intestinal wall

Table 5: Variables contributing to the MaRIA score

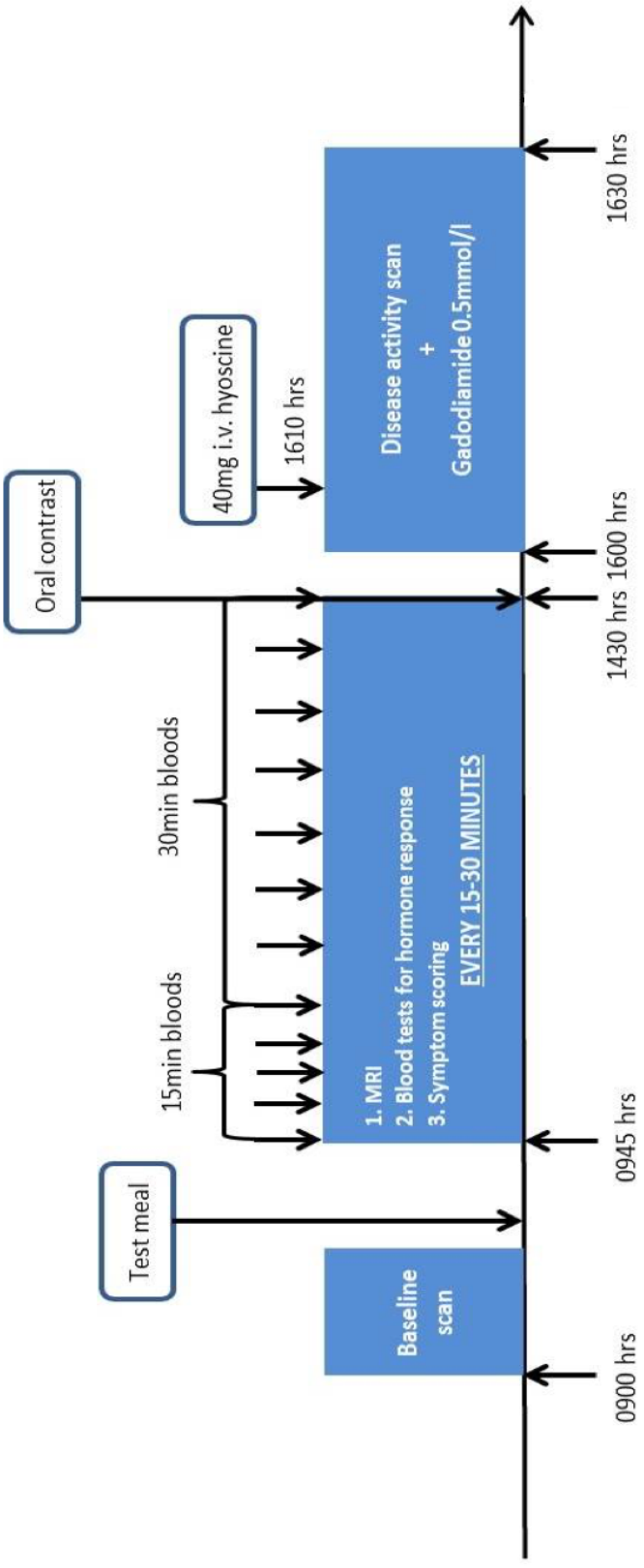

Figure 28: Diagram of MIC2's study protocol.

4.2.7 Data analysis

Small bowel motility, gastric volume, gall bladder volume and small bowel water content were processed and analysed as mentioned previously in Chapter 2.

4.2.8 Statistical analyses

The data are expressed as mean±standard error of the mean (SEM). Normality of the data were assessed using Shapiro–Wilk's test. All statistical analyses were performed using GraphPad Prism 7.01 (La Jolla, USA). A p-value less than 0.05 was considered statistically significant. ANOVA was used to assess the significance of differences. When the analysis of variance was significant, post hoc test assessments of the individual time points were performed using the Dunnett's (for parametric data) or Dunn's test (for nonparametric data) to account for multiple comparisons. The Pearson correlation coefficient was used to measure the strength of correlation between MaRIA scores and the different variables.

4.3 Results

All twenty healthy volunteers and 16 CD subjects completed the study and tolerated the experimental procedures well without any adverse event. One CD subject's data were excluded because of low MaRIA score.

Subject	Age (years)	Gender	MaRIA score	HBI	CRP (mg/dl)	fC (µg/g)
P01	24	F	16.10	2	41	933
P04	29	F	11.37	2	7	177
P06	39	F	16.72	13	<5	1435
P07	57	M	27.48	1	15	393
P11	20	F	6.75	6	<5	275
P08	52	F	27.07	7	<5	107
P09	30	M	24.54	9	32	unavailable
P10	33	M	13.65	2	<5	577
P13	46	M	17.50	2	10	unavailable
P14	33	M	33.75	2	<5	1023
P15	51	F	17.00	5	9	535
P16	30	F	17.06	6	<5	604
P17	53	M	23.68	2	<5	1800
P18	23	F	24.49	6	13	1587
P19	19	M	27.48	18	<5	unavailable

Table 6: Table summarising the demographics and key clinical variables of the CD subjects.

Small bowel motility

The healthy volunteers started with a significantly higher ($p<0.05$) fasting motility index (106±13 a.u) compared to CD subjects (70±8 a.u.) (Figure 29). Both groups reached their maximum motility immediately after

feeding. This was followed by a gradual decline in motility to around baseline at 240 min in HV and 270 min in CD. Small bowel motility was significantly higher ($p<0.05$) at the different time points in CD group compared to fasting motility except at t=45, t=120, and from t=210 to t=270 min. The percentage of change in small bowel motility from fasting state was greater in CD subjects possibly because of their underlying fasting hypomotility compared to HV (Figure 29C).

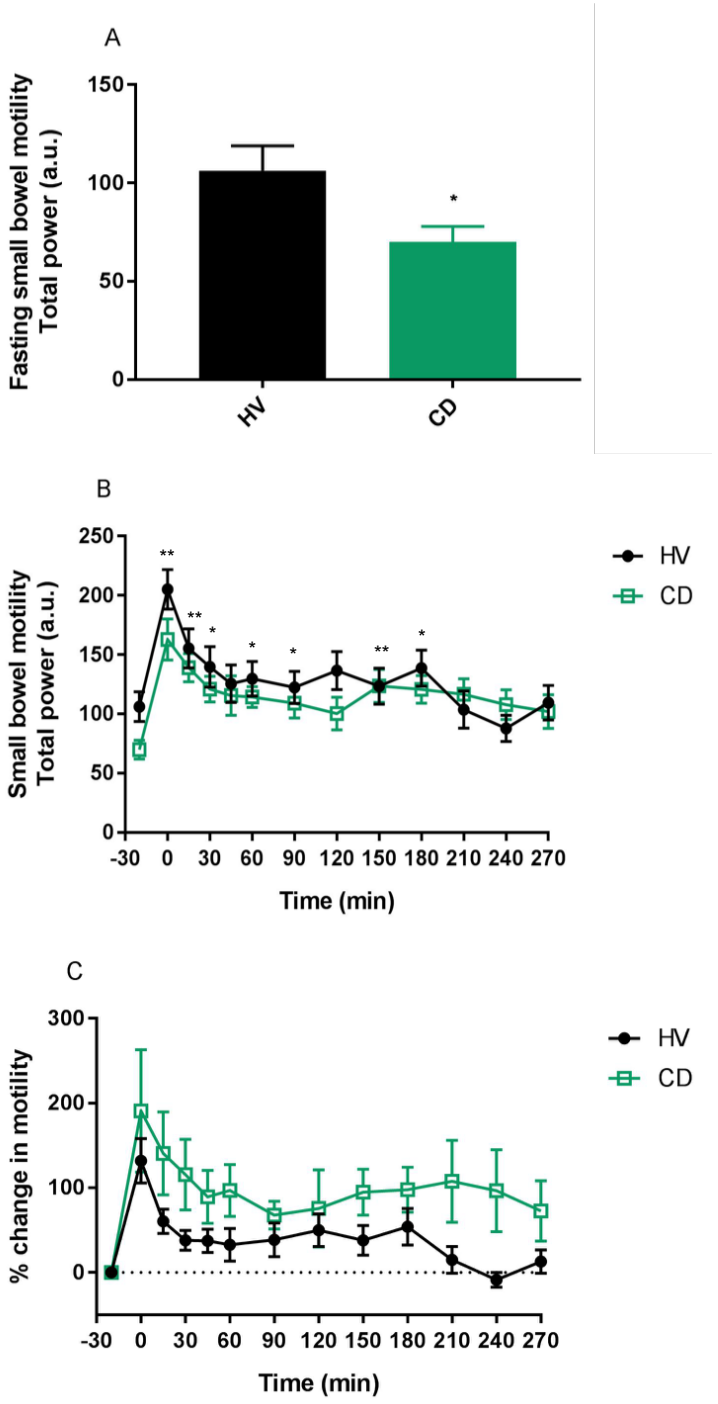

Figure 29: Time courses of the small bowel motility in CD and in HV. A. Fasting small bowel motility for CD and HV. B. Time courses of the small bowel motility for CD and HV. C. Percentage of change in small bowel motility from fasting across the time courses for CD and HV. (HV: n=20, CD: n=14). **p<0.01 and *p<0.05 versus fasting value for CD.

Gallbladder volumes

The difference in gallbladder volumes between healthy volunteers and CD subjects from fasting to 150 min are shown in Figure 30. The volume decreased upon feeding in both groups and stayed stable throughout the postprandial period. The gall bladder contracted immediately from fasting volumes of 21±2 mL and 36±9 mL in healthy volunteers and CD subjects respectively to 13±2 mL and 22±8 mL upon feeding (respectively). In the CD group, the gall bladder volumes after feeding were significantly lower than fasting baseline ($p<0.05$) at all time points but the t=60 min and t=120 min.

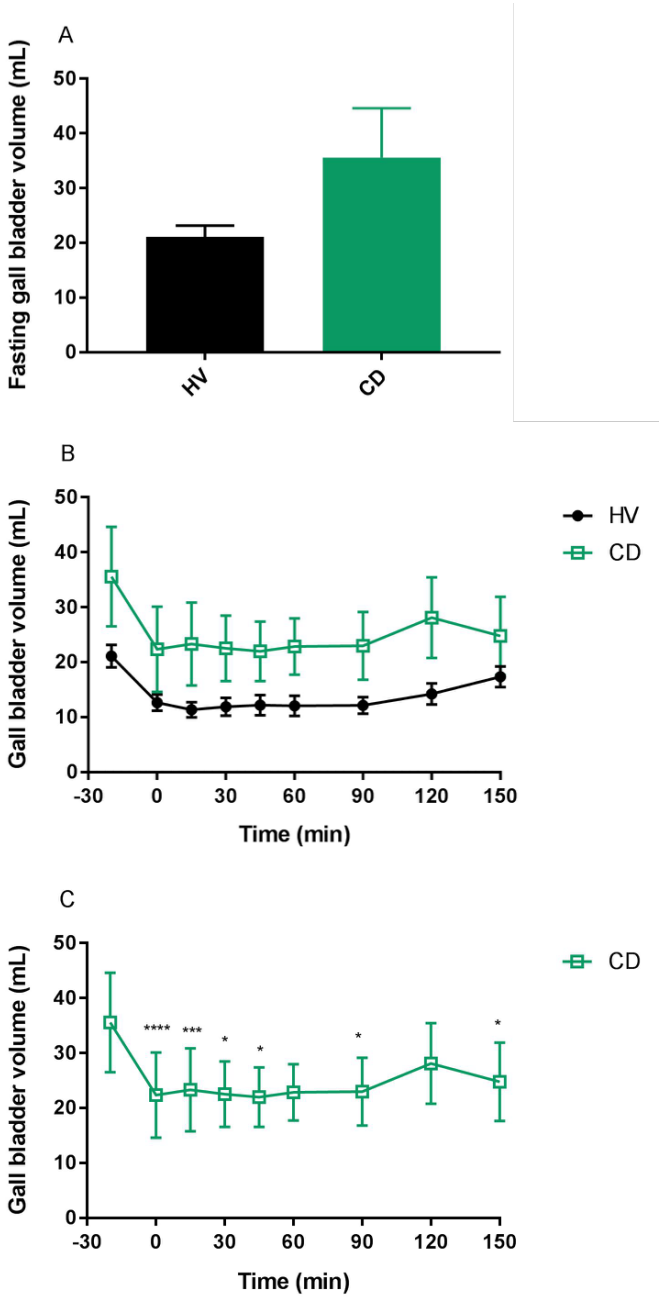

Figure 30: Time courses of the gallbladder volumes in CD and in HV. A. Fasting gall bladder volumes for CD and HV. B. Time courses of the gall bladder volumes in CD and HV. C. Time courses of the gallbladder volume in CD. Data are mean ± SEM (HV: n=20, CD: n=13). **** p<0.0001, *** p<0.001 and *p<0.05 versus fasting value.

Gastric volumes

The baseline gastric volumes showed a small amount of resting gastric juices in both groups (Figure 31, HV: 29±5 mL, CD: 25±4 mL) followed by the expected increase upon feeding (HV: 388±18 mL, CD: 324±26 mL). This was followed by a decline in volume as the stomach emptied, reaching baseline values at 150min. The average time to empty half of the stomach contents ($T_{1/2}$) in healthy volunteers and CD subjects was 43±4 min, 63±7.5 min respectively. In the CD group, the stomach volumes were significantly higher than the fasting baseline volume ($p<0.05$) at all postprandial time points except at t=150 min.

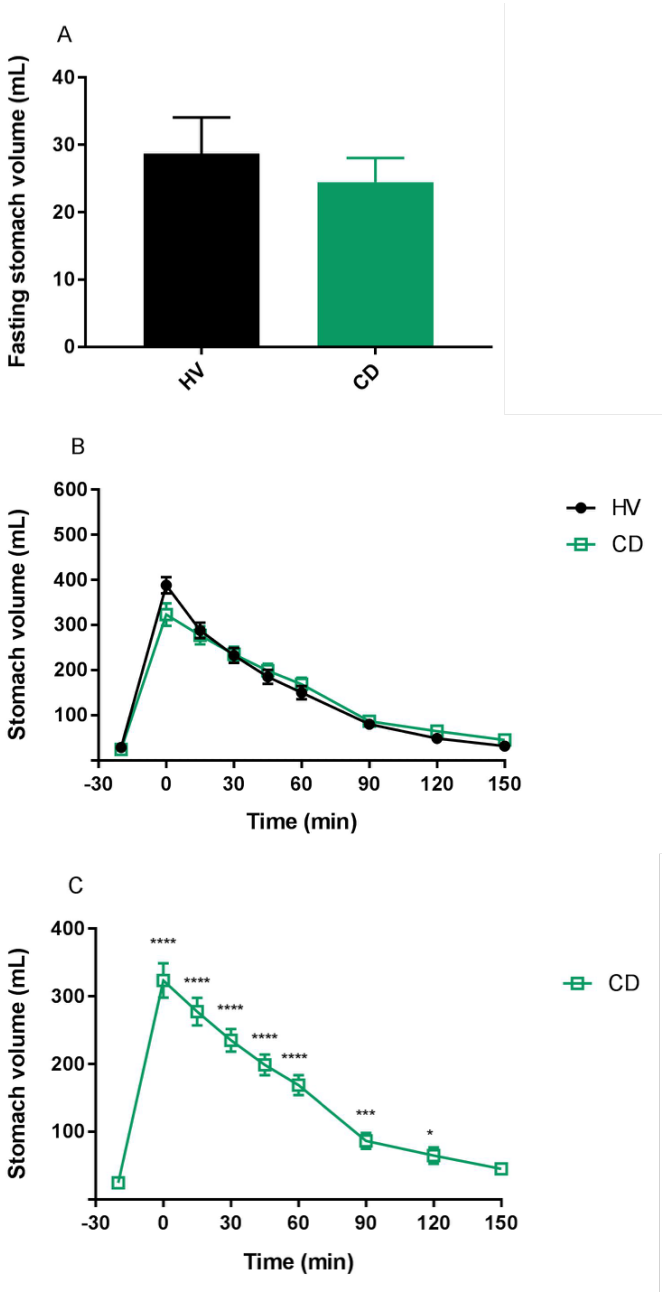

Figure 31: Time courses of the stomach content volumes in CD and in HV. A. Fasting stomach volumes for CD and HV. B. Time courses of the stomach volumes for CD and HV. C. Time courses of the stomach volumes in CD. Data are mean ± SEM (HV: n=20, CD: n=15). **** p<0.0001, *** p<0.001 and *p<0.05 versus fasting value.

Small bowel water content

The data in Figure 32 show a small amount of fasting small bowel water content in both groups (HV: 44±6 mL, CD: 36±9 mL). A significant increase ($p<0.05$) was seen in small bowel water content in CD subjects compared to HV (measured as area under the curve (AUC) CD: 19778±2119 mL/min, HV: 14197±1249 mL/min). Upon feeding, the small bowel water content increased at 15 min followed by a decrease in volume in healthy subjects. A second peak in volume at 180 min was seen in the healthy volunteers group. CD subjects responded differently as the increase upon feeding continued to reach the maximum at 210 min ($p<0.05$). In CD group, a significant increase ($p<0.0001$) in SBWC was seen from t=150 to t=270 min when compared to fasting volume.

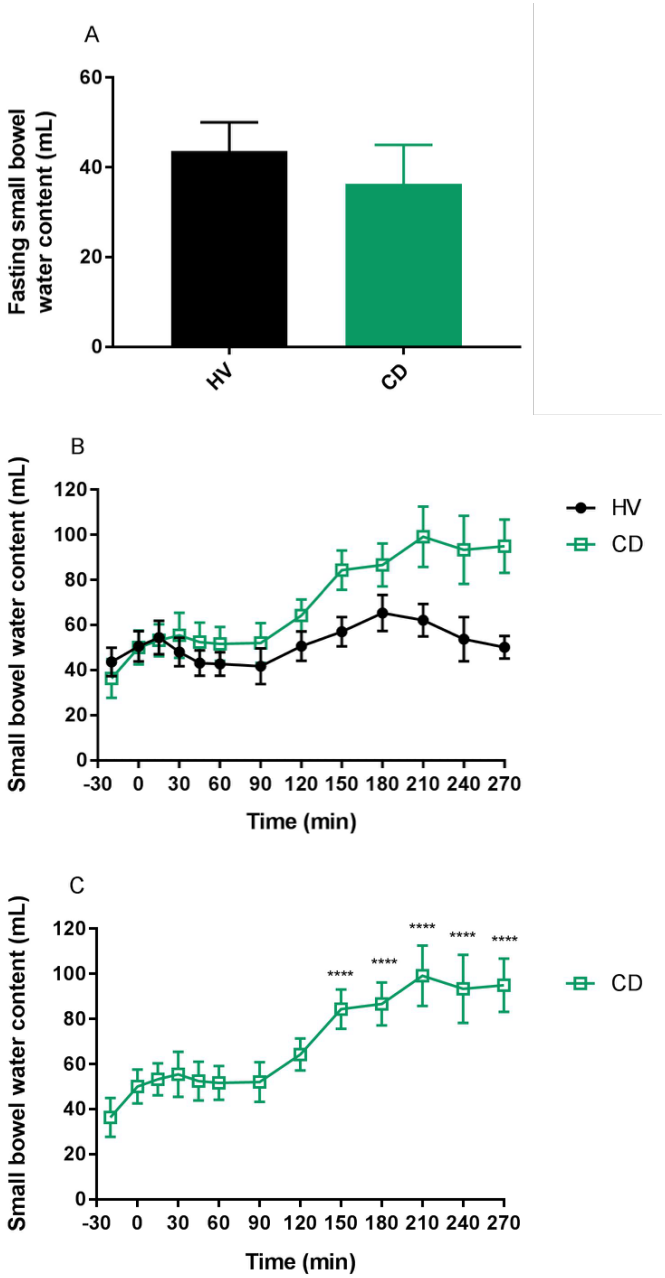

Figure 32: Time courses of the small bowel water content in CD and in HV. A. Fasting small bowel water content for CD and HV. B. Time courses of the small bowel water content for CD and HV. C. Time courses of the small bowel water content in CD. Data are mean ± SEM (HV: n=20, CD: n=15) **** p<0.0001 versus fasting value.

Total GLP-1

Figure 33 shows a significant increase ($p<0.0001$) in plasma measures of total GLP-1 in CD subjects compared to healthy volunteers (AUC CD: 12725 µg/mL, HV: 2400 µg/mL). Significantly higher ($P<0.0001$) fasting GLP-1 levels were noted in CD subjects compared to healthy volunteers (CD: 50±8 µg/mL, HV: 13±3 µg/mL). This was followed by a drop in GLP-1 levels after 30 minutes in healthy volunteers. The levels were stable across the study time points. No significant difference was observed within the CD patients across the different time points.

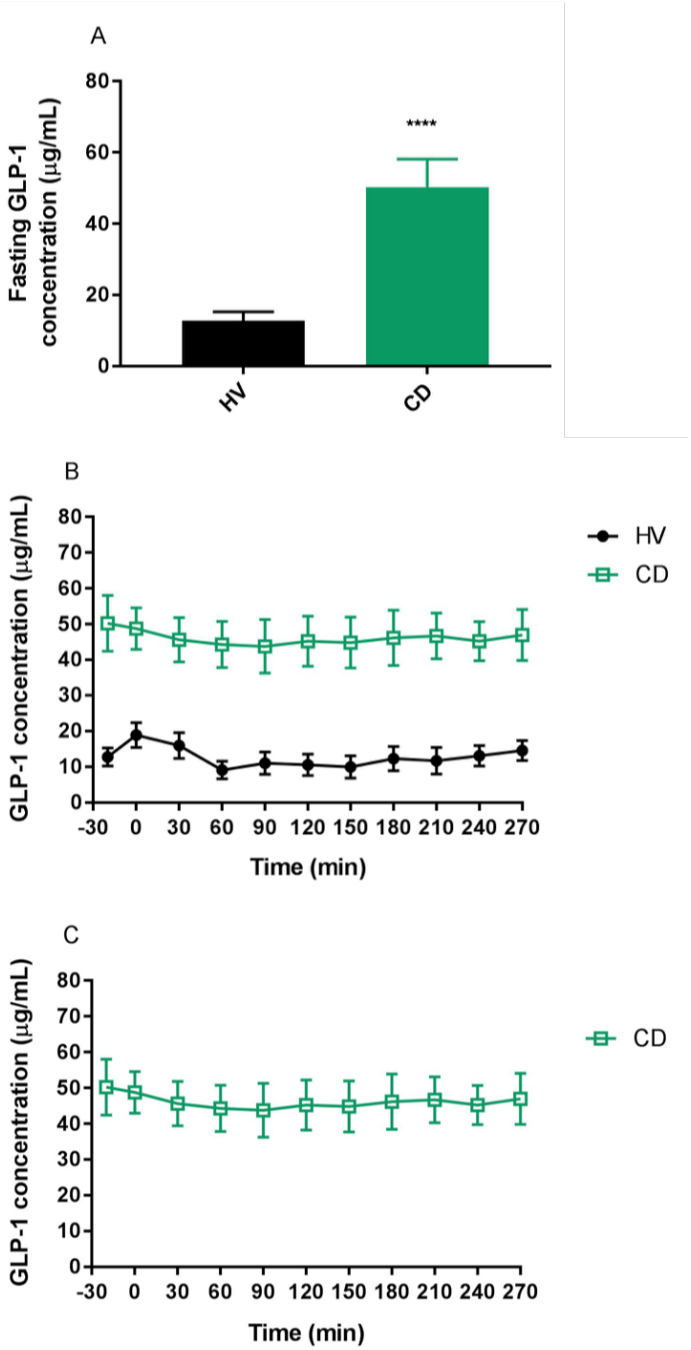

Figure 33: Time courses of the GLP-1 concentrations in CD and in HV. A. Fasting GLP-1 concentrations for CD and HV. B. Time courses of the GLP-1 concentrations for CD and HV. C. Time courses of the GLP-1 concentrations in CD. Data are mean ± SEM (HV: n=20, CD n=15). **** p<0.0001 versus fasting value.

PYY

PYY levels increased significantly ($p<0.0001$) postprandially in CD subjects compared to the healthy volunteers (AUC CD: 62782±4313 pg /mL HV: 34744±3169 pg/mL) (Figure 34). The CD subjects showed a significantly higher (236±16 pg/mL, $p<0.0001$) fasting PYY concentrations compared to healthy volunteers (118±12 pg/mL). The meal induced a significant postprandial increase in PYY concentration in both groups, followed by a gradual decline reaching the baseline by the end of the study. PYY in the CD group were significantly higher ($p<0.05$) levels across the different time points.

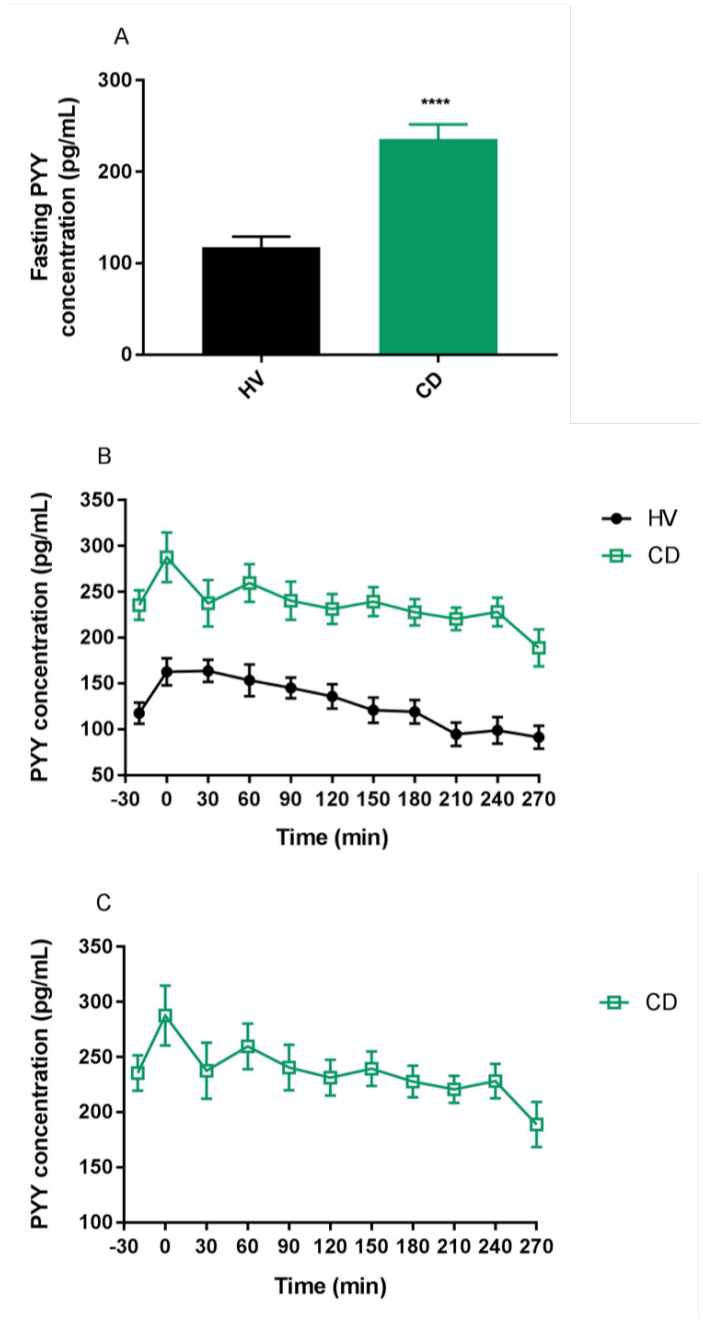

Figure 34: Time courses of the PYY concentrations in CD and in HV. A. Fasting PYY concentrations for CD and HV. B. Time courses of the PYY concentrations for CD and HV. C. Time courses of the PYY concentrations in CD. Data are mean ± SEM (HV: n=20, CD n=15). **** p<0.0001 versus fasting value.

CCK

The plasma CCK levels increased in both groups upon feeding reaching the maximum concentrations at 30 min in the healthy volunteers group and at 45min in the CD subjects (Figure 35). This was followed by a steadily decline after 90 min, reaching baseline values towards the end of the study day. In CD group, a significant difference ($p<0.0001$) was seen across the different time points with a significant increase ($p<0.05$) from time 0 to 90 min compared to fasting concentration.

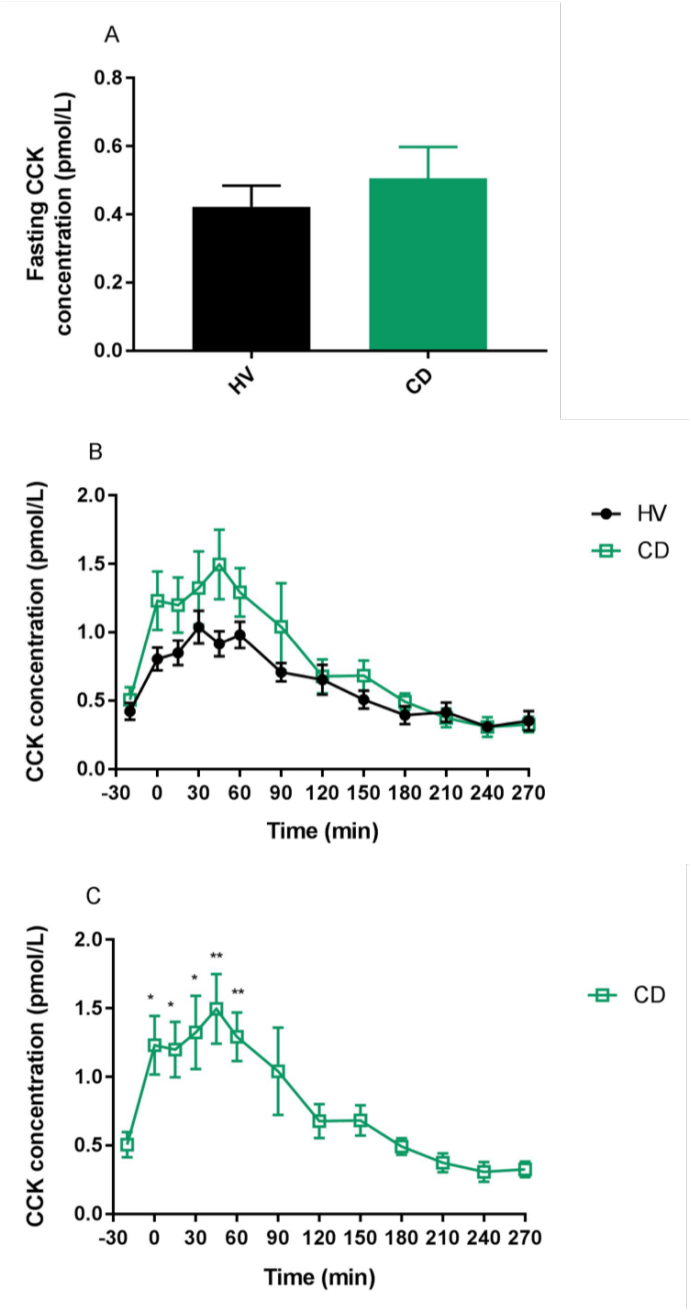

Figure 35: Time courses of the CCK concentrations in CD and in HV. A. Fasting CCK concentrations for CD and HV. B. Time courses of the CCK concentrations for CD and HV. C. Time courses of the CCK concentrations in CD. Data are mean ± SEM (HV: n=20, CD n=15) ** p<0.01 and *p<0.05 versus fasting value.

Symptom VAS data

Fullness

Fullness scores recorded from CD subjects and HV are shown in Figure 36. CD subjects showed a significantly higher ($p<0.01$) fasting fullness scores compared to healthy volunteers (CD: 21±6 mm, HV: 5±3 mm). The meal induced a significant ($p<0.05$) postprandial increase in the feeling of fullness in CD subjects compared to healthy volunteers (AUC CD: 6795±1440 mm/min HV: 2907±703 mm/min). The feeling returned to baseline thereafter. An overall significant difference ($p<0.0001$) was seen in the fullness scores in the CD group across the time points with a significant change from t=0 min to t=45 min compared to fasting (t=-20 min).

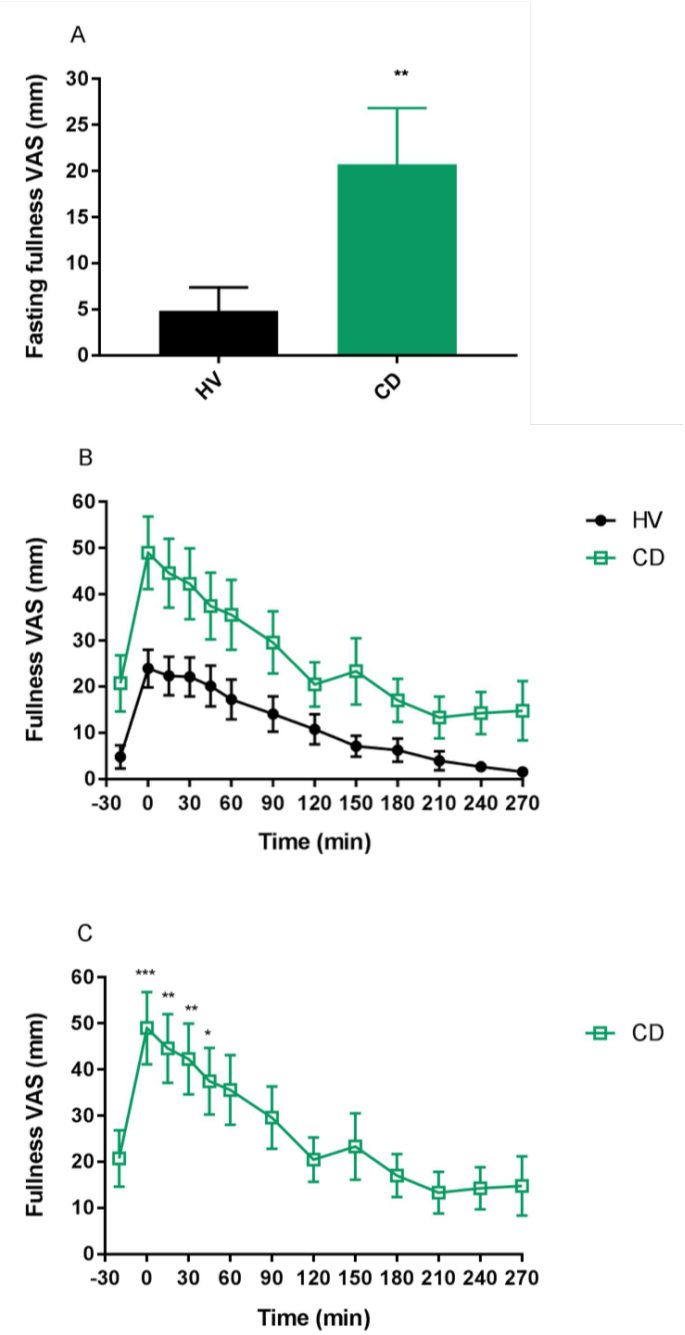

Figure 36: Time courses of the Fullness VAS scores in HV and in CD patients. A. Fullness fasting VAS scores for CD and HV. B. Time courses of the fullness VAS scores for CD and HV. C. Time courses of the fullness scores in CD. Data are mean ± SEM (HV: n=20, CD n=15). *** p<0.001, **p<0.01, and *p<0.05 versus fasting value.

Bloating

Figure 37 shows the time courses of the symptom of bloating. A significant postprandial increase ($p<0.0001$) in bloating was noted in CD subjects compared to healthy volunteers (AUC CD: 5558±1293 mm/min, HV: 565±257 mm/min). Bloating scores retuned to baseline by the end of the study time. An overall significant difference ($p<0.0001$) was noted in the bloating scores in the CD group across the time points.

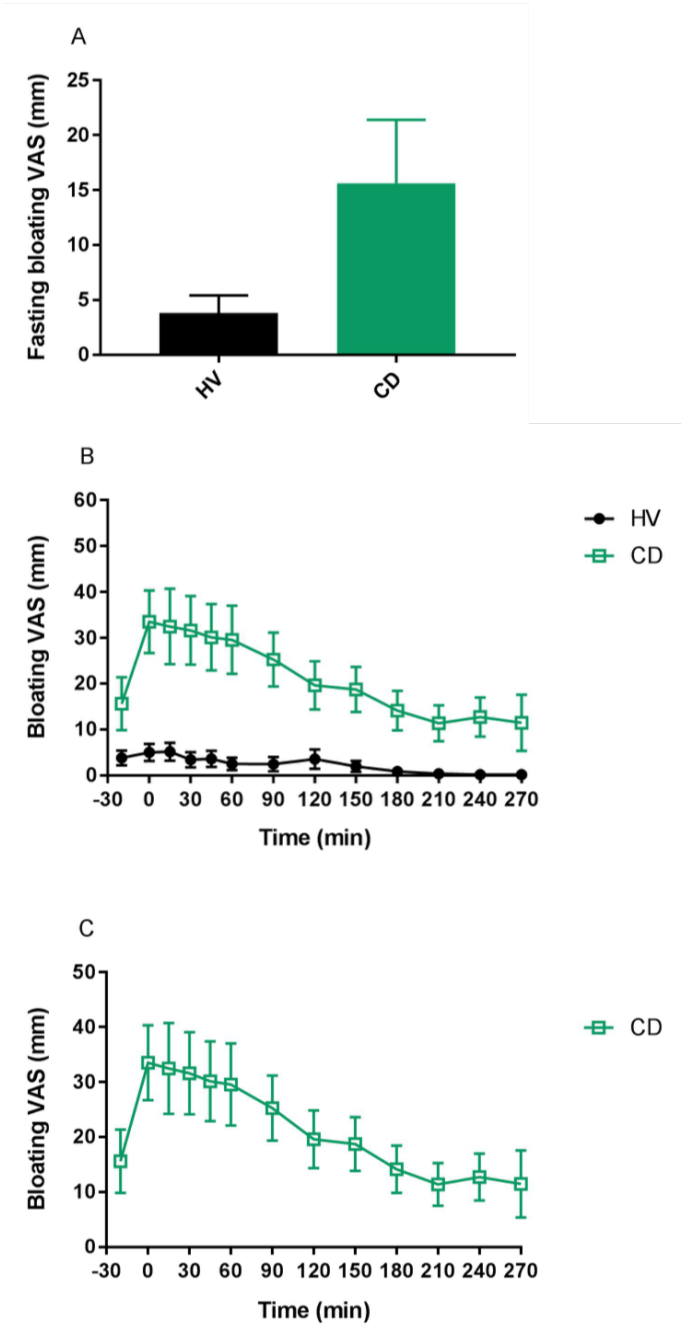

Figure 37: Time courses of the bloating VAS scores in HV and in CD patients. Bloating fasting VAS scores for CD and HV. B. Time courses of the bloating VAS scores for CD and HV. C. Time courses of the bloating scores in CD. Data are mean ± SEM (HV: n=20, CD n=15).

Distention

The time courses of the distention VAS scores are shown in Figure 38. Fasting scores showed a significantly higher ($p<0.05$) distention score in CD subjects compared to control (CD: 14±5 mm, HV: 2±1 mm). CD subjects showed a significant ($p<0.0001$) postprandial increase in the feeling of distention compared to healthy volunteers (AUC, CD: 5071±1253 mm/min, HV: 303±191 mm/min). The feeling retuned to baseline by the end of the study time. An overall significant difference ($p<0.0001$) was noted in the distention scores in the CD group across the time points.

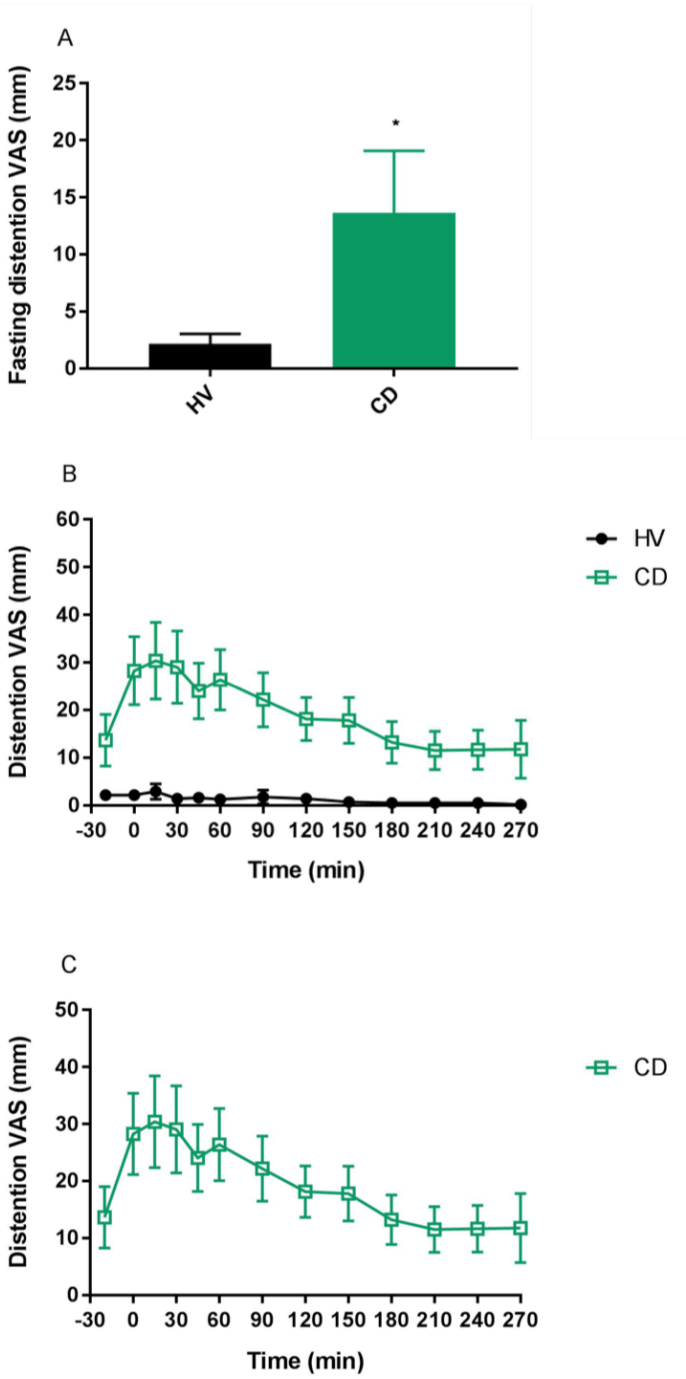

Figure 38: Time courses of the distention VAS scores in HV and in CD patients. A. Distention fasting VAS scores for CD and HV. B. Time courses of the distention VAS scores for CD and HV. C. Time courses of the distention scores in CD. Data are mean ± SEM (HV: n=20, CD n=15). * p<0.05 versus fasting value.

Abdominal pain

The recorded abdominal pain scores are shown in Figure 39. CD subjects reported a significant increase ($p<0.01$) in the fasting abdominal pain scores that continues to the end of the study time (CD: 18±5 mm, HV: 0.5±0.3 mm). A significant ($p<0.0001$) postprandial increase in abdominal pain was seen in CD subjects compared to healthy volunteers (AUC, CD: 3187±873 mm/min HV: 7±5 mm/min). No change was reported within the CD group across the different time points.

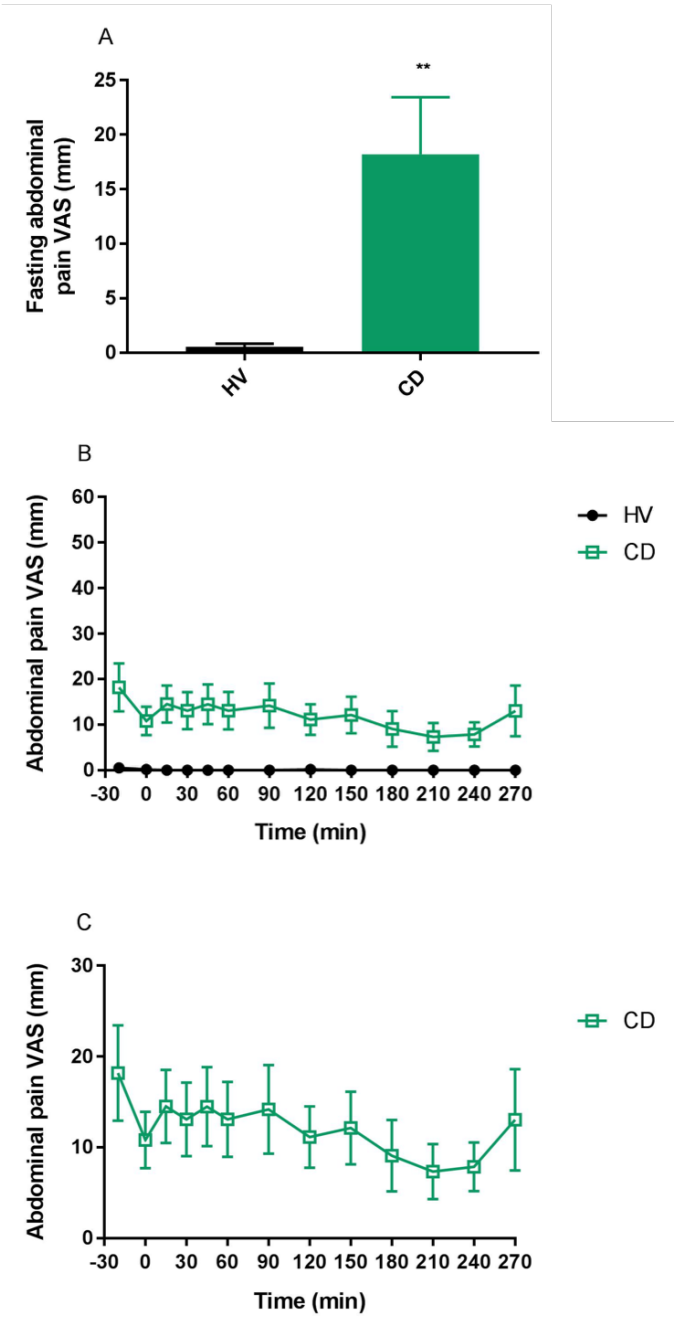

Figure 39: Time courses of the abdominal pain VAS scores in HV and in CD patients. Fasting abdominal pain VAS scores for CD and HV. B. Time courses of the abdominal pain VAS scores for CD and HV. C. Time courses of the abdominal pain scores in CD. Data are mean ± SEM (HV: n=20, CD n=15). ** p<0.01 versus fasting value.

Sickness/nausea

Figure 40 illustrated the reported sickness scores in both groups. The CD subjects showed a significant ($p<0.01$) increase in the feeling of sickness compared to healthy volunteers (AUC, CD: 2024±927 mm/min HV: 75±75 mm/min). The feeling returned to baseline at 270 min. No change was reported within the CD group across the different time points.

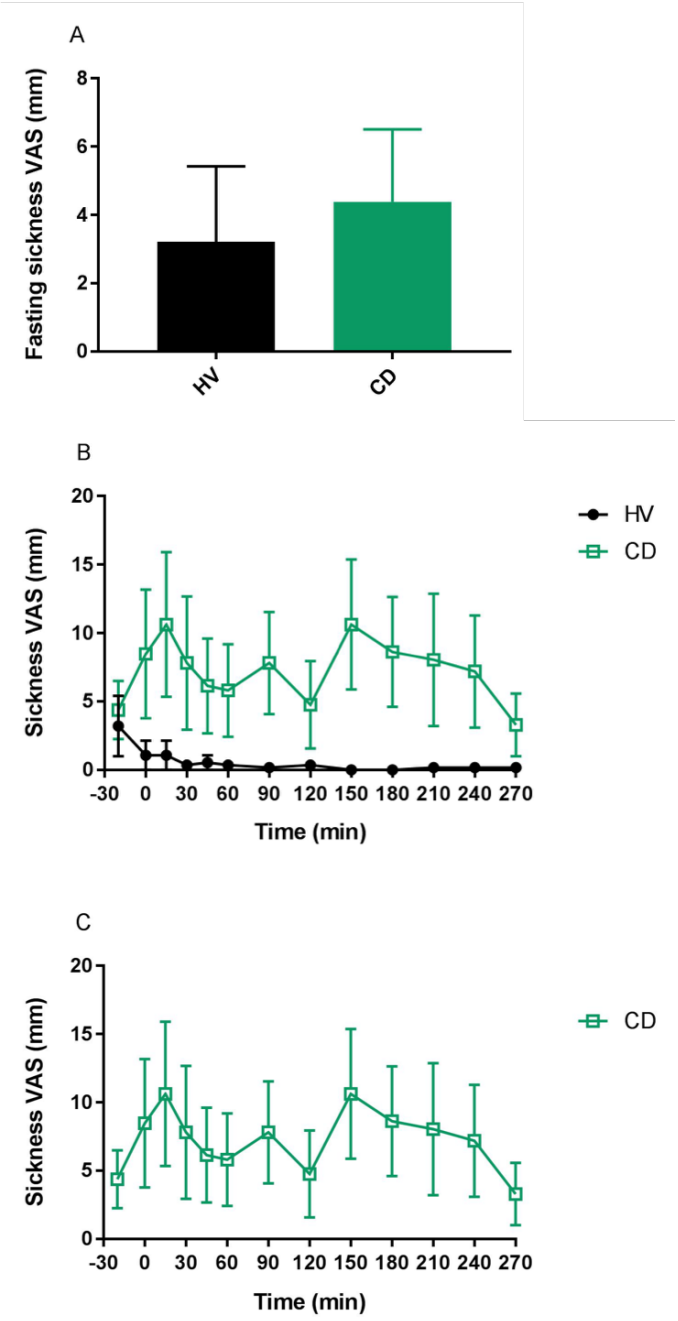

Figure 40: Time courses of the sickness VAS scores in HV and in CD patients. Sickness fasting VAS scores for CD and HV. B. Time courses of the sickness VAS scores for CD and HV. C. Time courses of the sickness scores in CD. Data are mean ± SEM (HV: n=20, CD n=15).

MaRIA

There was no significant correlation between MaRIA scores and small bowel motility and between MaRIA scores and small bowel water content (Figure 41). Also, there was no significant correlation between MaRIA scores and GLP-1, PYY or CCK levels (Figure 42).

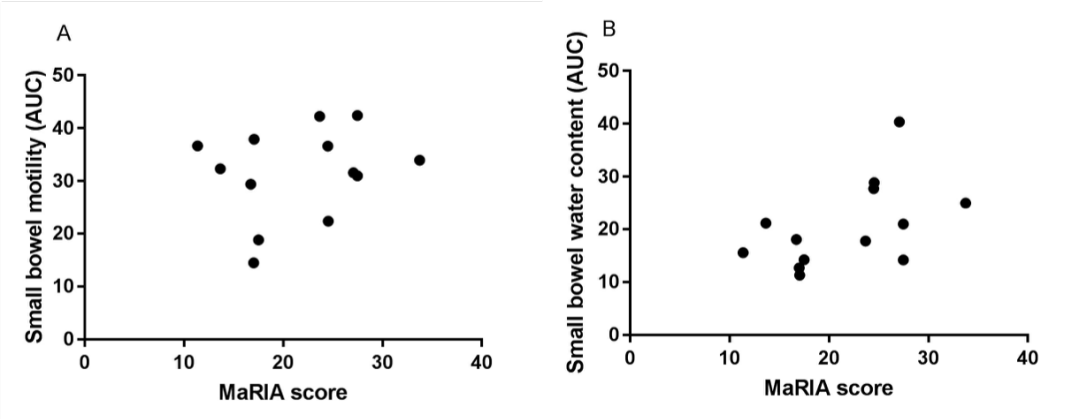

Figure 41: B. Correlation between MaRIA scores and different MRI parameters. A. Correlation between small bowel motility measured as AUC and MaRIA scores. (r=0.23, p=0.45, n=13). B. Correlation between small bowel water content measured as AUC and MaRIA scores. (r=0.51, p=0.07, n=26).

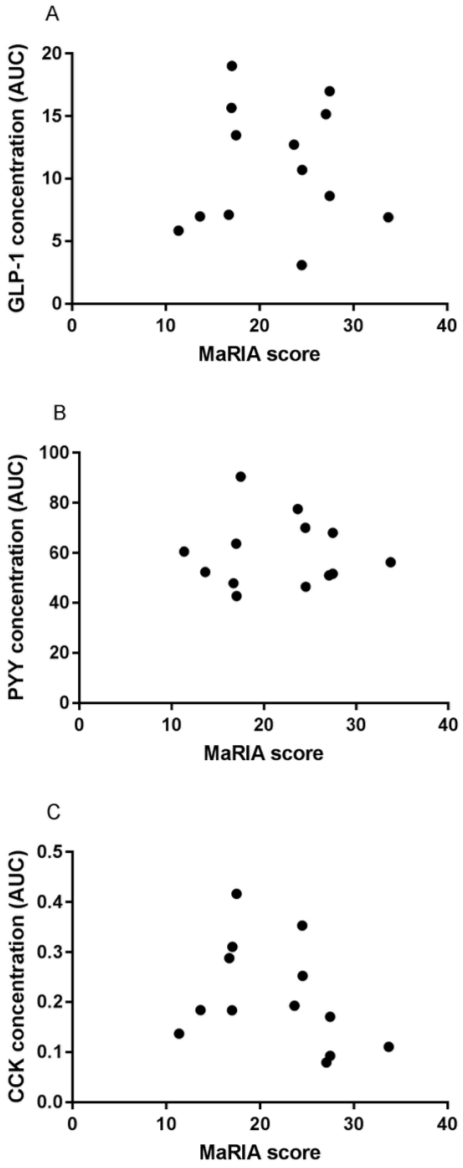

Figure 42: Correlation between MaRIA scores and different peptides. A. Correlation between GLP-1 concentrations measured as AUC and MaRIA scores. (r=0.03, p=0.93, n=13). B. Correlation between PYY concentrations measured as AUC and MaRIA scores. (r=-0.02, p=0.96, n=13). C. Correlation between CCK concentrations measured as AUC and MaRIA scores. (r=-0.36, p=0.23, n=13).

Outcome	Fasting	Postprandial
Gall bladder volumes	↑	↑
Gastric volumes	-	-
Small bowel motility	↑↑	-
Small bowel water content	-	↑↑
Total GLP-1	↑↑	↑↑
PYY	↑↑	↑↑
CCK	-	↑
Fullness	↑↑	↑↑
Bloating	↑	↑↑
Distention	↑↑	↑↑
Abdominal pain	↑↑	↑↑
Sickness	-	↑↑

Table 7: A summary table describing the differences seen between CD subjects and HV in each measured outcome. (No difference - ; ↑ some difference; ↑↑ a significant difference).

4.4 Discussion

This is the first work measuring small bowel motility in the unprepared small bowel of CD patients and comparing this to healthy volunteers. The measured fasting small bowel motility was significantly ($p<0.05$) lower in CD group compared to healthy controls. In parallel, similar results were found in previous study but performed on prepared

bowel[164]. Patients with active terminal ileum CD showed a significantly reduced small bowel motility compared to healthy subjects[164]. In our data, this was followed by immediate maximum increase in motility after feeding in both groups.

The fasting and postprandial plasma levels of GLP-1 were significantly ($p<0.0001$) higher in CD compared to healthy volunteers. This was confirmed in previous studies in which the measured postprandial GLP-1 levels were elevated in IBD patients[118]. PYY levels were significantly elevated in CD group compared to healthy controls with significant higher fasting levels in CD. This was noted in previous studies in which plasma peptide levels were elevated in CD[109, 118]. Healthy volunteers and CD patients had similar fasting CCK levels.

No significant difference was seen in the fasting and postprandial gall bladder volumes in CD compared to healthy volunteers. The lack of difference in CCK levels between the two groups explains the lack of difference in the gall bladder volumes. Additionally, previous data showed a similar non-significant fasting gall bladder volumes in both healthy volunteers and patients with small bowel CD[165, 166]. The soup meal used in our studies has a homogenous appearances in MRI images. The half gastric emptying time ($T_{1/2}$) was 43±4 min in healthy volunteers and 63±7.5 min in CD subjects. In both groups the gastric emptying was approximately linear from t=0 min to t=90 min. Gastric emptying is controlled by gut hormones. Fasting and postprandial CCK levels did not show a significant difference, however, fasting and

postprandial PYY and GLP-1 were significantly higher in CD compared to HV. A delay in gastric emptying in CD group was expected but no significant decrease was noted.

As discussed earlier for the MIC1 study, small bowel water contents in healthy volunteers showed two peaks. The first peak presented the gastric phase and the second peak presented the intestinal phase. A bimodal postprandial peaks were also seen in the SBWC in CD group, with significant postprandial difference ($p<0.05$) in volume compared to healthy volunteers. None of the CD subjects had predominant stricture which may have caused a delay in intestinal transit and might explain the increase in small bowel water content. The noted increase could be due to the high CCK levels which leads to an increase in bile acid production and pancreatic secretion. Additionally, the meal can act as an osmotic stimulus causing the increase in the small bowel water content. We believe that the increase in SBWC in CD group from t=90 min might cause the increase in small bowel motility by stimulating smooth muscle contraction.

The CD group demonstrated a significantly higher ($p<0.05$) postprandial symptom's VAS scores, with significantly higher ($p<0.05$) fasting fullness, distention and abdominal pain scores compared to healthy volunteers. The bowel distention in CD and the increase in small bowel water content might explain the significant difference in the measured symptoms.

There were limitations of this work, the soup meal used was small in volume and nutrients. However, it was well tolerated by all the patients and it was a good stimulus that produced GI responses reliably. Another limitation is the small patient population with only 15 active CD patients and 20 healthy volunteers and also the broad age range. Active disease was defined using the MaRIA score as the HBI was not a sensitive marker of the disease activity while MaRIA, CRP and fC were. Moreover, we only measured the plasma levels of the gut hormones, no cytokines were measured.

This study is observational, it would have been good to repeat this in a mechanistic study with a specific GI peptide inhibitor and examine the effect of the peptides and cytokines on the different parameters. Furthermore, repeating the study in remission would have been useful too but in that case the GI peptides and the cytokines will be normalised.

In this work we successfully quantified small bowel motility and different physiological outcomes in unprepared small bowel during fasting and after a nutrient soup meal. The assessment of fasted and fed small bowel motility using MRI is important to more accurately design and monitor diagnosis and therapeutic strategies. Further future work may be able to normalise such dysmotility through GI peptide inhibitors.

5. Gastric emptying by MRI and gamma scintigraphy (GEMRIGS)

After the successful use of the soup meal in both cohorts, in healthy volunteers and in CD, we wanted to explore its possible use with different image modality.

5.1 Introduction

The importance of measuring gastric emptying in the clinical and in the research arenas has long been recognised for a range of conditions including gastroparesis[167], dyspepsia[168] and dumping syndrome[169]. Various techniques have been used over the years to measure gastric emptying. Methods such as dilution-intubation techniques[170], paracetamol absorption test[171], stable isotope breath tests[172] and ultrasound[173] have limitations. GS has gained an established role and is very often considered the 'gold standard' for gastric emptying[174]. The use of MRI of gastric emptying[175] has however recently increased[176, 177] due to its lack of use of ionizing radiation, multi-planar ability, spatial resolution and richness of contrast mechanisms[47].

Gastric MRI and GS however have image inherently different physical parameters. MRI is based on the radiofrequency signal arising from the spatial distribution of water hydrogen protons in a test meal; GS is based on the radiation counts emitted by a radiolabelled test meal in the stomach. This physical difference indicated a need to compare the

gastric emptying parameters obtained with the two techniques. Historical comparison studies between MRI and GS showed good correlation of the two modalities[175, 178] although these studies were performed on separate days and in a limited number of subjects. In more recent literature there has been renewed interest in comparing the two techniques for gastric emptying. Two study found good correlation between the two modalities, once the additional contribution of secretion volume had been considered[142, 149]. Another recent study of gastrointestinal complications after lung transplantation found no significant differences in gastric emptying parameters between MRI and GS[179].

These studies were however necessarily performed on two separate study days. This may add potential intra-individual confounds and does not allow for a direct comparison of gastric emptying curves acquired on the same study day.

In our research facilities, there is a MRI scanner unit located next to a gamma camera unit. Is this study we exploited the physical proximity of the two modalities. We aimed to evaluate the correlation of gastric emptying between MRI and GS performed on the same day in the same healthy participants, alternating the two modalities throughout the emptying of a test meal.

5.2 Methodology

5.2.1 Subjects

Twelve healthy volunteers (age 22±0.4 years, BMI 24±1.0 kg/m^2), were recruited from the local campus population by poster advertisement from January 2018 to March 2018. This study was approved by the Administration of Radioactive Substances advisory Committee (ARSAC approval RPC 253/3849/37292), the Research Ethics Committee (REC approval 17/EM/0151) and the Health research Authority (Protocol Number 17016). Informed written consent was obtained from all individual participants included in the study. This study was funded by Kuwait Foundation for the Advancement of Sciences (KFAS) under project code CB17-63NR-01.

5.2.2 Test meal challenge

The soup meal challenge was the same as for MIC1 and MIC2. The soup was radiolabelled with 5MBq of 99mTc which resulted in an effective radiation dose of 0.125 mSv. This dose was low and is similar approximately to that provided by a skull X-Ray or that provided by approximately three weeks of natural background radiation. This dose and radiolabelling methods have been used previously by our group in healthy volunteer studies[149].

Radiopharmaceuticals (99mTc-DTPA) were supplied by the Radiopharmacy Unit, Medical Physics and Clinical Engineering at Queen's Medical Centre Campus, Nottingham University Hospitals NHS

Trust, Nottingham. The radiolabelling was performed by study personnel under Good Manufacturing Practice (GMP) conditions.

Preparation of the test meal conformed to food hygiene legislation and prepared in a designated radiolabelling food preparation area. All manufacturing details were recorded within the Trial Master File (TMF). The radiolabelled test meal was administered orally on the morning of the study following an overnight fast, and details of ingestion of the meal was observed and recorded.

5.2.3 Eligibility

Inclusion criteria:

- Healthy volunteer, male or female.
- Age – 18-75 years.
- BMI – 18-30 kg/m^2.
- Able to understand English language.

Exclusion criteria:

- Any history of gastrointestinal disease
- If a smoker, unable to refrain from midnight until after test finishes.
- Subjects currently (or in the last three months) participating in another research project.
- Pregnancy or breastfeeding.
- MRI contraindication (e.g. pacemaker).
- Use of medication that could affect gastrointestinal function.

5.2.4 *In vitro* validation

The use of the soup meal has been validated before the start of the study. Canned chicken soup was mixed with simulated gastric fluid and 5MBq of 99mTc in a glass beaker. Images were taken using gamma scintigraphy.

Figure 43: images illustrating the in vitro experiment. The soup meal was mixed with simulated gastric fluid and 99mTc.

5.2.5 Study design

Visit1

Participants attended the Nottingham Digestive Disease Centre (NDDC) division in the School of Medicine. They had the participant information sheet posted to them in advance in order for them to be able to give an informed consent. They met one of the investigators and went through the study information and eligibility questionnaire. Once eligible and wished to participate, they gave informed consent. They were informed of their study day details and discharged.

On the day before the arranged study day (Visit 2) the subjects were asked to fast from 2000 h and to avoid alcohol, caffeine, strenuous exercise and any self-reported medication that could affect gastrointestinal function for 18 h before the experiment.

Visit 2

On the day of the scans, they were only be allowed a small glass of water on waking. The participants once again attended at the NDDC unit at 0800 hrs. They were asked to fill in a questionnaire to ensure adherence to the study day restrictions. They were asked to change their clothing into a gown which was provided and to remove all metal objects (e.g. watches, jewellery).

A baseline measurement was taken by MRI. The participants were then transported rapidly by wheelchair to the adjacent gamma scintigraphy unit (100 meters down the same corridor of the Medical School) (Figure 42). Small Radioactive markers were affixed to the subject at the right costal margin, both anteriorly and posteriorly.

They were then asked to consume the radiolabelled soup test meal within 20 minutes. They then stood in front of the gamma camera and anterior and posterior images each of 30 seconds duration were recorded using a Mediso Gamma Camera (Nucline X-Ring-R, Budapest, Hungary) connected to a dedicated nuclear medicine computer as described previously[149].

The participant was transported quickly by wheelchair back to the adjacent MRI unit where MRI data point were acquired. The subject was then transported back to the GS unit and this was repeated approximately every 30 minutes for a total of 150 minutes, which previous studies suggest is the time by which most people will have emptied all the meal from the stomach. By doing so we collected at 6 data points per technique, per subject as required.

Figure 44: The Mediso Gamma Camera (Nucline X-Ring-R, Budapest, Hungary) at QMC.

5.2.6 MRI protocol and data analysis

MRI imaging was performed using a 1.5T GE Signa HDx MRI scanner (GE Healthcare, Milwaukee, WI). At each time point, scans were acquired using a balanced steady-state gradient echo sequence (FIESTA) sequence with slice thickness 5 mm, echo time (TE)=1.2 ms, repetition time (TR)=3.5 ms, flip angle 80º, within one breath hold of ~16 seconds. This imaging sequence yields good contrast between the stomach contents and other abdominal organs.

Gastric volumes from the MRI datasets were quantified using in house software written in IDL[142] as previously described in our previous studies. The retention rates (RR) (%) of gastric content volumes were also calculated, as the percentage of gastric content volume in the stomach at each time point relative to the gastric content volume measured at time 0[179].

5.2.7 GS protocol and data analysis

A Mediso Gamma Camera (Nucline X-Ring-R, Budapest, Hungary) was used as described previously[149]. Two small radiolabelled markers were affixed to the costal margin of the participants for the duration of the gastric emptying study. At each time point the participants stood in front of the gamma camera. Anterior and posterior images each of 30 seconds duration were recorded.

Gastric volumes were analysed from the coded, anonymised images using methods described previously[142]. To measure gastric

emptying by GS ROIs were defined around the labelled meal in the stomach and around an area of background activity in the anterior and posterior images[149]. All counts were corrected for background radiation and radioactive decay. The values for each participant at each time point were then expressed as the percentage of activity relative to the counts obtained at time 0. The same process was repeated for all subsequent scans. $T_{1/2}$ was then calculated using the same equation fit as for the MRI data.

5.2.8 Statistical analysis

Data analysis were performed using GraphPad Prism version 7.01 (GraphPad Software Inc., La Jolla, CA, USA). Results are presented as mean±SEM. All data were tested for normality using the D'Agostino and Shapiro–Wilk's test. Paired Student's t test was used to assess the significance of differences in $T_{1/2}$. Pearson correlation coefficient was used to measure the strength of correlation between the two modalities for $T_{1/2}$ and for the RRs at different time points.

5.3 Results

All 12 participants tolerated the study procedures well and completed the study. Example of MRI and gamma scintigraphy images of the stomach at different time points are shown in Figure 43.

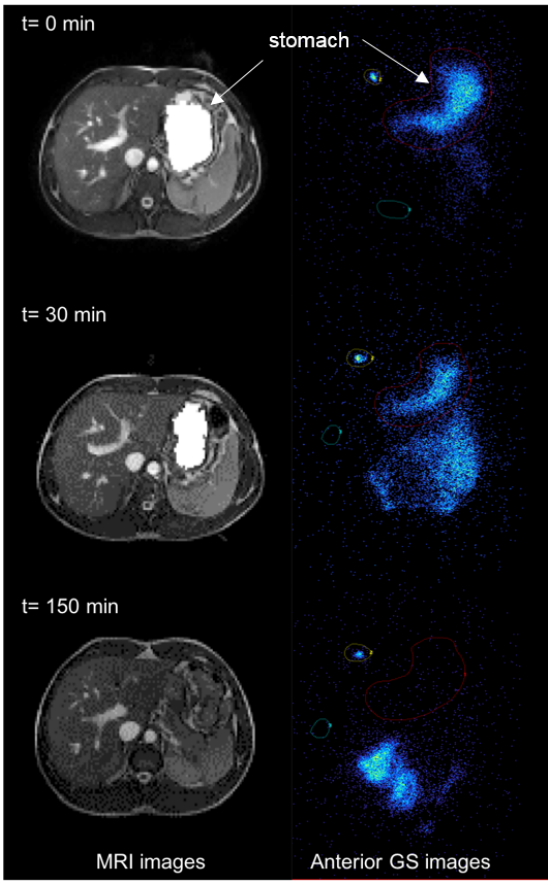

Figure 45: Example of MRI and GS images of the stomach at different time points after a participant consume the soup meal. (t=0 just after feeding, t=30 min after feeding and t=150 min at the end of the study period). The axial, moderately T2 weighted images are shown on the left hand of the panel and the coronal gamma scintigraphy images are shown on the right hand of the panel, with labels and arrows to indicate stomach.

MRI

The fasted baseline gastric volumes (Figure 44) showed a small amount of resting gastric juices of 41±10 mL. After the ingestion of the meal, volumes increased significantly ($p<0.0001$) to reach the maximum immediately after feeding (367±14 mL). This was followed by a decline

in the volumes reaching the baseline at 150 min (35.5±6.2 mL). The average time to empty half of the stomach contents ($T_{1/2}$) was 44±6 min.

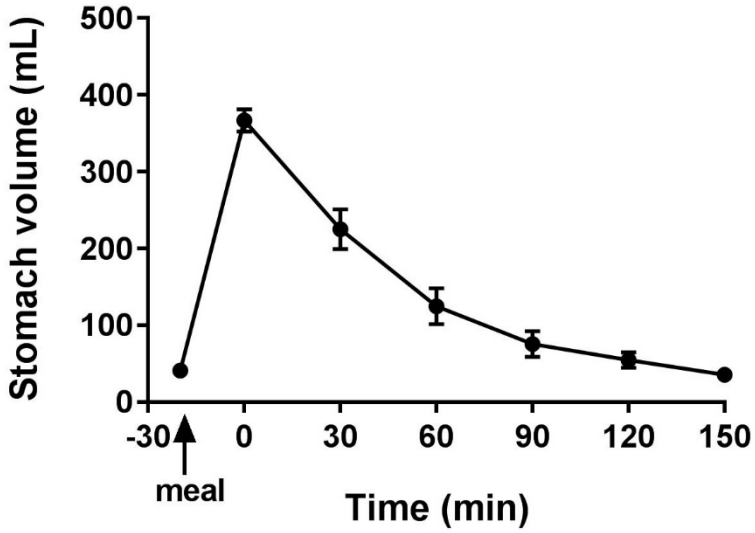

Figure 46: Gastric volumes measured with MRI plotted against time before and after feeding the soup test meal with arrow to indicate the meal time. n=12 participants, data are shown as mean ± SEM.

GS

The gastric emptying curve of n=12 subjects presented by the percentage of activity in the radiolabelled meal is shown in Figure 45. The average time to empty half of the stomach contents ($T_{1/2}$) was of 35±4 min with a modest but significant difference from the $T_{1/2}$ measured by MRI ($p<0.004$).

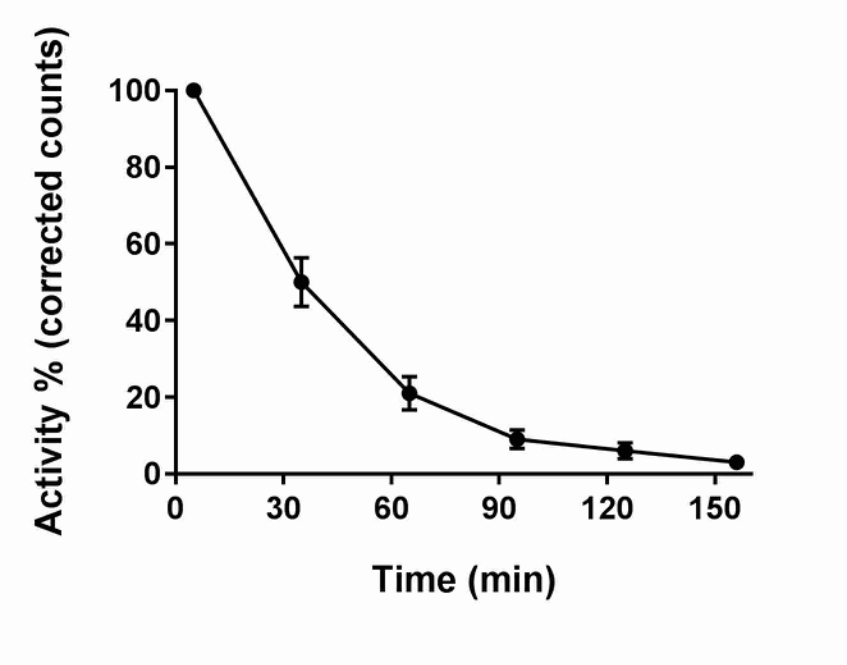

Figure 47: Percentage of activity in the stomach's region of interest measured with GS plotted against time after feeding the soup test meal. n=12 participants, data are shown as mean ± SEM. Counts were corrected for background radioactivity and radioisotope decay.

Correlation of MRI and GS

We examined the strength of correlation between the two imaging modalities using the half-emptying time ($T_{1/2}$) .The correlation between MRI and GS (Figure 46) showed a good positive correlation between both techniques MRI and GS (n=12, Pearson's r=0.95, p<0.0001). The RRs at different time points also correlated well at all time points but the last t=150 min with the parameters being Pearson's r=0.91, p<0.00004 for RR30; Pearson's r=0.95, p<0.000002 for RR60; Pearson's r=0.94, p<0.00004 for RR90; Spearman's r=0.64, p<0.03 for RR120 and Spearman's r=0.20, p<0.54 for RR150.

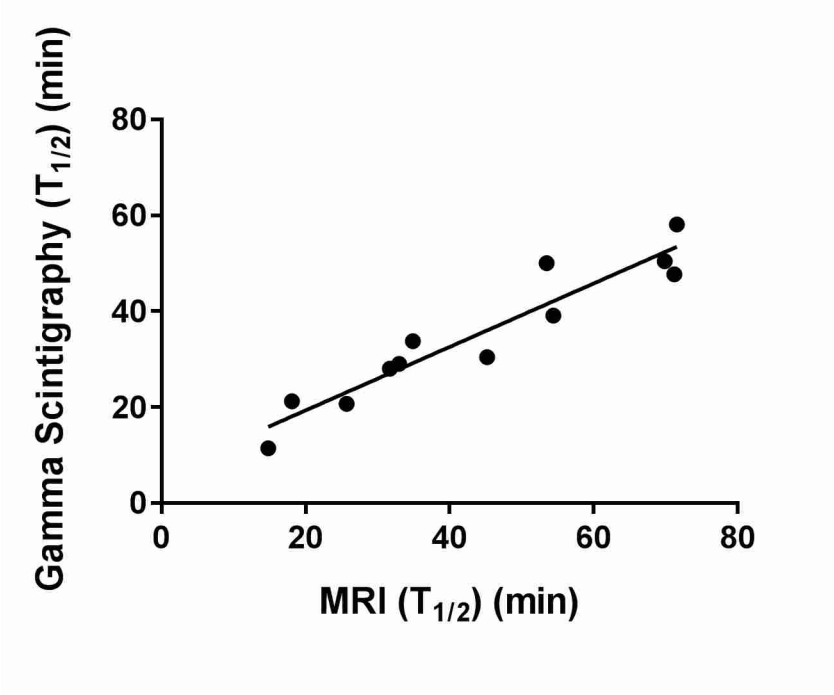

Figure 48: Plot of the correlation between gastric half emptying times measured by MRI and GS (n=12, Pearson's r=0.95, p<0.0001). Each data point represent the $T_{1/2}$% for a given participant measured, respectively, by MRI and gamma scintigraphy.

5.4 Discussion

Alteration in gastric emptying has been linked to patient symptoms in functional gastrointestinal diseases. This led to the development of variety of techniques to assess and study gastric emptying. Different techniques have been used each with limitations and disadvantages. Some of these disadvantages include exposure to a small amount of radiation during gamma scintigraphy, difficulties in measuring gastric emptying using ultrasonography due to the presence of air[180], and possible alteration in normal physiology with gastrointestinal

intubation[181]. MRI has been used to measure fasting and postprandial gastric volumes[143, 175, 176] and most recently semi-automatic MRI analysis has been validated against gamma scintigraphy[142]. To our knowledge there are no studies whereby gastric empting of a meal has been validated concomitantly, on the same day, with both MRI and gamma scintigraphy.

This study had various limitations. MRI scanning was carried out in the supine position, which is different from the standing GS position. However, the soup meal remains homogeneous thus we would not expect any possible layering effect on gastric emptying and the MRI scan time was also very brief. The significantly longer time measured by MRI could reflect the ability of MRI to include secretions in the measured gastric volumes, not just the emptying of a label.

In conclusion, in this study gastric emptying was measured by MRI and GS on the same study day for the first time, to avoid confounds. The time to half emptying and the retention rates correlated well. This may help translating the use of this simple soup meal known to elicit reliable physiological and pathological gastrointestinal motor, peptide and appetite responses.

6. Conclusion and future directions

In this work, we were able to quantify and monitor successfully different MRI parameters of gastrointestinal function fasting and postprandially after a soup meal intervention. The measurements were carried out in CD and compared to physiological GI peptide responses and symptoms in healthy volunteers. Although the soup meal was small in volume and nutrients and absorbed quickly in the gut, it provided a good and reliable stimulus for GI responses which highlighted differences between the groups rather than having a supra-physiological stimulus in which could have masked differences between groups. Moreover, it was well tolerated in the patient population and it could be prepared and administered easily and in a timely fashion in a clinical setting.

We also developed a technique for the analysis of small bowel motility from cine MRI images of the unprepared bowel in both fasting and fed states. This will be useful in studying the time scales of global or regional contractile activity and patterns along the gastrointestinal tract in health and disease. Monitoring small bowel motility using MRI could have an impact on the diagnosis of small bowel pathologies like CD. Considering the increasing clinical availability of MRI scanners, this technique has the potential to improve our knowledge of the pathophysiology of gastrointestinal tract under normal physiological conditions.

The disease location might have an important impact in studying CD. The CD location in this recruited cohort was predominantly ileal rather than proximal in the duodenum where the CCK secreting I cells are located. This might explain the lack of difference in CCK concentration between both groups. Although earlier data in IBD murine models suggested that EEC upregulation occurs irrespective of the anatomical location of intestinal inflammation[182], this observation was later refuted in CD[116].

In this work, the bowel distention in CD and the increase in small bowel water content might explain the significant difference in the measured symptoms although the actual difference in small bowel water content accounts to only 40 mL that might not have been enough to account for such a radical difference in symptoms. It is interesting that the correlation between small bowel water content and MaRIA scores fell just outside the significance threshold, whilst no conclusions can be drawn at this stage future work should consider this again, perhaps in a larger cohort with increased power. Additionlly, both groups had a similar fasting small bowel water content volumes, but symptoms scores were significantly elevated in CD subjects. Possibly, a central effect of an otherwise upregulated gut-brain axis via vagal nerve might be a more possible cause for these exaggerated symptoms. Further future studies are needed to examine the role of the gut-brain axis in CD.

In addition, identifying the link between gut peptides, motility and aversive symptoms has pharmacological relevance. Pharmacological

EEC peptide modulators (exendin 9-39[183] and dexloxiglumide[184]) are now available. With the use of the peptides modulators and with the increased knowledge of the relationship between dysmotility and aversive symptoms, gut peptides could be targeted pharmacologically. This work can potentially open a new therapeutic pathway in CD therapy by targeting motility and consequent symptoms, thus improving nutritional status, disease outcomes and quality of life in a significant number of individuals.

Therefore, It would be interesting to replicate this pilot work in a larger cohort with a specific GI peptide inhibitor and to examine the effect of the peptide modulators on the different measured parameters. It would be also be very interesting to use this methodology to study CD patients in remission when the GI peptide response would have been normalised, and examine the different MRI parameters.

In conculsion, we have shown a significant difference in fasting motility, postprandial water content, EEC peptide response and key patient symptoms in CD compared to healthy volnteers. This work is starting to provide novel insights into the possible aetiology of the altered intestinal physiology and aversive manifestations that CD patients experience.

References

1. Bruen CM, O'Halloran F, Cashman KD, et al. The effects of food components on hormonal signalling in gastrointestinal enteroendocrine cells. Food & Function 2012;3:1131-1143.
2. Mushref MA, Srinivasan S. Effect of high fat-diet and obesity on gastrointestinal motility. Annals of Translational Medicine 2013;1:14.
3. Hellstrom PM, Gryback P, Jacobsson H. The physiology of gastric emptying. Best Practice & Research. Clinical Anaesthesiology 2006;20:397-407.
4. Hunt JN. Mechanisms and disorders of gastric emptying. Annual Review of Medicine 1983;34:219-29.
5. Toms AP, Farghal A, Kasmai B, et al. Physiology of the small bowel: A new approach using MRI and proposal for a new metric of function. Medical Hypotheses 2011;76:834-839.
6. McCoy EJ, Baker RD. Effect of feeding on electrical activity of dog's small intestine. The American Journal of Physiology 1968;214:1291-1295.
7. Carlson GM, Bedi BS, Code CF. Mechanism of Propagation of Intestinal Interdigestive Myoelectric Complex. American Journal of Physiology 1972;222:1027-&.
8. McLaughlin J. Gastrointestinal physiology. Surgery (Oxford) 2009;27:225-230.

9. Sadik R, Abrahamsson H, Stotzer PO. Gender differences in gut transit shown with a newly developed radiological procedure. Scand J Gastroenterol 2003;38:36-42.

10. Sternini C, Anselmi L, Rozengurt E. Enteroendocrine cells: a site of 'taste' in gastrointestinal chemosensing. Current Opinion in Endocrinology Diabetes and Obesity 2008;15:73-78.

11. Posovszky C, Wabitsch M. Regulation of appetite, satiation, and body weight by enteroendocrine cells. Part 1: characteristics of enteroendocrine cells and their capability of weight regulation. Hormone Research in Paediatrics 2015;83:1-10.

12. Huda MSB, Wilding JPH, Pinkney JH. Gut peptides and the regulation of appetite. Obesity Reviews 2006;7:163-182.

13. Janssen P, Vanden Berghe P, Verschueren S, et al. Review article: the role of gastric motility in the control of food intake. Alimentary Pharmacology & Therapeutics 2011;33:880-894.

14. Gibbs J, Young RC, Smith GP. Cholecystokinin Elicits Satiety in Rats with Open Gastric Fistulas. Nature 1973;245:323-325.

15. McLaughlin J, Luca MG, Jones MN, et al. Fatty acid chain length determines cholecystokinin secretion and effect on human gastric motility. Gastroenterology 1999;116:46-53.

16. Liou AP, Lu XP, Sei Y, et al. The G-Protein-Coupled Receptor GPR40 Directly Mediates Long-Chain Fatty Acid-Induced Secretion of Cholecystokinin. Gastroenterology 2011;140:903-912.

17. Kissileff HR, Pi-Sunyer FX, Thornton J, et al. C-terminal octapeptide of cholecystokinin decreases food intake in man. The American Journal of Clinical Nutrition 1981;34:154-60.

18. Field BCT, Wren AM, Cooke D, et al. Gut hormones as potential new targets for appetite regulation and the treatment of obesity. Drugs 2008;68:147-163.

19. Anini Y, Fu-Cheng XM, Cuber JC, et al. Comparison of the postprandial release of peptide YY and proglucagon-derived peptides in the rat. Pflugers Archiv-European Journal of Physiology 1999;438:299-306.

20. Batterham RL, Cohen MA, Ellis SM, et al. Inhibition of food intake in obese subjects by peptide YY3-36. New England Journal of Medicine 2003;349:941-948.

21. Spiller RC, Trotman IF, Adrian TE, et al. Further Characterization of the Ileal Brake Reflex in Man - Effect of Ileal Infusion of Partial Digests of Fat, Protein, and Starch on Jejunal Motility and Release of Neurotensin, Enteroglucagon, and Peptide Yy. Gut 1988;29:1042-1051.

22. Wen J, Phillips SF, Sarr MG, et al. PYY and GLP-1 contribute to feedback inhibition from the canine ileum and colon. The American Journal of Physiology 1995;269:G945-52.

23. Witte AB, Gryback P, Holst JJ, et al. Differential effect of PYY1-36 and PYY3-36 on gastric emptying in man. Regulatory Peptides 2009;158:57-62.

24. Lin HC, Chey WY, Zhao X. Release of distal gut peptide YY (PYY) by fat in proximal gut depends on CCK. Peptides 2000;21:1561-3.

25. Little TJ, Pilichiewicz AN, Russo A, et al. Effects of intravenous glucagon-like peptide-1 on gastric emptying and intragastric distribution in healthy subjects: Relationships with postprandial glycemic and insulinemic responses. Journal of Clinical Endocrinology & Metabolism 2006;91:1916-1923.

26. Drucker DJ. The biology of incretin hormones. Cell Metabolism 2006;3:153-165.

27. Baggio LL, Drucker DJ. Biology of incretins: GLP-1 and GIP. Gastroenterology 2007;132:2131-2157.

28. Ludwig DS. The glycemic index - Physiological mechanisms relating to obesity, diabetes, and cardiovascular disease. Jama-Journal of the American Medical Association 2002;287:2414-2423.

29. Tolessa T, Gutniak M, Holst JJ, et al. Inhibitory effect of glucagon-like peptide-1 on small bowel motility. Fasting but not fed motility inhibited via nitric oxide independently of insulin and somatostatin. The Journal of Clinical Investigation 1998;102:764-74.

30. Schirra J, Nicolaus M, Roggel R, et al. Endogenous glucagon-like peptide 1 controls endocrine pancreatic secretion and antro-pyloro-duodenal motility in humans. Gut 2006;55:243-251.

31. Hellstrom PM, Naslund E, Edholm T, et al. GLP-1 suppresses gastrointestinal motility and inhibits the migrating motor complex in

healthy subjects and patients with irritable bowel syndrome. Neurogastroenterology and Motility 2008;20:649-59.

32. Patcharatrakul T, Gonlachanvit S. Technique of Functional and Motility Test: How to Perform Antroduodenal Manometry. Journal of Neurogastroenterology and Motility 2013;19:395-404.

33. Hamilton MJ. The valuable role of endoscopy in inflammatory bowel disease. Diagnostic and Therapeutic Endoscopy 2012;2012:1-8.

34. Sarosiek I, Selover KH, Katz LA, et al. The assessment of regional gut transit times in healthy controls and patients with gastroparesis using wireless motility technology. Alimentary Pharmacology & Therapeutics 2010;31:313-322.

35. O'Donnell S, Qasim A, Ryan BM, et al. The role of capsule endoscopy in small bowel Crohn's disease. Journal of Crohns & Colitis 2009;3:282-286.

36. Solem CA, Loftus EV, Fletcher JG, et al. Small-bowel imaging in Crohn's disease: a prospective, blinded, 4-way comparison trial. Gastrointestinal Endoscopy 2008;68:255-266.

37. Frokjaer JB, Drewes AM, Gregersen H. Imaging of the gastrointestinal tract-novel technologies. World Journal of Gastroenterology 2009;15:160-168.

38. Di Sabatino A, Armellini E, Corazza GR. Doppler sonography in the diagnosis of inflammatory bowel disease. Digestive Diseases 2004;22:63-66.

39. Haruma K, Kusunoki H, Manabe N, et al. Real-time assessment of gastroduodenal motility by ultrasonography. Digestion 2008;77:48-51.

40. Aschoff AJ. MDCT of the abdomen. European Radiology 2006;16 Suppl 7:54-57.

41. Ryan ER, Heaslip ISE. Magnetic resonance enteroclysis compared with conventional enteroclysis and computed tomography enteroclysis: a critically appraised topic. Abdominal Imaging 2008;33:34-37.

42. Brenner DJ, Hall EJ. Current concepts - Computed tomography - An increasing source of radiation exposure. New England Journal of Medicine 2007;357:2277-2284.

43. Mariani G, Boni G, Barreca M, et al. Radionuclide gastroesophageal motor studies. Journal of Nuclear Medicine 2004;45:1004-1028.

44. Giaffer MH, Tindale WB, Holdsworth D. Value of technetium-99m HMPAO-labelled leucocyte scintigraphy as an Initial screening test in patients suspected of having inflammatory bowel disease. European Journal of Gastroenterology & Hepatology 1996;8:1195-1200.

45. Scholmerich J, Schmidt E, Schumichen C, et al. Scintigraphic assessment of bowel involvement and disease activity in Crohn's disease using technetium 99m-hexamethyl propylene amine oxine as leukocyte label. Gastroenterology 1988;95:1287-93.

46. Sans M, Fuster D, Llach J, et al. Optimization of technetium-99m-HMPAO leukocyte scintigraphy in evaluation of active inflammatory bowel disease. Digestive Diseases and Sciences 2000;45:1828-1835.

47. Marciani L. Assessment of gastrointestinal motor functions by MRI: a comprehensive review. Neurogastroenterology and Motility 2011;23:399-407.

48. Sinha R, Rajiah P, Murphy P, et al. Utility of High-Resolution MR Imaging in Demonstrating Transmural Pathologic Changes in Crohn Disease. Radiographics 2009;29:1847-1867.

49. McRobbie DW, Moore EA, Graves MJ, et al. MRI from picture to proton. Cambridge, UK ; New York: Cambridge University Press, 2003.

50. Knuesel PR, Kubik RA, Crook DW, et al. Assessment of dynamic contrast enhancement of the small bowel in active Crohn's disease using 3D MR enterography. European Journal of Radiology 2010;73:607-13.

51. Cronin CG, Lohan DG, Browne AM, et al. MR enterography in the evaluation of small bowel dilation. Clinical Radiology 2009;64:1026-1034.

52. Fidler JL, Guimaraes L, Einstein DM. MR Imaging of the Small Bowel. Radiographics 2009;29:1811-1826.

53. Patak MA, Froehlich JM, von Weymarn C, et al. Non-invasive distension of the small bowel for magnetic-resonance imaging. Lancet 2001;358:987-8.

54. Froehlich JM, Patak MA, von Weymarn C, et al. Small bowel motility assessment with magnetic resonance imaging. Journal of Magnetic Resonance Imaging 2005;21:370-5.

55. Menys A, Taylor SA, Emmanuel A, et al. Global Small Bowel Motility: Assessment with Dynamic MR Imaging. Radiology 2013;269:442-449.

56. Hahnemann ML, Nensa F, Kinner S, et al. Motility Mapping as Evaluation Tool for Bowel Motility: Initial Results on the Development of an Automated Color-Coding Algorithm in Cine MRI. Journal of Magnetic Resonance Imaging 2015;41:354-360.

57. Odille F, Menys A, Ahmed A, et al. Quantitative assessment of small bowel motility by nonrigid registration of dynamic MR images. Magnetic Resonance in Medicine 2012;68:783-793.

58. Bickelhaupt S, Froehlich JM, Cattin R, et al. Software-assisted small bowel motility analysis using free-breathing MRI: feasibility study. Journal of Magnetic Resonance Imaging 2014;39:17-23.

59. van der Paardt MP, Sprengers AMJ, Zijta FM, et al. Noninvasive Automated Motion Assessment of Intestinal Motility by Continuously Tagged MR Imaging. Journal of Magnetic Resonance Imaging 2014;39:9-16.

60. Van Assche G, Dignass A, Panes J, et al. The second European evidence-based Consensus on the diagnosis and management of Crohn's disease: Definitions and diagnosis. Journal of Crohns & Colitis 2010;4:7-27.

61. Mowat C, Cole A, Windsor A, et al. Guidelines for the management of inflammatory bowel disease in adults. Gut 2011;60:571-607.

62. Luces C, Bodger K. Economic burden of inflammatory bowel disease: a UK perspective. Expert Review of Pharmacoeconomics Outcomes Research 2006;6:471-482.

63. Lala S, Ogura Y, Osborne C, et al. Crohn's disease and the NOD2 gene: a role for paneth cells. Gastroenterology 2003;125:47-57.

64. Tlaskalova-Hogenova H, Stepankova R, Kozakova H, et al. The role of gut microbiota (commensal bacteria) and the mucosal barrier in the pathogenesis of inflammatory and autoimmune diseases and cancer: contribution of germ-free and gnotobiotic animal models of human diseases. Cellular & Molecular Immunology 2011;8:110-120.

65. Baumgart DC, Sandborn WJ. Crohn's disease. Lancet 2012;380:1590-1605.

66. Wallace KL, Zheng LB, Kanazawa Y, et al. Immunopathology of inflammatory bowel disease. World Journal of Gastroenterology 2014;20:6-21.

67. Sokol H, Seksik P, Rigottier-Gois L, et al. Specificities of the fecal microbiota in inflammatory bowel disease. Inflammatory Bowel Diseases 2006;12:106-111.

68. Emge JR, Huynh K, Miller EN, et al. Modulation of the microbiota-gut-brain axis by probiotics in a murine model of inflammatory bowel disease. American Journal of Physiology-Gastrointestinal and Liver Physiology 2016;310:G989-G998.

69. Ott SJ, Kuhbacher T, Musfeldt M, et al. Fungi and inflammatory bowel diseases: Alterations of composition and diversity. Scandinavian Journal of Gastroenterology 2008;43:831-841.

70. Zeissig S, Burgel N, Gunzel D, et al. Changes in expression and distribution of claudin 2, 5 and 8 lead to discontinuous tight junctions and barrier dysfunction in active Crohn's disease. Gut 2007;56:61-72.

71. Silverberg MS, Satsangi J, Ahmad T, et al. Toward an integrated clinical, molecular and serological classification of inflammatory bowel disease: Report of a Working Party of the 2005 Montreal World Congress of Gastroenterology. Canadian Journal of Gastroenterology and Hepatology 2005;19:5A-36A.

72. Gassull MA, Cabre E. Nutrition in inflammatory bowel disease. Current Opinion in Clinical Nutrition and Metabolic Care 2001;4:561-569.

73. Filippi J, Al-Jaouni R, Wiroth JB, et al. Nutritional deficiencies in patients with Crohn's disease in remission. Inflammatory Bowel Diseases 2006;12:185-191.

74. Lochs H, Dejong C, Hammarqvist F, et al. ESPEN guidelines on enteral nutrition: Gastroenterology. Clinical Nutrition 2006;25:260-274.

75. Ghosh S, Mitchell R. Impact of inflammatory bowel disease on quality of life: Results of the European Federation of Crohn's and Ulcerative Colitis Associations (EFCCA) patient survey. Journal of Crohns & Colitis 2007;1:10-20.

76. Lin JF, Chen JM, Zuo JH, et al. Meta-analysis: Fecal Calprotectin for Assessment of Inflammatory Bowel Disease Activity. Inflammatory Bowel Diseases 2014;20:1407-1415.

77. Mosli MH, Zou GY, Garg SK, et al. C-Reactive Protein, Fecal Calprotectin, and Stool Lactoferrin for Detection of Endoscopic Activity in Symptomatic Inflammatory Bowel Disease Patients: A Systematic Review and Meta-Analysis. American Journal of Gastroenterology 2015;110:802-819.

78. Mao R, Xiao YL, Gao X, et al. Fecal calprotectin in predicting relapse of inflammatory bowel diseases: A meta-analysis of prospective studies. Inflammatory Bowel Diseases 2012;18:1894-1899.

79. D'Inca R, Dal Pont E, Di Leo V, et al. Can calprotectin predict relapse risk in inflammatory bowel disease? American Journal of Gastroenterology 2008;103:2007-2014.

80. Sipponen T, Savilahti E, Kolho KL, et al. Crohn's disease activity assessed by fecal calprotectin and lactoferrin: correlation with Crohn's disease activity index and endoscopic findings. Inflammatory Bowel Diseases 2008;14:40-46.

81. Koutroumpakis E, Katsanos KH. Implementation of the simple endoscopic activity score in crohn's disease. Saudi Journal of Gastroenterology 2016;22:183-191.

82. Voderholzer WA, Beinhoelzl J, Rogalla P, et al. Small bowel involvement in Crohn's disease: a prospective comparison of wireless capsule

endoscopy and computed tomography enteroclysis. Gut 2005;54:369-373.

83. Romanini L, Passamonti M, Navarria M, et al. Quantitative analysis of contrast-enhanced ultrasonography of the bowel wall can predict disease activity in inflammatory bowel disease. European Journal of Radiology 2014;83:1317-1323.

84. Paredes JM, Ripolles T, Cortes X, et al. Contrast-enhanced ultrasonography: usefulness in the assessment of postoperative recurrence of Crohn's disease. Journal of Crohns & Colitis 2013;7:192-201.

85. Kucharzik T, Kannengiesser K, Petersen F. The use of ultrasound in inflammatory bowel disease. Annals of Gastroenterology 2017;30:135-144.

86. Baumgart DC, Muller HP, Grittner U, et al. US-based Real-time Elastography for the Detection of Fibrotic Gut Tissue in Patients with Stricturing Crohn Disease. Radiology 2015;275:889-899.

87. Dillman JR, Stidham RW, Higgins PDR, et al. US Elastography-derived Shear Wave Velocity Helps Distinguish Acutely Inflamed from Fibrotic Bowel in a Crohn Disease Animal Model. Radiology 2013;267:757-766.

88. Taylor S, Mallett S, Bhatnagar G, et al. METRIC (MREnterography or ulTRasound in Crohn's disease): a study protocol for a multicentre, non-randomised, single-arm, prospective comparison study of magnetic resonance enterography and small bowel ultrasound compared to a

reference standard in those aged 16 and over. BMC Gastroenterology 2014;14:142-151.

89. Yacoub JH, Obara P, Oto A. Evolving role of MRI in Crohn's disease. Journal of Magnetic Resonance Imaging 2013;37:1277-1289.

90. Punwani S, Rodriguez-Justo M, Bainbridge A, et al. Mural Inflammation in Crohn Disease: Location-Matched Histologic Validation of MR Imaging Features. Radiology 2009;252:712-720.

91. Froehlich JM, Waldherr C, Stoupis C, et al. MR motility imaging in Crohn's disease improves lesion detection compared with standard MR imaging. European Radiology 2010;20:1945-1951.

92. Amitai MM, Ben-Horin S, Eliakim R, et al. Magnetic resonance enterography in Crohn's disease: A guide to common imaging manifestations for the IBD physician. Journal of Crohns & Colitis 2013;7:603-615.

93. Schaffler A, Herfarth H. Creeping fat in Crohn's disease: travelling in a creeper lane of research? Gut 2005;54:742-744.

94. Cullmann JL, Bickelhaupt S, Froehlich JM, et al. MR imaging in Crohn's disease: correlation of MR motility measurement with histopathology in the terminal ileum. Neurogastroenterology and Motility 2013;25:749-756.

95. Desmond AN, O'Regan K, Curran C, et al. Crohn's disease: factors associated with exposure to high levels of diagnostic radiation. Gut 2008;57:1524-1529.

96. Savoye-Collet C, Savoye G, Koning E, et al. Fistulizing Perianal Crohn's Disease: Contrast-enhanced Magnetic Resonance Imaging Assessment at 1 Year on Maintenance Anti-TNF-alpha Therapy. Inflammatory Bowel Diseases 2011;17:1751-1758.

97. Ng SC, Plamondon S, Gupta A, et al. Prospective Evaluation of Anti-Tumor Necrosis Factor Therapy Guided by Magnetic Resonance Imaging for Crohn's Perineal Fistulas. American Journal of Gastroenterology 2009;104:2973-2986.

98. Sempere GAJ, Sanjuan VM, Chulia EM, et al. MRI evaluation of inflammatory activity in Crohn's disease. American Journal of Roentgenology 2005;184:1829-1835.

99. Rimola J, Planell N, Rodriguez S, et al. Characterization of Inflammation and Fibrosis in Crohn's Disease Lesions by Magnetic Resonance Imaging (January 110, pg 432, 2015). American Journal of Gastroenterology 2015;110:480-480.

100. Umschaden HW, Szolar D, Gasser J, et al. Small-bowel disease: Comparison of MR enteroclysis images with conventional enteroclysis and surgical findings. Radiology 2000;215:717-725.

101. Schreyer AG, Geissler A, Albrich H, et al. Abdominal MRI After Enteroclysis or With Oral Contrast in Patients With Suspected or Proven Crohn's Disease. Clinical Gastroenterology and Hepatology 2004;2:491-497.

102. Frokjaer JB, Larsen E, Steffensen E, et al. Magnetic resonance imaging of the small bowel in Crohn's disease. Scandinavian Journal of Gastroenterology 2005;40:832-842.

103. Dignass A, Van Assche G, Lindsay JO, et al. The second European evidence-based Consensus on the diagnosis and management of Crohn's disease: Current management. J Crohns Colitis 2010;4:28-62.

104. Johnson GJ, Cosnes J, Mansfield JC. Review article: smoking cessation as primary therapy to modify the course of Crohn's disease. Alimentary Pharmacology & Therapeutics 2005;21:921-931.

105. Bernell O, Lapidus A, Hellers G. Risk factors for surgery and postoperative recurrence in Crohn's disease. Annals of Surgery 2000;231:38-45.

106. Kaplan GG, Jackson T, Sands BE, et al. The risk of developing Crohn's disease after an appendectomy: a meta-analysis. The American Journal of Gastroenterology 2008;103:2925-31.

107. Ma C, Moran GW, Benchimol EI, et al. Surgical Rates for Crohn's Disease Are Decreasing: A Population-Based Time Trend Analysis and Validation Study (vol 112, pg 1840, 2017). American Journal of Gastroenterology 2018;113:310-310.

108. Moran GW, Leslie FC, Levison SE, et al. Enteroendocrine cells: neglected players in gastrointestinal disorders? Therapeutic Adavnces in Gastroenterology 2008;1:51-60.

109. Moran GW, Leslie FC, McLaughlin JT. Crohn's disease affecting the small bowel is associated with reduced appetite and elevated levels of circulating gut peptides. Clinical Nutrition 2013;32:404-11.

110. McDermott JR, Leslie FC, D'Amato M, et al. Immune control of food intake: enteroendocrine cells are regulated by CD4(+) T lymphocytes during small intestinal inflammation. Gut 2006;55:492-497.

111. Worthington JJ, Samuelson LC, Grencis RK, et al. Adaptive Immunity Alters Distinct Host Feeding Pathways during Nematode Induced Inflammation, a Novel Mechanism in Parasite Expulsion. Plos Pathogens 2013;9.

112. Besterman HS, Cook GC, Sarson DL, et al. Gut Hormones in Tropical Malabsorption. British Medical Journal 1979;2:1252-1255.

113. Adrian TE, Savage AP, Bacaresehamilton AJ, et al. Peptide-Yy Abnormalities in Gastrointestinal-Diseases. Gastroenterology 1986;90:379-384.

114. Leslie FC, Thompson DG, McLaughlin JT, et al. Plasma cholecystokinin concentrations are elevated in acute upper gastrointestinal infections. Qjm-an International Journal of Medicine 2003;96:870-871.

115. Bishop AE, Pietroletti R, Taat CW, et al. Increased Populations of Endocrine-Cells in Crohns Ileitis. Virchows Archiv a-Pathological Anatomy and Histopathology 1987;410:391-396.

116. Moran GW, Pennock J, McLaughlin JT. Enteroendocrine cells in terminal ileal Crohn's disease. Journal of Crohns & Colitis 2012;6:871-80.

117. Keller J, Beglinger C, Holst JJ, et al. Mechanisms of gastric emptying disturbances in chronic and acute inflammation of the distal gastrointestinal tract. American Journal of Physiology-Gastrointestinal and Liver Physiology 2009;297:G861-G868.

118. Keller J, Binnewies U, Rosch M, et al. Gastric emptying and disease activity in inflammatory bowel disease. European Journal of Clinical Investigation 2015;45:1234-1242.

119. Harrison E, Lal S, McLaughlin JT. Enteroendocrine cells in gastrointestinal pathophysiology. Current Opinion in Pharmacology 2013;13:941-5.

120. Hordonneau C, Buisson A, Scanzi J, et al. Diffusion-weighted magnetic resonance imaging in ileocolonic Crohn's disease: validation of quantitative index of activity. American Journal of Gastroenterology 2014;109:89-98.

121. Rimola J, Rodriguez S, Garcia-Bosch O, et al. Magnetic resonance for assessment of disease activity and severity in ileocolonic Crohn's disease. Gut 2009;58:1113-1120.

122. Samuel S, Bruining DH, Loftus EV, Jr., et al. Endoscopic skipping of the distal terminal ileum in Crohn's disease can lead to negative results from ileocolonoscopy. Clinical Gastroenterology and Hepatology 2012;10:1253-9.

123. Panes J, Bouhnik Y, Reinisch W, et al. Imaging techniques for assessment of inflammatory bowel disease: Joint ECCO and ESGAR evidence-based consensus guidelines. Journal of Crohns & Colitis 2013;7:556-585.

124. Bru C, Sans M, Defelitto MM, et al. Hydrocolonic sonography for evaluating inflammatory bowel disease. American Journal of Roentgenology 2001;177:99-105.

125. Horsthuis K, Bipat S, Stokkers PCF, et al. Magnetic resonance imaging for evaluation of disease activity in Crohn's disease: a systematic review. European Radiology 2009;19:1450-1460.

126. Horsthuis K, Bipat S, Bennink RJ, et al. Inflammatory bowel disease diagnosed with US, MR, scintigraphy, and CT: Meta-analysis of prospective studies. Radiology 2008;247:64-79.

127. Panes J, Bouzas R, Chaparro M, et al. Systematic review: the use of ultrasonography, computed tomography and magnetic resonance imaging for the diagnosis, assessment of activity and abdominal complications of Crohn's disease. Alimentary Pharmacology & Therapeutics 2011;34:125-145.

128. Rimola J, Ordas I, Rodriguez S, et al. Magnetic Resonance Imaging for Evaluation of Crohn's Disease: Validation of Parameters of Severity and Quantitative Index of Activity. Inflammatory Bowel Diseases 2011;17:1759-1768.

129. Rozendorn N, Amitai MM, Eliakim RA, et al. A review of magnetic resonance enterography-based indices for quantification of Crohn's

disease inflammation. Therapeutic Advances in Gastroenterology 2018;11:1-21.

130. Steward MJ, Punwani S, Proctor I, et al. Non-perforating small bowel Crohn's disease assessed by MRI enterography: Derivation and histopathological validation of an MR-based activity index. European Journal of Radiology 2012;81:2080-2088.

131. Makanyanga JC, Pendse D, Dikaios N, et al. Evaluation of Crohn's disease activity: Initial validation of a magnetic resonance enterography global score (MEGS) against faecal calprotectin. European Radiology 2014;24:277-287.

132. Ajaj WM, Lauenstein TC, Pelster G, et al. Magnetic resonance colonography for the detection of inflammatory diseases of the large bowel: quantifying the inflammatory activity. Gut 2005;54:257-63.

133. Prezzi D, Bhatnagar G, Vega R, et al. Monitoring Crohn's disease during anti-TNF-alpha therapy: validation of the magnetic resonance enterography global score (MEGS) against a combined clinical reference standard. European Radiology 2016;26:2107-2117.

134. Menys A, Helbren E, Makanyanga J, et al. Small bowel strictures in Crohn's disease: a quantitative investigation of intestinal motility using MR enterography. Neurogastroenterology and Motility 2013;25:967-975.

135. Menys A, Atkinson D, Odille F, et al. Quantified terminal ileal motility during MR enterography as a potential biomarker of Crohn's disease activity: a preliminary study. European Radiology 2012;22:2494-2501.

136. Bickelhaupt S, Pazahr S, Chuck N, et al. Crohn's disease: small bowel motility impairment correlates with inflammatory-related markers C-reactive protein and calprotectin. Neurogastroenterology and Motility 2013;25.

137. Plumb AA, Menys A, Russo E, et al. Magnetic resonance imaging-quantified small bowel motility is a sensitive marker of response to medical therapy in Crohn's disease. Alimentary Pharmacology & Therapeutics 2015;42:343-355.

138. Khalaf A, Hoad CL, Spiller RC, et al. Magnetic resonance imaging biomarkers of gastrointestinal motor function and fluid distribution. World Journal of Gastrointestinal Pathophysiology 2015;6:140-149.

139. Khalaf A, Hoad CL, Menys A, et al. MRI assessment of the postprandial gastrointestinal motility and peptide response in healthy humans. Neurogastroenterology and Motility 2018;30.

140. Khalaf A, Nowak A, Menys A, et al. Cine MRI assessment of motility in the unprepared small bowel in the fasting and fed state: Beyond the breath-hold. Neurogastroenterol Motil 2018:e13466.

141. Chaddock G, Lam C, Hoad CL, et al. Novel MRI tests of orocecal transit time and whole gut transit time: studies in normal subjects. Neurogastroenterology and Motility 2014;26:205-214.

142. Hoad CL, Parker H, Hudders N, et al. Measurement of gastric meal and secretion volumes using magnetic resonance imaging. Physics in Medicine and Biology 2015;60:1367-1383.

143. Marciani L, Pritchard SE, Hellier-Woods C, et al. Delayed gastric emptying and reduced postprandial small bowel water content of equicaloric whole meal bread versus rice meals in healthy subjects: novel MRI insights. European Journal of Clinical Nutrition 2013;67:754-8.

144. Hoad CL, Marciani L, Foley S, et al. Non-invasive quantification of small bowel water content by MRI: a validation study. Physics in Medicine and Biology 2007;52:6909-22.

145. Eggers H, Brendel B, Duijndam A, et al. Dual-Echo Dixon Imaging with Flexible Choice of Echo Times. Magnetic Resonance in Medicine 2011;65:96-107.

146. Astbury NM, Taylor MA, Macdonald IA. Breakfast consumption affects appetite, energy intake, and the metabolic and endocrine responses to foods consumed later in the day in male habitual breakfast eaters. The Journal of Nutrition 2011;141:1381-1389.

147. Hamy V, Dikaios N, Punwani S, et al. Respiratory motion correction in dynamic MRI using robust data decomposition registration - Application to DCE-MRI. Medical Image Analysis 2014;18:301-313.

148. Silverthorn DU. Human Physiology: an integrated Approach. 6th ed. London: Pearson, 2012:Chapter 21.

149. Parker HL, Tucker E, Hoad CL, et al. Development and validation of a large, modular test meal with liquid and solid components for assessment of gastric motor and sensory function by non-invasive imaging. Neurogastroenterology and Motility 2016;28:554-68.

150. Marciani L, Cox EF, Hoad CL, et al. Postprandial changes in small bowel water content in healthy subjects and patients with irritable bowel syndrome. Gastroenterology 2010;138:469-477.

151. Marciani L, Hall N, Pritchard SE, et al. Preventing Gastric Sieving by Blending a Solid/Water Meal Enhances Satiation in Healthy Humans. Journal of Nutrition 2012;142:1253-1258.

152. Pironi L, Stanghellini V, Miglioli M, et al. Fat-Induced Ileal Brake in Humans - a Dose-Dependent Phenomenon Correlated to the Plasma-Levels of Peptide-Yy. Gastroenterology 1993;105:733-739.

153. Marathe CS, Rayner CK, Jones KL, et al. Effects of GLP-1 and incretin-based therapies on gastrointestinal motor function. Experimental Diabetes Research 2011;2011:1-10.

154. Edelbroek M, Horowitz M, Dent J, et al. Effects of duodenal distention on fasting and postprandial antropyloroduodenal motility in humans. Gastroenterology 1994;106:583-92.

155. Kellum JM, Albuquerque FC, Stoner MC, et al. Stroking human jejunal mucosa induces 5-HT release and Cl- secretion via afferent neurons and 5-HT4 receptors. The American Journal of Physiology 1999;277:G515-20.

156. Gentilcore D, Nair NS, Vanis L, et al. Comparative effects of oral and intraduodenal glucose on blood pressure, heart rate, and splanchnic blood flow in healthy older subjects. Am J Physiol Regul Integr Comp Physiol 2009;297:R716-22.

157. Bland JM, Altman DG. Statistical methods for assessing agreement between two methods of clinical measurement. Lancet 1986;1:307-10.

158. Maurer AH. Gastrointestinal Motility, Part 2: Small-Bowel and Colon Transit. Journal of Nuclear Medicine Technology 2016;44:12-8.

159. Menys A, Makanyanga J, Plumb A, et al. Aberrant Motility in Unaffected Small Bowel is Linked to Inflammatory Burden and Patient Symptoms in Crohn's Disease. Inflammatory Bowel Diseases 2016;22:424-432.

160. Harvey RF, Bradshaw JM. A simple index of Crohn's-disease activity. Lancet 1980;1:514.

161. Schoepfer AM, Beglinger C, Straumann A, et al. Fecal Calprotectin Correlates More Closely With the Simple Endoscopic Score for Crohn's Disease (SES-CD) than CRP, Blood Leukocytes, and the CDAI. American Journal of Gastroenterology 2010;105:162-169.

162. Turvill J. Mapping of Crohn's disease outcomes to faecal calprotectin levels in patients maintained on biologic therapy. Frontline Gastroenterol 2014;5:167-175.

163. Ordas I, Rimola J, Rodriguez S, et al. Accuracy of Magnetic Resonance Enterography in Assessing Response to Therapy and Mucosal Healing in Patients With Crohn's Disease. Gastroenterology 2014;146:374-382.

164. Bickelhaupt S, Froehlich JM, Cattin R, et al. Differentiation between active and chronic Crohn's disease using MRI small-bowel motility examinations - Initial experience. Clinical Radiology 2013;68:1247-1253.

165. Murray FE, McNicholas M, Stack W, et al. Impaired fatty-meal-stimulated gallbladder contractility in patients with Crohn's disease. Clinical Science 1992;83:689-93.

166. Vu MK, Gielkens HA, van Hogezand RA, et al. Gallbladder motility in Crohn disease: influence of disease localization and bowel resection. Scandinavian Journal of Gastroenterology 2000;35:1157-62.

167. Camilleri M, Parkman HP, Shafi MA, et al. Clinical guideline: management of gastroparesis. The American Journal of Gastroenterology 2013;108:18-37; quiz 38.

168. Scott AM, Kellow JE, Shuter B, et al. Intragastric Distribution and Gastric-Emptying of Solids and Liquids in Functional Dyspepsia - Lack of Influence of Symptom Subgroups and H-Pylori-Associated Gastritis. Digestive Diseases and Sciences 1993;38:2247-2254.

169. Tack J, Arts J, Caenepeel P, et al. Pathophysiology, diagnosis and management of postoperative dumping syndrome. Nature Reviews Gastroenterology & Hepatology 2009;6:583-590.

170. George JD. New clinical method for measuring the rate of gastric emptying: the double sampling test meal. Gut 1968;9:237-42.

171. Medhus AW, Sandstad O, Bredesen J, et al. Delay of gastric emptying by duodenal intubation: sensitive measurement of gastric emptying by the paracetamol absorption test. Alimentary Pharmacology & Therapeutics 1999;13:609-620.

172. Ghoos YF, Maes BD, Geypens BJ, et al. Measurement of Gastric-Emptying Rate of Solids by Means of a Carbon-Labeled Octanoic-Acid Breath Test. Gastroenterology 1993;104:1640-1647.

173. Bateman DN, Whittingham TA. Measurement of Gastric-Emptying by Real-Time Ultrasound. Gut 1982;23:524-527.

174. Abell TL, Camilleri M, Donohoe K, et al. Consensus Recommendations for Gastric Emptying Scintigraphy: A Joint Report of the American Neurogastroenterology and Motility Society and the Society of Nuclear Medicine. American Journal of Gastroenterology 2008;103:753-763.

175. Schwizer W, Maecke H, Fried M. Measurement of Gastric-Emptying by Magnetic-Resonance-Imaging in Humans. Gastroenterology 1992;103:369-376.

176. Fidler J, Bharucha AE, Camilleri M, et al. Application of magnetic resonance imaging to measure fasting and postprandial volumes in humans. Neurogastroenterology and Motility 2009;21:42-51.

177. Goetze O, Steingoetter A, Menne D, et al. The effect of macronutrients on gastric volume responses and gastric emptying in humans: a magnetic resonance imaging study. American Journal of Physiology-Gastrointestinal and Liver Physiology 2007;292:G11-G17.

178. Feinle C, Kunz P, Boesiger P, et al. Scintigraphic validation of a magnetic resonance imaging method to study gastric emptying of a solid meal in humans. Gut 1999;44:106-111.

179. Hayakawa N, Nakamoto Y, Chen-Yoshikawa TF, et al. Gastric motility and emptying assessment by magnetic resonance imaging after lung transplantation: correlation with gastric emptying scintigraphy. Abdominal Radiology 2017;42:818-824.

180. Holt S, Cervantes J, Wilkinson AA, et al. Measurement of Gastric-Emptying Rate in Humans by Real-Time Ultrasound. Gastroenterology 1986;90:918-923.

181. Read NW, Al Janabi MN, Bates TE, et al. Effect of gastrointestinal intubation on the passage of a solid meal through the stomach and small intestine in humans. Gastroenterology 1983;84:1568-1572.

182. O'Hara JR, Lomax AE, Mawe GM, et al. Ileitis alters neuronal and enteroendocrine signalling in guinea pig distal colon. Gut 2007;56:186-194.

183. Serre V, Dolci W, Schaerer E, et al. Exendin-(9-39) is an inverse agonist of the murine glucagon-like peptide-1 receptor: Implications for basal intracellular cyclic adenosine 3 ',5 '-monophosphate levels and beta-cell glucose competence. Endocrinology 1998;139:4448-4454.

184. Lassman DJ, McKie S, Gregory LJ, et al. Defining the role of cholecystokinin in the lipid-induced human brain activation matrix. Gastroenterology 2010;138:1514-24.

Appendix

(A): Visual analogue scale (VAS) symptoms questionnaire:

Study day symptom questionnaire: Motility in Crohn's disease
Investigators: Dr. Gordon W. Moran, Dr Caroline Hoad, Dr. Luca Marciani, Dr Khalid Latief, Professor Penny Gowland, Professor Robin Spiller

The University of Nottingham

SUBJECT.....DATE.....VISIT .....

TIME POINT .....

Please answer each of the following questions by putting on the scale a cross at the point that corresponds to the intensity of your satiety feelings.

QUESTION A: How full do you feel ?

Not full — Extremely full

QUESTION B: How bloated do you feel ?

Not bloated — Extremely bloated

QUESTION C: How distended do you feel?

Not at all — Very distended

QUESTION D: Do you feel any abdominal pain / discomfort?

No discomfort — Severe discomfort

QUESTION E: Do you feel any nausea/ sickness?

Not feeling sick — Feeling very sick

Motility in Crohn's disease. Study Day Symptom Questionnaire V1.0 10th November 2014

(B): The standard operating procedures (SOP) for the preparation of the oral contrast solution:

Introduction

These SOP contain the procedures to correctly prepare 1 litre of the oral contrast agent used for Magnetic Resonance Enterography examinations. This oral contrast agent contains 2.5% mannitol and 0.2% locust bean gum and is used to distend the small bowel lumen for MRI examination.

Procedures

- Wash hands before starting the preparation and make sure preparation surfaces are clean and tidy.
- Preparation time for this contrast agent takes a minimum time of 30 mins, please allow adequate time to prepare the solution before it is needed to be ingested.
- Water: Use a new 2 Litre bottle of mineral water.
- Preparation of Mannitol solution: Using a clean measuring cylinder, measure out 300 mL of water and place in a 1L or 2L glass beaker. Place a new weighing boat on the accurate scales and zero. Using a clean plastic spoon measure out 25 g of mannitol powder into the weighing boat. Carefully empty the mannitol from the weighing boat into the water and stir until dissolved using the plastic spoon. This solution should now be placed into the fridge to cool. The minimum time for the solution to be left in the fridge is 15 minutes. Set a timer if necessary.

- Preparation of Locust Bean Gum: Using a clean measuring cylinder measure out 520 mL of mineral water and put in a kettle and boil. Once boiled leave to cool as the hot water will be needed later in the preparation. Using a clean measuring cylinder, measure out 200 mL of water and place into a 1 L conical flask. Carefully slide a clean magnetic flea into the flask. Place a new weighing boat on the accurate scales and zero. Using a clean plastic spoon, measure out 2 g of locust bean gum powder into the weighing boat. Place the conical flask onto the magnetic stirrer and slowly set the flea rotating. Increase the speed of the rotation slowly until it reaches 7 on the dial. Slowly add the locust bean powder to the stirring water ensuring that large lumps of powder do not drop into the solution. This is achieved best by gently tapping the weighing boat to knock off the loose powder at the end of the boat. Once all the powder has been added to the water solution, allow to stir for 2-3 minutes until the solution looks smooth. Using a clean measuring cylinder and heat protective gloves measure out 500 mL of hot water (this may be done in 2 parts of 250 mL). Using the heat protective gloves slowly pour the hot water onto the locust bean gum solution in the conical flask whilst the stirrer is rotating. Leave the solution stirring for at least 10 minutes, this will allow for adequate mixing of the locust bean gum and some cooling of the solution.

- Combining the two solutions: Take the mannitol solution out of the fridge and slowly add to the locust bean gum solution whilst the solution is still being stirred. Stir the full solution for a further 2-3 minutes and then using the heat protective gloves pour the full solution into a 2L beaker (including the flea) and place back into the fridge until it is needed.
- Dispensing of Solution: The solution should be given to the participant in 2 separate 500 mL doses. The first dose should be given 30-40 minutes before the subject is due to be scanned. The second dose should be given 5-10 minutes before the scan and ideally should be finished immediately before scanning commences. To dispense the contrast agent, take the 2L beaker out of the fridge and check that the temperature of the solution is not too hot by feeling the temperature of the beaker on the back of your hand, if the beaker feels very hot place back in the fridge and wait a further 5 minutes. If the temperature of the beaker feels ok, place on the magnetic stirrer. Allow the mixture to stir at level 7 on the dial for 2-3 minutes before pouring out approximately 500 mL into a 500 mL plastic glass and serve immediately to the participant. Repeat this for the second glass at the appropriate time.
- Should the participant not consume the full drink, measure the remaining solution in the glasses using the measuring cylinder and make a note of the amount on the case report form (CRF).

- Tidying of kitchen area. Plastic glasses, spoons and weighing boats should be thrown away into the general waste. Any unused solution may be poured down the sink together with a small amount of running water. All beakers, flasks, magnetic fleas and measuring cylinders should be washed up and the put away when dry. If there have been any spillages please ensure these are cleaned up appropriately and leave the kitchen area in a clean and tidy condition for the next user.